A Study of Polycarbonate / Poly (butylene terephthalate) Compounding in a Twin Screw Extruder

by

Vahid Noeei Ancheh

A thesis
presented to the University of Waterloo
in fulfillment of the
thesis requirement for the degree of
Master of Applied Science
in
Chemical Engineering

Waterloo, Ontario, Canada, 2008

I hereby declare that I am the sole author of this thesis. This is a true copy of the thesis, including any required final revisions, as accepted by my examiners.

I understand that my thesis may be made electronically available to the public.

Abstract

Blends of poly butylene terephthalate (PBT) and polycarbonate (PC) form a very important class of commercial blends in numerous applications requiring materials with good chemical resistance, impact resistance even at low temperatures, and aesthetic and flow characteristics. PC and PBT are usually blended in a twin screw extruder (TSE). Product melt volume flow rate (MVR) is a property used to monitor product quality while blending the PC/PBT in a twin screw extruder. It is usually measured off line in a quality control laboratory using extrusion plastometer on samples collected discretely during the compounding operation. Typically a target value representing the desired value of the quality characteristics for an in-control process, along with upper and lower control limits are specified. As long as the MVR measurement is within the control limits, the sample is approved and the whole compounded blend is assumed to meet the specification. Otherwise, the blend is rejected. Because of infrequent discrete sampling, corrective actions are usually applied with delay, thus resulting in wasted material.

It is important that the produced PC/PBT blend pellets have consistent properties. Variability and fault usually arise from three sources: human errors, feed material variability, and machine operation (i.e. steady state variation). Among these, the latter two are the major ones affecting product quality. The resulting variation in resin properties contributes to increased waste products, larger production cost and dissatisfied customers. Motivated by this, the objective of this project was to study the compounding operation of PC/PBT blend in a twin screw extruder and to develop a feasible methodology that can be applied on-line for monitoring properties of blends on industrial compounding operations employing available extruder input and output variables such as screw speed, material flow rate, die pressure and torque.

To achieve this objective, a physics-based model for a twin screw extruder along with a MVR model were developed, examined and adapted for this study, and verified through designed experiments. This dynamic model for a TSE captures the important dynamics, and

relates measurable process variables (screw speed, torque, feed rates, pressure etc.) to ones that are not being measured (material holdups and compositions at the partially and filled section along a TSE barrel). This model also provides product quality sensors or inferential estimation techniques for prediction of viscosity and accordingly MVR. The usefulness of the model for inferential MVR sensing and fault diagnosis was demonstrated on experiments performed on a 58 mm co-rotating twin-screw extruder for an industrial compounding operation at a SABIC Innovative Plastics plant involving polycarbonate – poly butylene terephthalate blends.

The results showed that the model has the capability of identifying faults (i.e., process deviation from the nominal conditions) in polymer compounding operations with the twin screw extruder. For instance, the die pressure exhibited a change as a function of changes in raw materials and feed composition of PC and PBT. In the presence of deviations from nominal conditions, the die pressure parameters are updated. These die pressure model parameters were identified and updated using the recursive parameter estimation method. The recursive identification of the die pressure parameters was able to capture very well the effects of changes in raw material and/or composition on the die pressure. In addition, the developed MVR model showed a good ability in monitoring product MVR on-line and inferentially from output process variables such as die pressure which enables quick quality control to maintain products within specification limits and to minimize waste production.

Acknowledgements

I would like to express my sincere gratitude and appreciation to my supervisors, professors Costas Tzoganakis and Tom Duever, for their guidance, suggestions and support.

Special thanks and appreciation to the SABIC Innovative Plastics at Cobourg Plant, ON, Canada, especially Mr. Paul Van Laren and Mr. Daniel Ross, for providing the materials, equipment, machinery, facility, financial and technical support for completion of this work.

My thanks are also expressed to my wife, my son- Aidyn - and my colleagues at the polymer processing lab.

Table of Contents

List of Figures

List of Tables

NOMENCLATURE

A, B	extruder geometry-dependent parameters for mass holdups
D	diameter of the screw, mm
DP	die pressure, psi
H	channel depth, mm
F_d	shape factor which accounts for the aspect ratio of the channel
I	number of screw lobes or flights
K	die and extruder-dependent parameter
k	screw design/geometry dependent parameters
l_c	length of the partially filled of screw, mm
L_m	length of the mixing section and melting section, mm
M_1	mass holdup in partially filled section of screw, kg
M_2	mass holdup in completely filled section of screw, kg
N	screw speed, rpm
Q_1	feed-rate of PC, kg/hr
Q_2	feed-rate of PBT, kg/hr
Q	total feed-rate at inlet, kg/hr
R1, R2	recycle ratios in partially and completely filled sections of screw
T	total torque(% motor load)
x_i	weight fraction PC at inlet = *Q1 /Q*
x_1	weight fraction PC in partially filled section of screw
x_2	weight fraction PC in completely filled section
V_p	filled volume in the conveying section due to pressure back flow
W	channel width, mm
α_i	parameters in torque relation
β_i	parameters in die pressure relation
θ	helix angle of the conveying element
μ_0	nominal viscosity at the nominal operating point
μ_1, μ_2, μ_3	gradient of viscosity with respect to composition , shear rate and temperature

Chapter 1
Introduction

Blends of poly (butylene terephthalate) (PBT) and polycarbonate (PC) form a very important class of commercial blends in numerous applications requiring materials with good chemical resistance, great impact resistance even at low temperatures, heat resistance, and outstanding aesthetic and flow characteristics. In these blends, the amorphous PC provides impact resistance and toughness, while, PBT because of its semi-crystalline structure, provides chemical resistance and thermal stability. By changing the percentage of PBT and PC in these blends, their properties can be tailor-made. For example, with increasing PC percentage, the viscosity of the blend will increase significantly. Because of the chemical structure of PC and PBT, the occurrence of transesterification reactions is possible, resulting in the formation of the PC–PBT co-polyester. Some additives may be added to the blend to control or prevent transesterification reactions between PC and PBT. Some other special additives may also be added to blends to enhance properties and processing.

PC and PBT are usually blended in a twin screw extruder (TSE) to achieve certain properties such as melt flow behavior, color and mechanical strength. Figure 1.1 presents a schematic diagram of a PC/PBT compounding line in a TSE. As demonstrated in this figure, PC and PBT are fed into the TSE from storage hoppers. The rotating action of the screws contributes to producing a homogeneous melt blend which is pumped through a shaping die. The melted material emerges from the die in continuous multiple strands that are cooled in a water bath which is located after the TSE. Subsequently, the cooled and solidified polymer resin strands are chopped into pellets in a pelletizer and packed and shipped to customers.

It is important that produced resin pellets have consistent properties. Product melt volume flow rate (MVR) is a property used to monitor product quality. It is usually measured off line in a quality control laboratory on samples that were collected discretely during the compounding operation. Because of the discrete sampling, corrective action is usually applied with delay which results in wasted products. Variability and fault in key quality

characteristics, such as MVR, usually arise from three sources: machine operation, human errors and feed material variability. Among these possible sources of faults, the major ones that affect product quality are associated with variations in raw material and feeder rate variations. The resulting variation in resin properties contributes to increased waste products, production cost and dissatisfied customers. Motivated by this, the objective of this project is to study the compounding operation of PC/PBT blends in a twin screw extruder and to develop a feasible methodology that can be applied on-line for monitoring properties of blends on industrial compounding operations employing available extruder input and output variables such as screw speed, material flow rate, die pressure and torque.

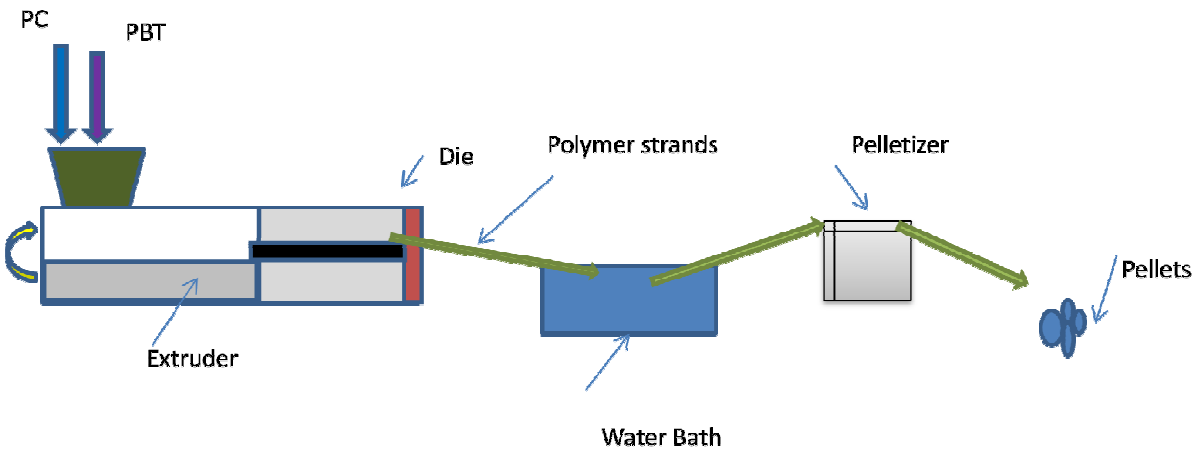

Figure 1.1: Polymer compounding line

Polymer blending has been studied extensively and there are numerous publications addressing various aspects of these systems. In chapter 2 of this thesis, an overview is provided focusing on polymer blends of PBT and PC and compounding of PC/PBT blends in twin-screw extruders (TSE) is reviewed with emphasis on processing, modeling and diagnostics aspects.

The nature of the flow characteristics in twin screw extruder physics is too complex, and it is hard to find a model for twin screw extruder that has the capability of implementation in typical compounding lines. A simple process model that captures the main aspects of the compounding operation in a TSE accurately is a significant achievement. The next step in the approach for this project was to develop a simple yet predictive model. In chapter 3, several general aspects of twin screw extruders are discussed along with the flow model employed in this work for blending of PBT with PC. Section 3.1 looks at TSEs in general and section 3.2 describes the physics-based lumped model based on previous literature work. In this physics-based lumped flow model for TSEs, in response to changes in input variables such as feeds rate and screw speed, the model predicts output variables such as die pressure and torque.

An overview of experimental methods including design of experiments, experimental set up, material selection along with the physical properties that would be measured to characterize the blend are presented in chapter 4.

Algorithms and experimental results to identify the flow model parameters along with validation experiments are described in chapter 5 of this thesis. These models for torque and die pressure in twin screw extruders have unknown parameters that depend on the specific extruder geometry and the product application and need to be identified from measured input/output data. Section 5.2 describes the Levenberg Marquardt algorithm (LMA) and results for estimation of torque model parameters. Section 5.3 describes the die pressure model parameters identification using recursive parameter estimation methods (RPE).

A major objective of process control for compounding of PC/PBT in a TSE is to quickly detect the occurrence of faults such as change in composition of raw materials. This quick identification of fault and a corrective action in successive stages will reduce significantly nonconforming products. In addition, the ability to monitor product MVR on-line from output process variables enables quick quality control to maintain products within specification limits. Sections 6.1 through 6.4 of chapter 6 describe the development of a

simple model for inferential estimation of MVR from die pressure model parameters and also check its validity using industrial experimental runs. Section 6.5 describes the fault identification method for the extruder using the developed modeling and adaptation methods. Finally, concluding remarks are made in chapter 7 along with some recommendations for future work.

Chapter 2
Literature Overview

Polymer blending has been studied extensively and there are numerous publications addressing various aspects of these systems. In this chapter, an overview is provided focusing on polymer blends of thermoplastic polyesters, namely poly butylene terephthalate (PBT), and polycarbonate (PC). In the first section, the mechanical, physical and morphological properties of PC/PBT blends are reviewed. In the next section, compounding of PC/PBT blends in twin-screw extruders (TSE) is reviewed with emphasis on processing, modeling and diagnostics aspects.

2.1 PC/PBT Blends

Commercial polymer blends normally consist of binary systems with partial solubility, thus containing two or more phases [1]. Occasionally, components may be added to serve as compatibilizers or as impact modifiers. Processing conditions such as feed rate, screw speed and temperature play an important role among the factors that influence the degree of mixing of the components and also the morphological structure of parts moulded from such blends [2]. The morphology also depends strongly on the composition. Halder et al. [3] studied the morphology of blends PC/PBT which were crystallized from the melt. They applied density measurements and small angle light scattering techniques and found that the rate of crystallization of these blends decreased with increasing amount of PC. Control of possible transesterification reactions is critical because the crystallinity of the PBT decreases with increasing transesterification extent. As a consequence of decreased crystallinity, the mechanical performance as well as chemical resistance and thermal stability of the blends are reduced. On the other hand, if the extent of the transesterification reactions is too limited, the interphase adhesion will be poor, leading to brittleness. Therefore, the introduction of impact modifiers, compatibilizers, and glass fibres into the composition is preferable to the use of the transesterification reaction for the improvement of impact resistance [4].

Various additives have been introduced into the blend composition to improve impact resistance at low extents of transesterification. Among the additives used, methyl acrylate-butadiene-styrene (MBS) impact modifiers have demonstrated a significant impact-modifying effect at low temperatures. Tseng and Lee [5] synthesized and characterized functional group containing MBS impact modifiers for PC/PBT alloys. They realized that introduction of a functional group would improve the adhesion between the MBS rubber and the PC/PBT alloy and, thus, would have a beneficial effect on the impact strength of these blends. Their results showed that a much smaller amount of the functional group containing MBS in the PC/PBT alloy could lead to higher impact strength. On the other hand, the PMMA-shell of this impact modifier gives good adhesion with the polycarbonate. The poly butadiene because of its rubbery properties is the component that causes the higher impact strength. The poly styrene has an aesthetic function [4]. Bai et al. [6] have reported the use of ethylene–butylacrylate–glycidyl methacrylate (EBGMA) as a toughening modifier for PC/PBT blends. Their results showed that the addition of EBGMA leads to great increases in impact strength, in elongation at break and in vicat softening temperature. However, the tensile strength and the flexural properties showed a reduction. Wu et al. [7] studied the static and impact fracture toughness of a PC/PBT/impact modifier blend at different temperatures. They found that, for PC/PBT/MBS blends, the increase in impact toughness with temperature is a consequence of the relaxation processes of the rubbery zones of the parent polymers.

The role of interphase interactions on the impact strength of PC/PBT and PC/PET blends has also been studied by Pesetskii et al. [8]. The major conclusion was that phase separation phenomena can cause variations in properties of both the amorphous and crystalline phases. They demonstrated that the adhesion strength decreases in the temperature range from the glass transition temperature (Tg) of PBT to that of PC. They also observed that over the temperature range where interphase interactions are strong and the two components are in the glassy state, the impact resistance of the blends is weak. Over the temperature range between the Tg of the PBT and the Tg of the PC the impact resistance of the blends increases. They

attributed this behavior to the dissipation of the energy of crack propagation in the PBT amorphous phase.

Devaux et al. [9] suggested three possible mechanisms for the PC/PBT transesterification. The exchange reaction can result either from an alcoholysis between an –OH terminated polycondensate (PC or PBT) and another macromolecular species (PBT or PC) or from an acidolysis reaction involving carboxyl terminated PBT. The transesterification can also proceed via a direct reaction between a PBT unit and a PC group. They suggested the main process is that of direct transesterification. As a consequence of this, copolymers act as compatibilizers in these blends. Tattum et al. [10] blended a series of 50:50 PC/PBT via reactive melt blending in a torque rheometer. In their study, a controlled degree of transesterification between the two homopolymers was initiated by the incorporation of an alkyl titanium catalyst during melt blending and finally quenched by the addition of a transesterification inhibitor. They showed that as the degree of transesterification increased, the composition of the blends became increasingly complex, comprising mixtures of the homopolymers and various AB-type copolymers of PC and PBT, resulting in significant changes in their thermal behavior. They suggested that a corresponding transformation in the morphology of the blends was observed due to the formation of increasing concentrations of copolyesters.

Hopfe et al. [11] studied the transesterification and crystallization behavior of melt blends of PC and PBT. They used Fourier transform infrared spectroscopy (FTIR) as well as nuclear magnetic resonance (NMR) spectroscopy and differential scanning calorimetry (DSC). They showed that at approximately 50/50 weight fraction of PC/PBT blends, partial miscibility exists both in the melt and after melt blending, with phase separation occurring during PBT crystallization. Marchese et al. [12] showed that miscibility was strictly correlated with the crystallizability of the system. The partial miscibility of the amorphous phases (amorphous PBT and amorphous PC) in this polymer blend has been attributed to various factors such as the morphology of the crystalline phase, transesterification reactions resulting in PC/PBT

copolyesters and the closeness of the solubility parameters of PC and PBT. Wahrmund et al. [13] studied melt blends of polycarbonate with PBT by differential thermal analysis (DTA) and dynamic mechanical behavior to determine their state of miscibility. Both techniques showed multiple glass transition temperatures which are indicative of incomplete miscibility in the amorphous phase. They suggested that there are amorphous phases containing both components, i.e., partial miscibility of the PC/PBT system. Birley and Chen [14] also concluded that PBT and PC show significant mixing in the melt but the partially mixed components phase-separate during dissolution. Partial melt miscibility of the PC/PBT system is also suggested by Hobbs et al. [15] and similar observations have also been reported by Dellimoy et al. [16].

The transesterification process can be kept under control and suppressed by added stabilizers. Additives used as stabilizers to prevent transesterification include phosphates and phosphorus containing acids [4].

2.2 Compounding of PC/PBT in Twin Screw Extruders

Twin screw extruders (TSE) are widely used in polymer compounding operations. The flow of molten polymers in TSE has been studied by various researchers. A particularly useful model for this work is that of Meijer et al. [17]. This a very simplified, fundamental model for a co-rotating TSE which can be used to examine the role of screw geometry and processing conditions on specific energy consumption and temperature rise along the machine. The model predictions were confirmed by visualization experiments for Newtonian fluids.

Due to complexity of compounding operations in extruders and because of the non-linearities frequently encountered, other approaches have been employed for model flows in TSEs. Neural networks [18] and genetic algorithms [19] have been used to develop inferential models for polymer viscosity in industrial plasticating extruders. McKay et al. [19]

demonstrated that both approaches work well. However, genetic algorithms produced models that performed better.

Traditionally the two methods of measuring polymer viscosity for process control have either been in the lab using a capillary rheometer or at the process extruder using a rheometer. The laboratory as always produced accurate results, however, the data collection period is often too long to be used for process control. In an effort to develop more comprehensive controls for composition and melt flow rate, the use of melt flow rheometer has been popular and is used widely as described by Dealy and Broadhead [20]. The most common type of process rheometer is the on-line type, in which a sample stream is withdrawn from a process line, usually by means of a gear pump, and fed to the rheometer. This is to be contrasted with an in-line rheometer, which is mounted directly in a process line. The cost, maintenance and generation of a waste stream of these sensors are major drawbacks. In addition, these polymer materials are often processed at elevated temperatures and not only must the rheometer be capable of functioning at these temperatures, but the effect of temperature on the rheological property measured must be taken into account [21]. The on-line sensors still require a QA lab for calibration and maintenance.

Gao and Bigio [22] presented and experimentally validated a physically motivated model for predicting the mean residence time in twin screw extruders. Accurate estimation of the mean residence time and the propagation delay through a plasticating extruder is critical for implementing feedback control schemes employing sensors mounted along the extruder. They carried out experiments on a 30 mm Krupp Werner and Pfleiderer co-rotating twin screw extruder equipped with reflectance optical probes over the melting section, the mixing section and at the die. They showed that the mean residence times predicted by their model are in good agreement with the experimentally measured mean residence times. Both the model and the experimental results of their works indicate that the mean residence volume has a linear relationship with the flow rate / screw speed (Q/N) ratio where Q stands for feed rate and N stands for screw speed. According to their study results, when the percent drag

flow is not large, their model can be used to predict the mean residence time with estimation error of no more than 10%. When the percent drag flow is large or higher estimation accuracy is required, their model should be modified. Kumar et al. [23,24] developed a framework for improved operation of extruders in a wide range of applications by incorporating intelligent means for (i) on-line product quality estimation (inferential sensing), (ii) diagnostics for common process material failures, and (iii) closed-loop control of product quality based on the on-line estimation. In their work, they have developed a novel model-based approach for the estimation, diagnostics and controls in a unified framework. Models that formed the basis of their work were first used by Gao and Bigio [22]. These models were originally aimed at studying residence time distributions for extruders and they have been adapted and extended as described in chapter 3 of this thesis.

Chapter 3

Polymer Compounding in Twin-Screw Extruders: Flow Modeling

In this chapter, several general aspects of twin screw extruders (TSEs) are discussed along with the flow model employed in this work for blending of poly butylene terephthalate (PBT) with polycarbonate (PC). Before trying to determine which variables are significant, it is important to understand the process, the variables involved, and the properties being affected. Section 3.1 looks at TSEs in general and section 3.2 describes the physics- based lumped model used in this work.

3.1 Twin Screw Extruders (TSEs)

Extruders are widely used, not only in polymer preparation, but throughout the petrochemical and food industries for mixing, blending, reacting, cooking, devolatilizing and numerous other tasks. The purpose of the extruder is to feed a die with a homogeneous material at constant temperature and pressure. This definition highlights three primary tasks that the extruder must accomplish while delivering material to a shaping die. First, it must homogenize, or satisfactorily mix, the material. Second, the material entering the die must have minimal temperature variation with respect to both time and position within the melt stream. Third, there must be minimal melt pressure variation with time [25].

Extruders are categorized in two types of single and twin screw extruder based on their number of screws. The single screw extrusion process is highly dependent on the frictional and viscous properties of the material and the conveying mechanism is based on frictional forces in the solids conveying zone and viscous forces in the melt conveying zone. In TSEs, the frictional and viscous properties of the material play a lesser role on the conveying behavior. TSEs can be designed to have positive conveying characteristics in which the material is more or less trapped in compartments formed by the two screws and the barrel. The better the seal between flight and channel of the opposite screw, the more positive will

be the conveying characteristics. The diversity among TSEs is large. We will only describe some important characteristics of the various TSEs. A summarized classification of twin screw extruders is shown in Table 3.1 [25].

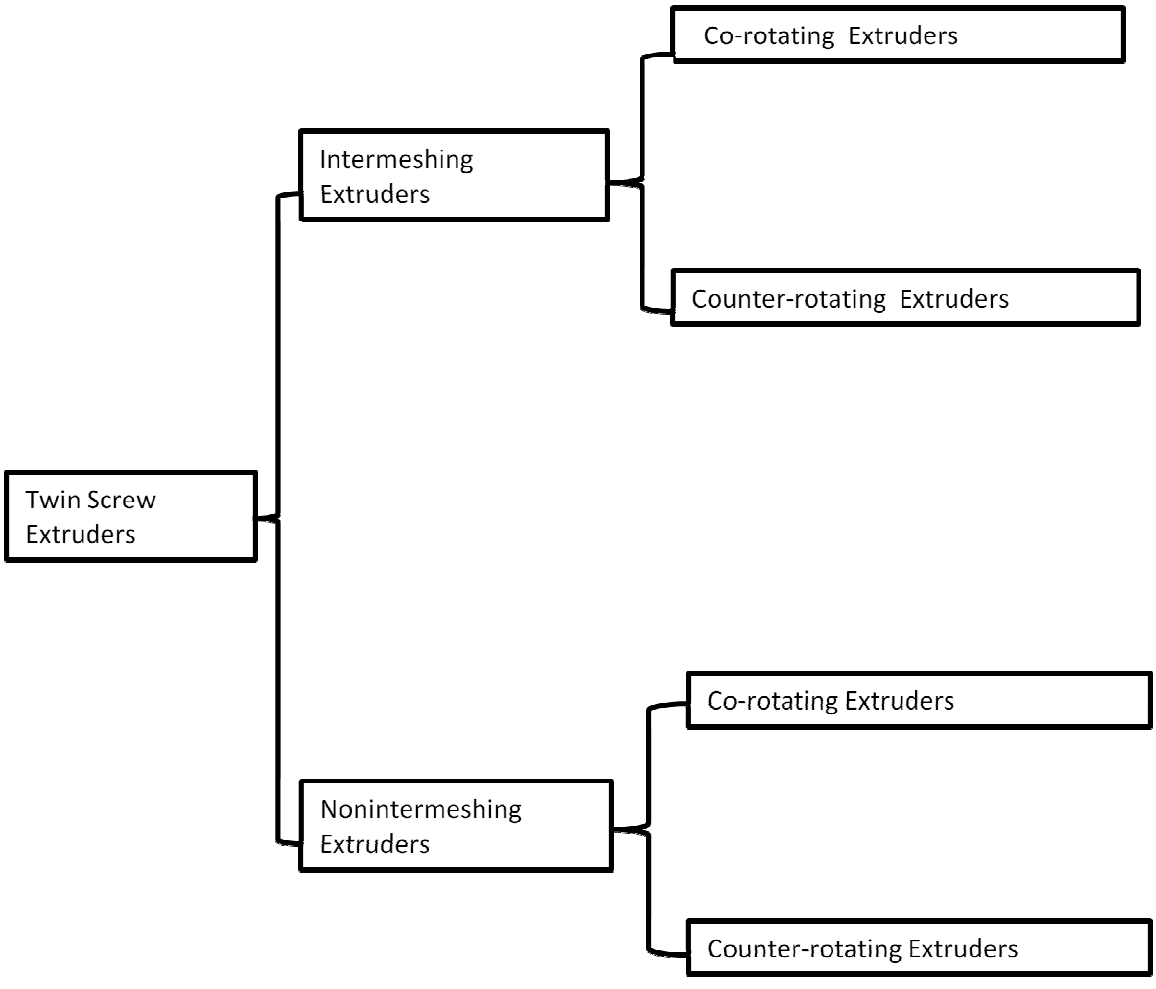

Table 3.1: Classification of Twin Screw Extruders

The main distinction is made between intermeshing and non-intermeshing TSEs. The non-intermeshing TSEs where the flights of one screw do not protrude into the channel of the other screw do not have the benefits of positive conveying characteristics. In intermeshing extruders, the degree of intermeshing can range from almost fully intermeshing to almost non-intermeshing with a corresponding range in the degree of positive conveying characteristics. Any amount of back leakage into upstream channel sections will adversely affect the positive conveying behavior.

The second distinguishing characteristic is the direction of rotation. There are only two possibilities: either co-or counter- rotating. In a counter-rotating twin screw extruder the material is sheared and pressurized in a mechanism similar to calendering i.e. the material is effectively squeezed between counter-rotating rolls [26]. In a co-rotating system the material is transferred from one screw to the other in a figure-of-eight pattern. The co-rotating extruders may be preferred for heat sensitive materials because the material is conveyed through the extruder quickly with little possibility of entrapment.

The intermeshing co-rotating extruders can be further subdivided in low and high speed machines. The low speed extruders have a closely fitting flight and channel profile. Therefore, they have a high degree of positive conveying characteristics. These machines are used primarily in profile extrusion applications. The high speed co-rotating extruders generally have self wiping characteristics. Because of the openness of the channels, material is easily transferred from one screw to another. These machines are primarily used in compounding operations [25]. A typical comparison of high and low speed co-rotating twin screw extruders is shown in Table 3.2.

Consider a typical polymer compounding extruder setup in Figure1.1, which consists of the main drive, the extruder barrel with two co-rotating screws, feeders for raw materials, water bath, and pelletizer unit. As demonstrated in this figure, raw materials are fed into the TSE from storage hoppers. The rotating action of the screws contributes to producing a

homogeneous melt blend which is pumped through a shaping die. The melted material emerges from die in continuous multiple strands that are cooled in a water bath which is located after TSE. Subsequently, the cooled and solidified polymer resin strands are chopped into pellets in a pelletizer and packed and shipped to customers.

Table 3.2: Comparison of low and high speed co-rotating twin-screw extruders [25]

Type	Low speed Co-rotating	High speed Co-rotating
Mixing efficiency	Medium	High
Shearing action	Medium	High
Energy efficiency	Medium	High
Heat generation	Medium	High
Max. revolving speed (rpm)	25-35	250-300
Length of Screw L/D	7-8	30-40

3.2 Physics-Based Lumped Flow Model for Twin Screw Extruders

This work focuses on the use of a co-rotating TSE in polymer compounding applications. Co-rotating twin-screw extruders are unique and versatile machines that are used widely in the plastics and food processing industries. The nature of the flow characteristics in twin screw extruder physics is too complex, and it is hard to find a model for twin screw extruders that have the capability of implementation in typical compounding lines. A simple process model that captures the main aspects of the compounding operation in a TSE accurately is a significant achievement. This section outlines the development of a dynamic model that captures the important dynamics, and relates measurable process variables (screw speed, torque, feed rates, pressure etc.) to ones that are not being measured. This model also provides product quality sensors or inferential estimation techniques for prediction of viscosity.

Kumar et al. [23, 24] derived models that were formed based on the work of Gao and Bigio [22]. They start with a dynamic model that describes the dominant characteristics associated with the mixing of the raw materials. They developed a lumped two-section dynamic mixing model that captures the effect of the inputs to the process (raw material feed-rates and screw speed) on the measured process outputs (total screw torque and die pressure, the pressure developed prior to the die plate as the molten product is stranded into the water bath). Figure 3.1 shows a schematic for this extrusion model. This model considers two flow zones along the extruder in which the first zone is partially- filled while the second zone is fully- filled.

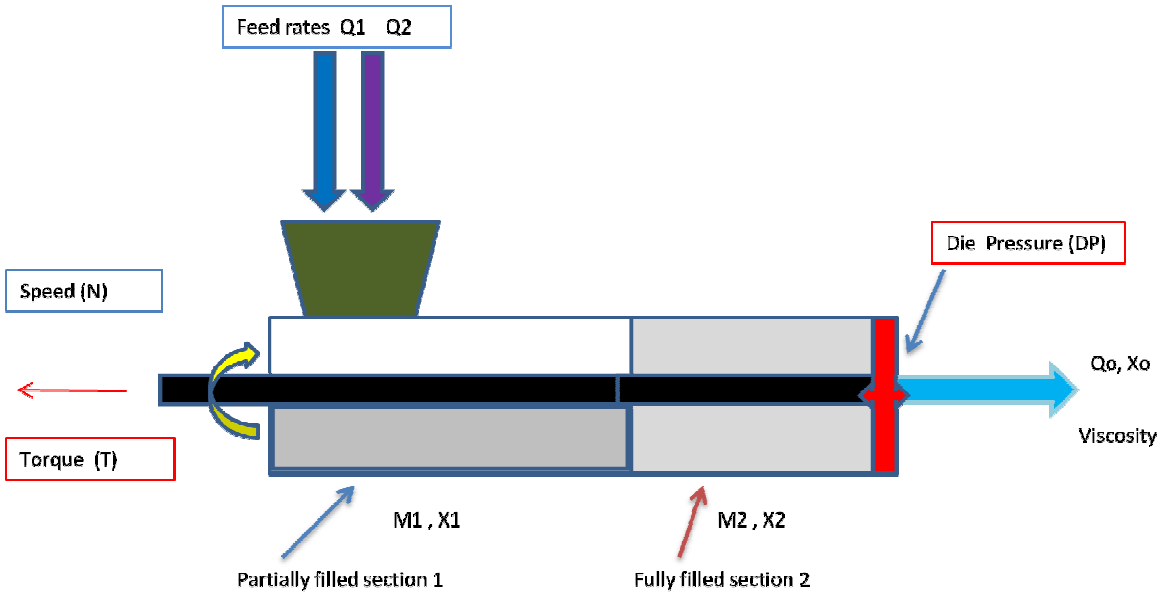

Figure 3.1: Schematic representation of extrusion model

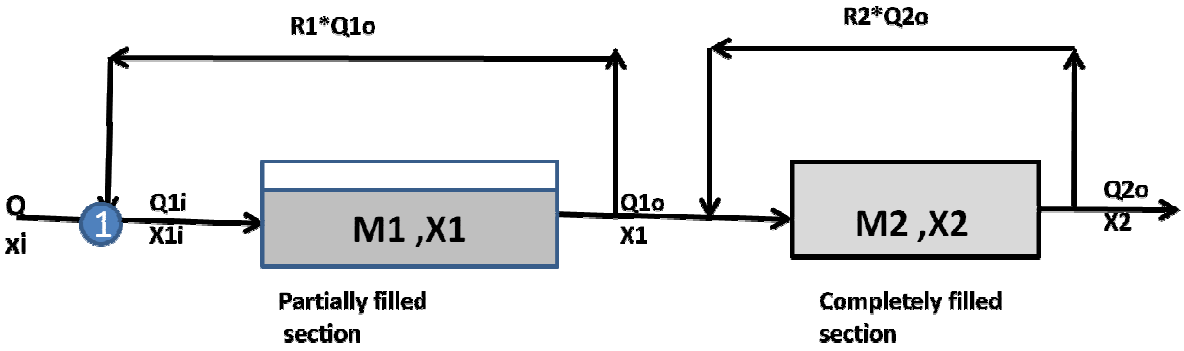

Figure 3.2: Schematic representation of mixing in partially and completely filled sections

In this model, two materials are being fed to the extruder at feed rates of Q_1 and Q_2 respectively while the screws rotate with speed N. Feed rate and screw speed are process input variables while die pressure (DP) and torque (T) on the screw are being monitored. They considered the extruder with two distinct sections during regular operation - a completely filled section (mixing, kneading) and a partially filled section (conveying). Under steady state operating conditions with total feed rate (throughput)$Q = Q_1 + Q_2$, and screw speed N, the total material holdup M_1 and M_2 in the partially and completely filled sections, respectively, are given by:

$$M_1 = B\frac{Q}{N} \;\; ; \;\; M_2 = A \qquad \textbf{(3.1)}$$

where the ratio *Q/N* is referred to as the specific throughput and the parameters *A, B* are related to the maximum capacities of the completely filled and partially filled sections, respectively, depending on the specific screw design/geometry. Based on the Gao et al. [22] work the specific throughput *Q/N* is an estimate of the degree of fill in the partially filled sections, which then affects residence time distribution. For different operating conditions with the same specific throughput and material viscosity, the degree of fill at a specific position of the screw tends to be the same. This result needs to be interpreted against the fact that the rheology changes with screw speed. Bigio et al. [27] found a correlation between the inverse of the percent drag flow and the number of screw revolutions a tracer takes between entering and exiting an extruder. This correlation can be expressed in the following equation, which separates the effect of screw speed and feed rate on the mean residence time(t_m):

$$t_m = \frac{A}{Q} + \frac{B}{N} \qquad \textbf{(3.2)}$$

where A and B are constant for specific screw configurations. This equation was presented as a quantitative observation. Gao et al. [22] presented specific relations for the constants A and B as:

$$A = A_f * L_m + V_p \quad , \quad B = \frac{2*A_f*l_c}{(2i-1)*\pi*D*cos\theta*W*H*F_d} \qquad \textbf{(3.3)}$$

where l_c is the length of the partially filled conveying section, L_m is the length of the mixing section and melting section, V_p is the filled volume in the conveying section due to pressure back flow, i is the number of screw lobes or flights , D is the diameter of the screw, H is the

channel depth, W is the channel width . The helix angle of the conveying element is labeled θ and $F_d$is a shape factor which accounts for the aspect ratio of the channel. Among the various model parameters, the value of V_p is probably the most difficult to obtain. V_p is the fully filled volume of the conveying screw elements. The forward conveying elements near the tip of the screw are expected to be fully filled due to the resistance of the die. In some cases the screw elements prior to mixing zone are also fully filled**.** Although V_p is affected by the percent drag flow, it is simply treated as constant and assumed to be composed of the free volume of the screw elements at the die end of the extruder. Both V_p and V_m should be dependent on the material viscosity, but this is not easily addressed in the simple model presented here.

While the holdup M_2 in the completely filled section is constant, the holdup M_1 in the partially filled section varies with the operating conditions, specifically the ratio *Q/N*. In particular, the transient variation in the holdup M_1 due to changes in total feed-rate *Q* and screw speed *N* is described by the total material balance:

$$\frac{dM_1}{dt} = Q - Q_{1o} \qquad \textbf{(3.4)}$$

In the above equation, the total inlet feed-rate to this section (from the feeders) is *Q* while the total outlet mass flow rate, denoted byQ_{1o}, varies with the operating conditions, in particular the fill fraction ∅ (i.e. the fraction of the total void volume filled with the material holdup) and the screw speed *N* with the proportionality constant k depending on the screw design/geometry. When this section is only partially filled the total outlet mass flow rate at steady state [23] is given by

$$\mathrm{Q_{1o}} = \mathrm{k\emptyset N} = \frac{\mathrm{M_1 N}}{\mathrm{B}} \qquad \textbf{(3.5)}$$

Combining equations 3.4 and 3.5 gives the dynamic mass balance relation for the holdup M_1:

$$\frac{dM_1}{dt} = Q - \frac{M_1 N}{B} \qquad \textbf{(3.6)}$$

At steady state, the inlet and outlet mass flow rates are equal, i.e.$Q = \mathrm{Q_{1o}}$, and the dynamic material balance in equation 3.6 reduces to the steady state version: $M_1 = B * Q/N$. In

contrast with the partially filled section, the total holdup M_2 in the filled section is constant (since the void volume is filled to maximum capacity). Furthermore, the outlet flow rate from this filled section is always the same as the inlet flow rate, which in turn is the same as the outlet flow rate from the partially filled section, i.e. $\mathrm{Q_{1o}}$.

We denote the weight fraction of material 1 in the material holdup in the partially and completely filled sections by x_1 and x_2, respectively. At steady state, these compositions are the same and are determined solely by the feed rates Q_1 and Q_2, i.e.

$$x_i = x_1 = x_2 = \frac{Q_1}{Q_1+Q_2} \quad \textbf{(3.7)}$$

The compositions $\mathrm{x_1}$ and $\mathrm{x_2}$ in the partially and completely filled sections change due to mixing of the two raw materials in the respective sections. We use a combination of plug flow with recycle to describe the overall effect of the mixing in the partially and completely filled sections. Consider the schematic representation in Figure 3.2, where raw material is fed to the partially filled section at a total flow rate

$$\mathrm{Q = Q_1 + Q_2}$$

and composition

$$\mathrm{x_i = Q_1/(Q_1 + Q_2)}$$

exits from this section to the completely filled section at a total flow rate $\mathrm{Q_{1o}}$ and composition x_1, Mass balance at point 1 results in:

$$\mathrm{x_{1i} = \frac{Q * x_i + R_1 * Q_{1o} * x_1}{Q + R_1 * Q_{1o}}}$$

where $\mathrm{x_{1i}}$is the inlet composition and $\mathrm{R_1}$ denotes the ratio of recycle to outlet flow rate. From pure plug flow concepts (i.e. first in first out), we have

$$\mathrm{x_1\ (t) = x_{1i}(t - t_{d1})}$$

with a time delay $\mathrm{t_{d1} = \frac{M_1}{Q_{1o}}}$.

Expressing the above relations in the Laplace domain and solving for $\mathrm{x_{1i}(s)}$ yields the overall input-output relation between the inlet composition $\mathrm{x_i(s)}$ and the outlet composition $\mathrm{x_1(s)}$ as shown below [23]:

$$x_1(s) = \frac{Qe^{-t_{d1}S}}{Q+R_1*Q_{10}(1-e^{-t_{d1}S})}\ x_i(s) \qquad where \quad t_{d1} = \frac{M_1}{Q_{10}} \tag{3.8}$$

The recycle ratio R_1 is the parameter that captures the actual degree of mixing in a given screw design [23]. In particular, the case $R_1=0$, i.e. no recycle, corresponds to no mixing and on the other hand, the case with infinite recycle, i.e. $R_1=\infty$, corresponds to perfect instantaneous mixing. Similarly, the mixing in the completely filled section can be captured through a combination of plug flow and recycle to obtain the following input-output relation:

$$x_2(s) = \frac{Qe^{-t_{d2}S}}{1+R_2*(1-e^{-t_{d2}S})}\ x_1(s) \qquad where \quad t_{d2} = \frac{M_2}{Q_{10}} \tag{3.9}$$

where R_2 denotes the ratio of recycle to outlet flow rate in filled section of extruder.

3.2.1 Torque and Die Pressure Relation

The above equations (3.6, 3.1 and 3.8, 3.9) describe the dynamics for the material holdup M_1, M_2 and the compositions x_1, x_2. However, these internal state variables are not measured on-line and need to be related to the output variables that are measured, namely torque (*T)* and die pressure (DP*)*. Based on Kumar et al. [23] work simple overall relationship for the total shaft torque can be expressed in the following general form:

$$T = \alpha_0 + \alpha_1 M_1(\alpha_2 + N)x_1 + \alpha_3 M_2 N x_2 \tag{3.10}$$

The above expression for torque has three key terms, the offset and the two contributions from the partially and completely filled sections, respectively. At steady state, using the corresponding steady state relations as

$$M_1 = B * \frac{Q}{N} \quad , \quad x_i = x_1 = x_2 \, , M_2 = B$$

Equation 3.10 for the torque reduces to the following relation:

$$T = \alpha_0 + \alpha_1\alpha_2 B\frac{Q}{N}x_i + \alpha_3 ANx_i + \alpha_1 BQx_i = c_0 + c_1\frac{Q}{N}x_i + c_2 Nx_i + c_3 Qx_i \tag{3.11}$$

In this work, we tested the validity of the above relationship, using the multiple measurements of torque at various steady state operating conditions, as discussed in Chapter 5 of this thesis.

The die pressure drop relates to the volumetric flow rate, viscosity of melt and geometry of die. Equation 3.12 outlines this relation where L, *D* denote the length and diameter of the die hole, ρ is the melt density of the material and Q_0 is the flow rate of the product through the die plate and μ denotes the viscosity of the product at the prevailing temperature and shear rate at the die.

$$DP = \left\lfloor \frac{128\,L}{\pi D^4 \rho} \right\rfloor Q_0 \mu = K Q_0 \mu \qquad \textbf{(3.12)}$$

The viscosity of the product depends on the composition, temperature (*To)* in the melt zone and the shear rate on the molten product as it flows through the die plate holes. While the melt temperature *To* is measured using a thermocouple in the melt pool just before the die plate, the shear rate is considered to be proportional to the total material flow rate Q_0. Based on Kumar et al. [23], we will use the following linear approximation for the product viscosity:

$$\mu = \mu_0 + \mu_1 (xo - \overline{xo}) - \mu_2 (Q_0 - \overline{Q_0}) - \mu_3 (T_0 - \overline{T_0}) \qquad \textbf{(3.13)}$$

where ($\bar{}$) denotes respective nominal steady state values at the nominal operating point. In the above linear approximation for viscosity,μ_0 denotes the nominal viscosity at the nominal operating point, while μ_1 , μ_2, μ_3 denote the gradient of viscosity with respect to composition, shear rate and temperature, respectively at this operating point. Substituting melt viscosity from equation 3.13 in equation 3.12 yields the following relationship for die pressure:

$$DP = KQ_O \left[\mu_0 + \mu_1 (xo - \overline{xo}) - \mu_2 (Q_0 - \overline{Q_0}) - \mu_3 (T_0 - \overline{T_0}) \right]$$

Or written in a compact form

$$DP = \beta_1 Q_0 + \beta_2 Q_0 \Delta x_0 - \beta_3 Q_0 \Delta Q_0 - \beta_4 Q_0 \Delta T \qquad \textbf{(3.14)}$$

In which

$$\beta_1 = K\mu_0 \quad \& \quad \beta_2 = K\mu_1 \qquad \textbf{(3.15)}$$

This simple equation (3.15) between μ_0 , $\mu_1$and β_1 , β_2 involves only the calibration parameter K. The flow model that has been explained in this chapter was amended and adapted for this work to inferentially estimate the melt viscosity (or accordingly the melt volume flow rate (MVR)) from the die pressure parameters and to identify the source of variability in the compounding of PC/PBT with the twin screw extruder. Details of the amendments and adaptations to the flow model and results are explained in chapter 5 and 6 of this thesis.

Chapter 4
Experiments

The experiments described in this chapter were all carried out on a WP ZSK 58 mm co-rotating extruder at the compounding facility of SABIC Innovative Plastics in Cobourg, Ontario. The materials used were from the commercial Xenoy® family of PC/PBT blends. In all, three sets of experiments were completed.

In the first set of experiments, the primary objectives were to: (i) obtain a basic understanding of the compounding process and identify the main factors/variables affecting the properties of PC/PBT blends and (ii) obtain an initial assessment of the levels of these factors that result in optimal process response in terms of product MVR and impact strength. To address this, a central composite design was used with a response surface methodology (RSM) as explained in section 4.1.

In the next set of experiments, the main objective was to evaluate the flow model derived earlier in chapter 3 of this thesis, to estimate the parameters in the torque and die pressure correlations and to examine the capability of the model for fault identification by employing blend composition changes. To address this objective, we used a 2-level factorial design in which the factors studied were screw speed, and PC and PBT flow rates. The factorial design and experimental set up for these experiments are explained in section 4.2.

Finally, a third set of verification experiments was carried out to test the validity of the model and its parameters. In addition, the ability of the model to diagnose variations in incoming raw material was tested. In this experiments the only variable was the composition of the PC feed stream. This stream was composed of two PC materials of high and low viscosity respectively. The ratio of these two materials was varied in blind experiments which were analyzed with the developed model. These experiments explained in section 4.3. Testing procedures for product properties are described in section 4.4.

4.1 First Set of Experiments- Central Composite Design

Response surface methodology (RSM) is a collection of mathematical and statistical techniques that are useful for the modeling and analysis of problems in which a response of interest is influenced by several variables and the objective is to optimize this response [28]. For example, to find the levels of screw speed (N) and feed rate (Q) that effect the melt volume flow rate (MVR) of the PC/PBT blends. In this case MVR would be a function of the levels of screw speed and feed rate that is:

$$MVR = f(N, Q) + \epsilon$$

where ε represents the noise or error observed in response MVR. If we denote the expected response by $(MVR) = f(N, Q) = \eta$, then the surface represented by η is called a response surface. In most RSM problems, the form of the relationship between the response and the independent variables is unknown. Thus, the first step is to find a suitable approximation for the true functional relationship. Usually, a polynomial model will be a reasonable approximation of the true functional relationship for a relatively small region. The design discussed in this section pertains to the estimation of response surfaces, following the general model equation [28]:

$$y = \beta_0 + \sum_{i=1}^{k} \beta_i x_i + \sum_{i=1}^{k} \beta_{ii} {x_i}^2 + \sum_{i<j} \sum \beta_{ij} x_i x_j + \epsilon$$

This general fitting model includes the observed values of the dependent variable y, main effects for factors (x_i), their interactions and their quadratic components. Fitting and analyzing response surface is greatly facilitated by the proper choice of an experimental design. Central composite design (CCD) is the most popular class of design used for fitting these models. Generally, CCD consists of a 2^kfactorial and 2k axial or star runs, which are augmented with center runs [28]. A typical coded CCD matrix with 3 factors, 6 star runs, and 6 center point is presented in table 4.1. The central composite design can be used to fit the data to the general model described above. One consideration for choosing standard central

composite designs is to find a design that is orthogonal, i.e., the sum of the products of column elements of the design matrix within each row is equal to zero.

Table 4.1: Variables of CCD design (coded)

Run order	x_1	x_2	x_3
15	-1	-1	-1
9	1	-1	-1
4	-1	1	-1
6	1	1	-1
14	-1	-1	1
13	1	-1	1
5	-1	1	1
18	1	1	1
8	-1.68179	0	0
16	1.68179	0	0
7	0	-1.68179	0
17	0	1.68179	0
2	0	0	-1.68179
10	0	0	1.68179
12	0	0	0
1	0	0	0
19	0	0	0
20	0	0	0
3	0	0	0
11	0	0	0

In this study, CCD consists of a 2^3 factorial in which factors are chosen as the total feed rate (kg/hr), the screw speed (rpm) and the die temperature (℃). The axial distance was chosen as 1.68179, and the design is augmented with 6 center points. These factors are coded as:

$x_1 = (feed\ rate - 400)/50$, total feed rate levels (350, 450)

$x_2 = (screw\ speed - 410)/40$, screw speed levels (370, 450)

$x_3 = (die\ temperature - 282)/5$, die temperature levels (277, 287)

The dependent variables monitored include the motor load, specific energy consumption, melt temperature, MVR and impact strength. The coded central composite design matrix has been presented in table 4.1. Table 4.2 presents of the uncoded design where Q is feed rate (Kg/hr), and N is screw speed (rpm).

As indicated earlier, these experiments were carried out at the SABIC Innovative Plastics, Cobourg plant, using a WP 58mm twin-screw extruder, with two feeders and a data acquisition system. The extruder was capable of running at a maximum screw speed of 620rpm. The extruder was powered by a 250HP drive, which provided a measurement of total screw load (estimated from motor current and voltage) and screw speed. The extruder had 9 thermocouples along the barrel length, 3 thermocouples along the die and heating elements to control the temperatures in the corresponding barrel zones. The signals for the machine variables were recorded using a data acquisition system. In this study, load, feed rates, screw speed, and melt temperature and water bath temperature was recorder at a sampling rate of 0.033 Hz. The material used was a blend of PC/PBT from the Xenoy® family. Polymer samples were collected during each runs. A total of 100 samples were collected at time intervals of 5, 10, 15, and 20 minutes for each run. The results of this experiment have been explained in appendix A of this thesis.

Table 4.2: Variables of CCD design (uncoded)

Run	Q(kg/hr)	N (rpm)	Temperature (°c)
1	400	410	292
2	450	450	290
3	400	343	285
4	400	477	293
5	400	410	290
6	450	400	291
7	350	450	291
8	350	370	286
9	400	410	289
10	350	370	300
11	484	420	295
12	400	410	290
13	400	410	289
14	450	400	290
15	450	450	294
16	350	450	293
17	400	410	291
18	316	410	291
19	400	410	305
20	400	410	296

4.2 Second Set of Experiments- Factorial Design

As explained in chapter 3 of this thesis, in the flow model for twin screw extruder, internal variables (i.e., material holdups and the compositions) are related to the output variables (i.e., torque and die pressure). Details of this relation between internal and output variables have been outlined in equations 3.10 and 3.14. These equations have machine, screw, materials and processing conditions related parameters that need to be determined. To address this and also to examine the validity of the flow model for TSEs, a factorial design was used. In this section the factorial design and experimental set- up are explained.

4.2.1 2^3 Factorial Design

A 2^3 $f$actorial design provides the smallest number of runs for which 3 factors can be studied in a complete factorial design because there are only two levels for each factor. In this study, the three factors were screw speed, PC flow rate (feeder 1) and PBT flow rate (feeder 2), each at two levels. These levels were approximately 10 % from the nominal conditions which were used as the center point. The design was augmented with 5 replicate runs at the center point. This design was run on two consecutive days as shown in tables 4.3 and 4.4. Due to machine experiment limitation, some of the combinations of the levels were not feasible and were adjusted to practical levels combination. These amended combinations are specified with red color numbers in Table 4.3 and 4.4.

In these experiments the load, die pressure, feed-rates, and screw speed were recorded at a sampling rate of 2 Hz. The die used on the first day had 17 holes each with 4 mm diameter and the die used on the second day had 17 holes but each with 3 mm diameter. The material used was again a Xenoy ® blend. Polymer samples were collected during each run. A total of 143 samples were collected on the first day at intervals of 0.5 , 1 , 1.5 , 2 , 2.5 , 3 , 3.5 , 4 , 9 , 14 and 19 minutes for each run. On the second day, a total of 156 samples were collected at intervals of 0.5 , 1 , 1.5 , 2 , 2.5 , 3 , 3.5 , 4 , 6 , 8 , 10 and 15 minutes for each run.

Table 4.3: DOE for day 1 experimental runs (die hole diameter = 4 mm)

Run Order	Screw Speed N (rpm)	Feed Rate Q (Kg/hr)	Feeder PC X1	Feeder PBT X2
1	410	425	0.61	0.39
2	451	434	0.66	0.34
3	451	383	0.61	0.39
4	410	425	0.61	0.39
5	369	383	0.61	0.39
6	410	425	0.61	0.39
7	369	434	0.66	0.34
8	451	468	0.61	0.39
9	410	425	0.61	0.39
10	451	416	0.56	0.44
11	400 **(410)**	468	0.61	0.39
12	400 **(369)**	416	0.56	0.44
13	410	425	0.61	0.39

Table 4.4: DOE for day 2 experimental runs (die hole diameter = 3 mm)

Run Order	Screw speed N(rpm)	Feed Rate Q (Kg/hr)	Feeder PC X1	Feeder PBT X2
1	410	425	0.61	0.39
2	451	434 **(456)**	0.63	0.34
3	451	383	0.61	0.39
4	410	425	0.61	0.39
5	369	383	0.61	0.39
6	410	425	0.61	0.39
7	369 **(390)**	434	0.66	0.34
8	451	468	0.61	0.39
9	410	425	0.61	0.39
10	451	416	0.56	0.44
11	400 **(451)**	468	0.61	0.39
12	400 **(369)**	416	0.56	0.44
13	410	425	0.61	0.39

4.3 Third Set of Experiments

The flow model that has been described in chapter 3 has unknown parameters which were estimated using data from the second set of experiments. In order to verify the validity of the estimated model parameters, a third set of experiments were performed. In addition, another purpose of these experiments was to examine the capability of the developed model in fault identification introduced by raw material variation.

In these experiments, screw speed, total feed rate and the total feed rate of PC (feeder 1) and PBT feed rate (feeder 2) were kept constant for all 8 runs. The only variable that was manipulated was the composition of PC material. Table 4.5 shows details of these experimental runs. These experiments were run randomly without any notice. In this table, Q is the total feed rate, N is the screw speed , Q(pc) is the total feed rate of polycarbonate in feeder 1 , Q(PBT) is the total feed rate of PBT in feeder 2 , X(PC1) is the weight fraction of polycarbonate type 1 in feeder 1 , and X(PC2) is the weight fraction of poly carbonate type 2 in feeder 1.

The experimental set up for these experiments were similar to one that was described in the second set of experiments. The die used had 17 holes each with 3 mm diameter. The material used was the same Xenoy® resin. A total of 32 polymer samples were collected at intervals of 1, 5, 10, and 15 minutes for each run.

Table 4.5: Third set of experiments (die hole diameter = 3 mm)

Run #	Q (Kg/hr)	N (rpm)	Q (PC) Kg/hr feeder1	Q(PBT) Kg/hr feeder2	XPC in feeder 1	XPBT in feeder 2	X(pc1) in feeder 1	X(pc2) in feeder1
1	425	410	259.25	165.75	0.61	0.39	0.428	0.389
2	425	410	259.25	165.75	0.61	0.39	0.428	0.389
3	425	410	259.25	165.75	0.61	0.39	0.478	0.339
4	425	410	259.25	165.75	0.61	0.39	0.378	0.439
5	425	410	259.25	165.75	0.61	0.39	0.428	0.389
6	425	410	259.25	165.75	0.61	0.39	0.328	0.389
7	425	410	259.25	165.75	0.61	0.39	0.528	0.489
8	425	410	259.25	165.75	0.61	0.39	0.428	0.289

4.4 Sample Testing Procedures

Plastic compound manufacturers use several tests to measure the quality of compounds and to specify the most suitable end use of a particular grade of the polymer. Two of the most important physical properties are melt flow rate, and impact strength which are measured in this study. A description of each physical property and the method of testing are presented in this section which also can be found in ASTM standards.

4.4.1 Melt Volume-Flow Rate (MVR)

The Melt Flow Index (MFI) was specified as a standard rheological quality control test in the ISO, BS, and ASTM. Selecting the appropriate conditions including temperature and load is necessary when using the test method for polymers. Despite the fact that melt flow index is an empirically defined parameter with certain limitations, it is still one of the most popular parameters in the plastics industry for distinguishing various grades of polymers. Polymer process ability, the physical, mechanical and thermal properties could be related with the MFI. For instance, increasing melt flow rate could result from decrease in viscosity and can cause decrease in hardness [29]. Melt flow rate is a single point viscosity measurement at relatively low shear rate and temperature.

Melt flow index (MFI) is basically defined as the weight of the polymer (g) extruded in 10 min through a capillary of specific diameter and length by the specific pressure applied under the specific temperature conditions. ASTM D1238 [30] specifies the details of the test conditions. In this work, the SABIC Innovative Plastics standard was used for conducting melt flow index tests on PC/PBT blends. That is, samples were preheated for 2 hr @ 120 ℃. Plastometer temperature was set at 250 °C. Load used was 4.9 kg with the die diameter of 0.0827 inches. The time interval for the test was chosen as 390 seconds. The amount of polymer collected after a specific interval is weighed and normalized to the number of grams that would have been extruded in 10 minutes. Furthermore, test results have been reported by melt volume flow rate (MVR) which is MFI divided by polymer melt density. That is:

MVR (cm^3/10 min) = MFI (g/10 min) / $\rho(\frac{g}{cm^3})$

4.4.2 Impact Strength

Impact strength test can be used as a quality control check for the estimation of toughness of specimens. In this test, a pendulum hammer is released from a predefined height striking a specimen which is clamped in a vice. The difference in the drop height and return height relates to the energy to break the test specimen. The test results depend on temperature, test bars dimensions and notching of the specimen. One of the prevalent methods is Izod impact method. Sometimes, Izod specimens are notched. The unnotched Izod test uses the same loading geometry with the exception that there is no notch cut into the specimen. The standard specimen for ASTM D256 [31] is 64 x 12.7 x 3.2 mm (2½ x ½ x 1/8 inch) and the result is expressed in J/m or ft-lb/in which is calculated by dividing impact energy in J (or ft-lb) by the thickness of the specimen.

Chapter 5
Model Parameter Identification

In chapter 3, a simple overall relationship for the total torque as a function of mass holdups (M_1, M_2) ,compositions (x_1,x_2) and the screw speed (N) in partially and completely filled sections of a twin screw extruder was presented in equation (3.10) :

$$T = \alpha_0 + \alpha_1 M_1(\alpha_2 + N)x_1 + \alpha_3 M_2 N x_2 \quad \textbf{(3.10)}$$

In this expression $\alpha_1 M_1(\alpha_2 + N)x_1$ and $\alpha_3 M_2 N x_2$ are contributions from the partially and completely filled sections of the screw. The validity of the above relationship for torque was tested using multiple measurements of torque at various steady state operating conditions and will be explained in section 5.1 of this chapter.

In chapter 3, equation 3.14 was developed which shows the linearized equation for die pressure as a function of flow rate of the molten compound through the die plate, the composition of the feed, and the temperature in the melt zone.

$$DP = \beta_1 Q_0 + \beta_2 Q_0 \Delta x_0 - \beta_3 Q_0 \Delta Q_0 - \beta_4 Q_0 \Delta T \quad \textbf{(3.14)}$$

These models for torque and die pressure in twin screw extruders have parameters that depend on the specific extruder geometry and the product properties and need to be identified from measured input/output data. These parameters can be categorized into two sets. The first set consisting of the parameters A and B (equations 3.1 and 3.6) depend on the specific screw and die geometry and will be invariant once the extruder screw and die geometry is fixed. The second set consisting of the parameters α_i and β_i depend on the particular process conditions and change from one product grade to another and these parameters need to be identified depending on the operating conditions. The torque model parameters were estimated using the Levenberg Marquardt Algorithm (LMA). Details of the torque model

parameter estimation method and results are given in section 5.2. The die pressure model parameters were estimated and adapted using recursive least-squares parameter estimation methods (LSPE) as shown in section 5.3.

5.1 Torque Model at Steady State

The latter two terms in equation 3.10 for torque depend on the respective holdups and compositions and the screw speed. At steady state using the corresponding steady state relations for the holdups (i.e. $M_1 = B * Q/N$ and $x_i = x_1 = x_2$), the equation for torque reduces to:

$$T = \alpha_0 + \alpha_1\alpha_2 B\frac{Q}{N}x_i + \alpha_3 ANx_i + \alpha_1 BQx_i = c_0 + c_1\frac{Q}{N}x_i + c_2 Nx_i + c_3 Qx_i \qquad \textbf{(3.11)}$$

The validity of the steady state relation for torque was tested during a two-day long trial in which input-output data were collected for feed-rates (Q1,Q2), screw speed (N) , composition of polycarbonate (PC) and torque at various steady state conditions. The experimental methods for these experiments have been explained in section 4.2 of this thesis. Table 5.1 presents experiment results at steady state for day 1 and day 2 of the second set of experiments. In this table X1 is weight fraction of PC in the feed and X2 is the weight fraction of PBT. Since torque measurements were not available, we used motor load data instead of torque. The method of least squares was used to estimate the regression coefficients in the torque model. We first fitted equation 3.11 using all 26 runs for two days. Table 5.2 presents Minitab output for 26 load data. From this table, the difference between the load observation and the fitted value (i.e. residual) corresponding to observation 14 (run 2.1) is -5.246 and the standardized residual corresponding to this run is -3.18. This large residual may indicate a possible outlier or unusual observation. Since run 2.1 denotes an observation with a large standardized residual, we refitted equation 3.11 after deleting this unusual observation to determine its effect on the regressors. Table 5.3 represents the computer output for 25 load data. The upper part of the table contains the numerical

estimates of the regression coefficients. R-sq -the coefficient of multiple determinations – which is defined as:

$$R^2 = \frac{SS_R}{SS_T}$$

is a measure of the amount of variability in load explained. In this equation, SS_R denotes the sum of squares regression and SS_T denotes the total sum squares. The coefficient of multiple determination for the regression model fit to the load data is R^2=94.9%. That is, about 94.9% of the variability in load has been explained when the three variables, Q/N*X1, N*X1 and Q*X1 are used. However, a large value of R^2=94.9% does not necessarily imply that the regression model is a good one. Residuals analysis is the best way to examine the fit of the model. The residual analysis did not show any irregular patterns. We also examined the adjusted R^2 statistic which is defined as [28]:

$$R^2(adj) = 1-(\frac{n-1}{n-p})*(1- R^2)$$

Here n denotes total number of observations and p denotes number of parameters in fitting regression models. In general, the adjusted R^2 statistic will not always increase as variables are added to the model. The adjusted R^2 for the load model in table 5.3 is computed as 94.1% which is very close to the ordinary R^2.

The lower portion of table 5.3 provides the test for significance of regression. Since the P-value is considerably less than 0.05 %, we conclude that the load model is significant. However, this does not necessarily imply that the relationship found is an appropriate model for predicting load as a function of input variables. We also carried out testing on the individual regression coefficient to determine model adequacy. For example, the model might be more effective with the inclusion of additional variables, or perhaps with the deletion of one or more of the regressors presently in the model. Testing hypotheses on the individual regression coefficient has been showed in the upper portion of Table 5.3. The test statistic for this hypothesis is defined by [28]:

$$T_0 = \frac{the\ regression\ coefficient - 0}{standard\ error\ of\ the\ coefficient}$$

The upper portion of Table 5.3 gives the least squares estimate of each parameter, the standard error (SE Coef), the t statistic, and the corresponding P-value. From this analysis, we would conclude that variables Q/N*X1, N*X1 and Q*X1 contribute significantly to the load model.

Table 5.1: Experiment results from the second set of experimental runs

Run	N	Q1	Q2	X1	X2	Q/N*X1	N*X1	Q*X1	% Load
1.1*	410.27	259.32	165.76	0.6102	0.39	0.6321	250.336	259.324	88.12
1.2	450.65	286.5	147.55	0.6601	0.34	0.6357	297.492	286.499	84.05
1.3	451.31	233.63	149.36	0.61	0.39	0.5177	275.291	233.625	75.92
1.4	410.27	259.32	165.76	0.6102	0.39	0.6321	250.336	259.324	87.61
1.5	368.88	233.65	149.41	0.61	0.3901	0.6334	225.032	233.649	88.33
1.6	410.27	259.32	165.76	0.6102	0.39	0.6321	250.336	259.324	86.89
1.7	369.08	286.59	147.59	0.6603	0.3401	0.7765	243.718	286.589	95.19
1.8	450.78	285.43	182.59	0.6099	0.3902	0.6332	274.924	285.429	89.24
1.9	410.27	259.32	165.76	0.6102	0.39	0.6321	250.336	259.324	86.83
1.10	451.31	232.91	183.05	0.5604	0.4404	0.5161	252.9	232.913	81.92
1.11	410.26	285.44	182.54	0.6099	0.39	0.6958	250.22	285.438	96.48
1.12	369.01	232.95	183.05	0.56	0.44	0.6313	206.633	232.949	94.28
1.13	410.27	259.32	165.76	0.6102	0.39	0.6321	250.336	259.324	89.06
2.1*	410.201	259.269	165.753	0.61	0.39	0.6321	250.241	259.269	83.71
2.2	451.255	286.472	169.292	0.6282	0.3713	0.6348	283.491	286.472	86.50
2.3	449.611	235.36	150.377	0.6145	0.3926	0.5235	276.294	235.36	77.25
2.4	410.201	259.269	165.753	0.61	0.39	0.6321	250.241	259.269	88.93
2.5	368.752	233.641	149.351	0.61	0.39	0.6336	224.949	233.641	88.89
2.6	410.201	259.269	165.753	0.61	0.39	0.6321	250.241	259.269	89.95
2.7	390.423	286.48	147.597	0.6601	0.3401	0.7338	257.715	286.48	95.02
2.8	451.213	285.565	182.66	0.6102	0.3903	0.6329	275.322	285.565	90.63
2.9	410.201	259.269	165.753	0.61	0.39	0.6321	250.241	259.269	89.76
2.10	450.434	232.941	183.085	0.56	0.4401	0.5171	252.223	232.941	83.27
2.11	450.546	285.509	182.526	0.6101	0.39	0.6337	274.861	285.509	91.59
2.12	368.762	233.011	183.014	0.5601	0.4399	0.6319	206.552	233.011	96.12
2.13	410.201	259.269	165.753	0.61	0.39	0.6321	250.241	259.269	90.47

1.1* Means Run number 1 from day 1 of the second set of experimental runs at the SABIC Innovative Plastics plant

2.1* Means Run number 1 from day 2 of the second set of experimental runs at the SABIC Innovative Plastics plant

Table 5.2* Regression Analysis: Load versus Q/N*X1, N*X1, Q*X1

The regression equation using data from day 1 and day 2 of the second set of experimental runs is
Load = 98.3 - 25.6 Q/N*X1 - 0.308 N*X1 + 0.324 Q*X1

Predictor	Coef	SE Coef	T	P
Constant	98.333	7.789	12.62	0.000
Q/N*X1	-25.56	16.49	-1.55	0.135
N*X1	-0.30836	0.04127	-7.47	0.000
Q*X1	0.32378	0.05491	5.90	0.000

S = 1.681 R-Sq = 90.8% R-Sq(adj) = 89.5%

Analysis of Variance

Source	DF	SS	MS	F	P
Regression	3	610.73	203.58	72.06	0.000
Residual Error	22	62.15	2.82		
Total	25	672.88			

Source	DF	Seq SS
Q/N*X1	1	434.37
N*X1	1	78.13
Q*X1	1	98.23

Unusual Observations

Obs	Q/N*X1	Load	Fit	SE Fit	Residual	St Residual
14	0.632	83.710	88.958	0.334	-5.246	-3.18R

*In all statistical tables presented in this thesis Coef, SE, SS, MS, T, P, and Obs are corresponding as:

Coef	:	the least squires estimate of each parameter
SE	:	Standard Error
SS	:	Sum of Squares
MS	:	Mean Square
T	:	the t statistic
P	:	P-value corresponding P-value
Obs	:	observation

Table 5. 3 Regression Analysis: Load versus Q/N*X1, N*X1, Q*X1

The regression equation using data from day 1 and day 2 of the second set of experimental runs deleting unusual observation (2.1) is
Load = 98.8 - 25.7 Q/N*X1 - 0.311 N*X1 + 0.325 Q*X1

Predictor	Coef	SE Coef	T	P
Constant	98.833	5.853	16.89	0.000
Q/N*X1	-25.71	12.39	-2.07	0.049
N*X1	-0.31055	0.03101	-10.02	0.000
Q*X1	0.32515	0.04125	7.88	0.000

S = 1.263 R-Sq = 94.9% R-Sq(adj) = 94.1%

Analysis of Variance

Source	DF	SS	MS	F	P
Regression	3	617.41	205.80	129.10	0.000
Residual Error	21	33.48	1.59		
Total	24	650.89			

Source	DF	Seq SS
Q/N*X1	1	437.98
N*X1	1	80.37
Q*X1	1	99.06

In particular, the model parameters in equation 3.11 were fitted using the data from day 1 experiments, and subsequently the results were tested by predicting day 2 load data. Table 5.4 represents output of the regression analysis for load from day 1 experimental runs at the SABIC Innovative Plastics with the coefficient of multiple determination of R^2=97%. The regression equation obtained from day 1 data was used to predict the load for the second day. The results showed that the model validates very well against the measured load data with an overall R^2 value of 91.8 %. Figure 5.1 shows the comparison of the measured and predicted load for steady state points obtained on two separate days.

Table 5. 4 Regression Analysis: Load versus Q/N*X1, N*X1, Q*X1

```
The regression equation using data from day 1 of the second experimental runs is
Load = 96.3 - 24.8 Q/N*X1 - 0.301 N*X1 + 0.320 Q*X1

Predictor        Coef     SE Coef          T        P
Constant       96.285       6.681      14.41    0.000
Q/N*X1         -24.75       14.89      -1.66    0.131
N*X1         -0.30056     0.03601      -8.35    0.000
Q*X1          0.32024     0.05066       6.32    0.000

S = 1.103       R-Sq = 97.0%     R-Sq(adj) = 96.0%

Analysis of Variance

Source            DF          SS          MS         F        P
Regression         3      356.14      118.71     97.64    0.000
Residual Error     9       10.94        1.22
Total             12      367.08

Source       DF      Seq SS
Q/N*X1        1      258.69
N*X1          1       48.87
Q*X1          1       48.57
```

Figure 5.1: Comparison of predicted load versus measured load

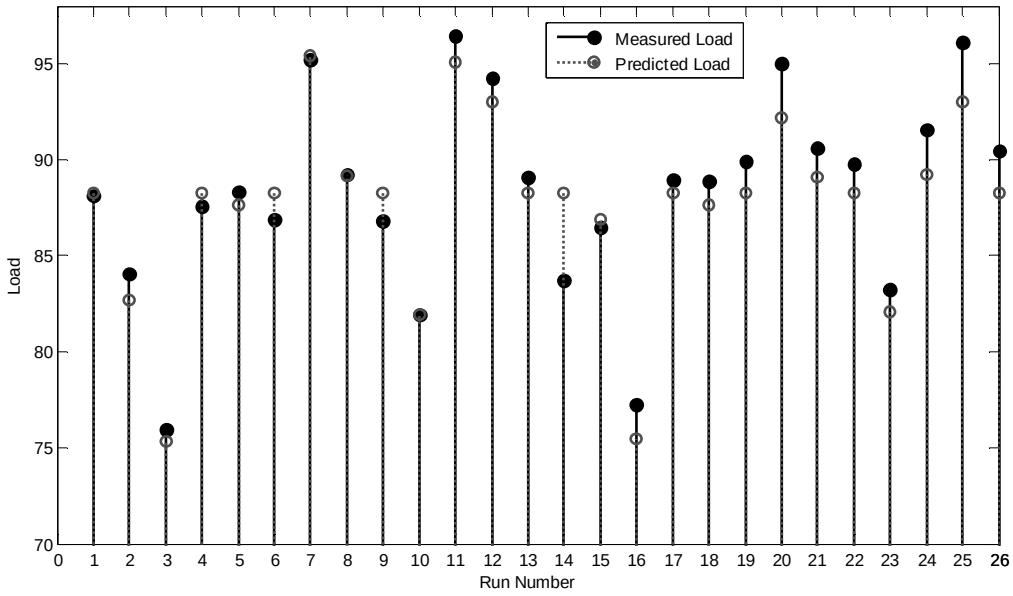

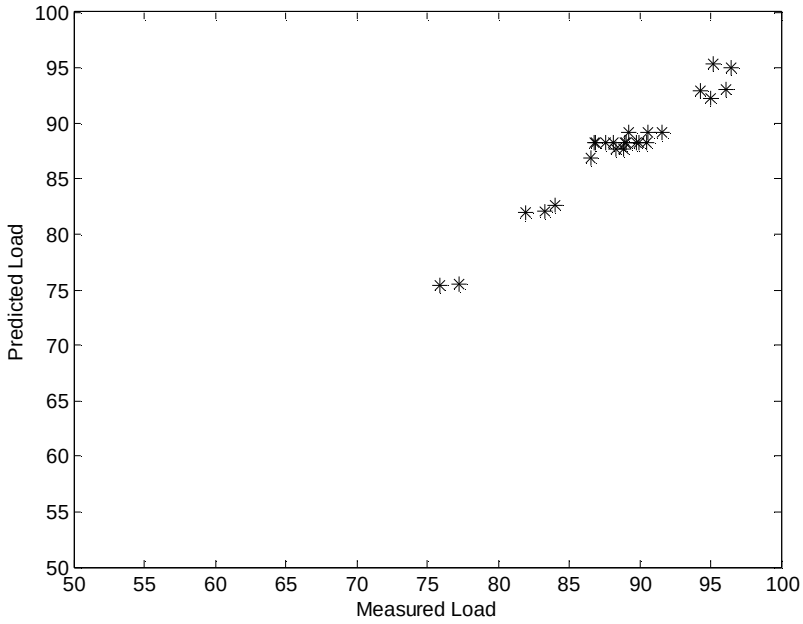

5.2 Torque Model Parameters Estimation using Levenberg Marquardt Algorithm

The torque model in equation 3.10 has several unknown parameters, which need to be identified for specific applications based on input-output measurements from experiments. However, the identification of these parameters is greatly simplified by grouping the parameters into machine-dependent and process condition-dependent sets. The former set of parameters need to be identified only once for a given extruder geometry, while the latter set of parameters will, in general, vary depending on the process conditions.

Input-output measurements from experiments were used to calculate the weight fraction of polycarbonate (PC) in a partially filled section of screw (x_1) and in a fully filled section of screw (x_2). As presented in figure 5.2, it seems that the weight fraction of PC in the partially and the fully filled section of the screw immediately becomes the same as the weight fraction of PC at the inlet (x_i) in any experiment.

Figure 5.2: Weight fraction of PC in feed composition, partially and fully filled section of the extruder, day 1 of the second set of experimental runs

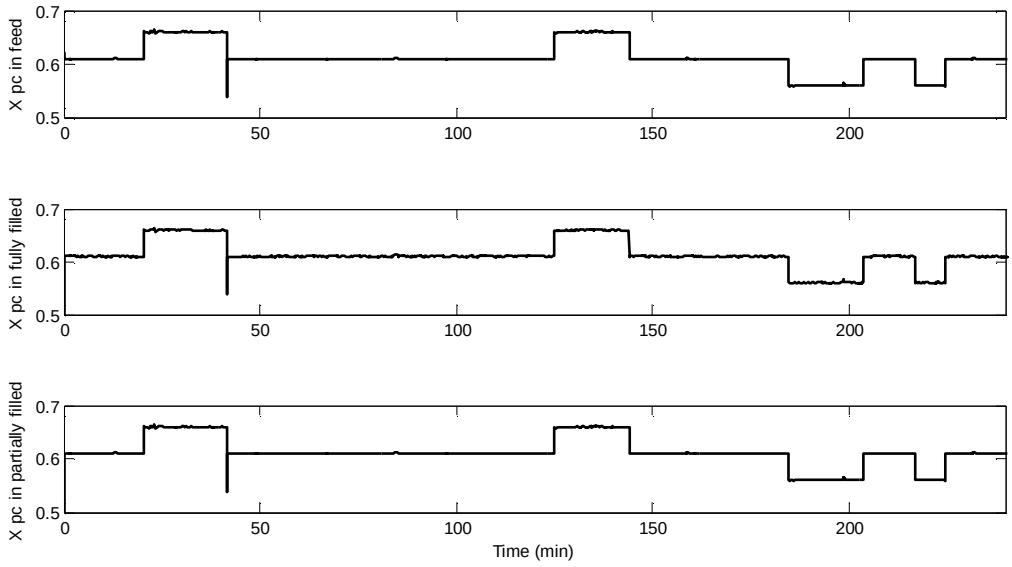

Assuming $x_i = x_1 = x_2$ and substituting M_2 =A in equation 3.10, yields

$$T = \alpha_0 + \alpha_1 * M_1 * (\alpha_2 + N)x_i + \alpha_3 ANx_i \quad \textbf{(5.1)}$$

As noted previously, the mass hold up (M_1) in the partially filled section of the screw is

$$\frac{dM_1}{dt} = Q - \frac{M_1 N}{B} \quad \textbf{(3.6)}$$

Rearranging the equation and taking the Laplace transform of both sides of the equation yields

$$\text{s } M_1(s) - M_1(0) + \frac{N}{B} M_1(s) = \text{Q/s} \quad \textbf{(5.2)}$$

Solving for $M_1(s)$ yields

$$M_1(s) = (M_1(0) * s + Q) / (s * (s * B + N)) \text{ *B} \quad \textbf{(5.3)}$$

Taking the inverse Laplace transform to find the general solution yields

$$M_1(t) = \frac{\left((M_1(0) * N - BQ)e^{-\frac{Nt}{B}} + BQ\right)}{N} \quad \textbf{(5.4)}$$

Finally, substituting $M_1(t)$ in equation 5.1, the torque model leads to Eq 5.5. In this equation $M_1(0)$ is the initial value of M_1.

$$T = \alpha_0 + \frac{\alpha_1 * \left((M_1(0) * N - BQ)e^{-\frac{Nt}{B}} + BQ\right)}{N} * (\alpha_2 + N)x_i + \alpha_3 ANx_i \quad \textbf{(5.5)}$$

The Levenberg Marquardt Algorithm (LMA) was used for estimation of A, B and α_i in the torque model**.** The Levenberg Marquardt Algorithm provides a solution to the problem of minimizing a nonlinear function, over a space of parameters of the function. The LMA in many cases finds a solution even if it starts very far off the minimum. The LMA algorithm is an iterative procedure in which initial guesses for the parameters have to be provided by the user. In each iteration step, the parameter vector is replaced by a new estimate and a damping factor is adjusted at each iteration. If a retrieved step length or the reduction of sum of squares to the latest parameter vector falls short to predefined limits, the iteration is aborted and the last parameter vector is considered to be the solution [32].

In this study, a Matlab M-file was written to estimate parameters A, B and α_i in the torque equation using the Levenberg Marquardt algorithm. This M-file is attached in appendix C of this thesis. An initial guess of all the parameters is obtained through off-line least squares fit using the measured input-output data. Various runs from day 1 and day 2 of the second set of experimental runs were used to estimate torque parameters. Estimated parameters A, B and α_i in the torque model from multiple runs with various operating conditions process (different screw speed and feed rates) have been summarized in Table of 5.5. We also verified the accuracy of the estimated parameters using actual recorded input/output data from the third set of experiments. Table 5.6 shows estimated torque parameters using data from the third set of experiments. It confirms that parameters α_i especially parameters α_1 and α_3 depend on the particular process conditions, i.e. they change depending on the operating conditions process and need to be updated using LMA. The parameters *A, B* depend on the specific screw and die geometry and are invariant once the extruder screw and die geometry are fixed. Figure 5.3 shows the comparison of measured torque with the torque predicted using the observed estimated parameters for a representative run (run 2) from the third set of experimental runs.

Table 5.5: Summary of estimated parameters A, B and α_i from multiple runs
(2nd set of experiments)

A	B	α_0	α_1	α_2	α_3	Run #
12.9892	24.1669	90.0105	-0.00187	46.6106	0.002653	1.9
13.0134	24.1427	89.9866	0.003091	46.5863	-0.00744	1.1
13.0043	23.9957	89.9957	0.001505	46.5957	-0.00351	1.13
13.0021	23.8417	89.9979	0.000907	46.598	-0.00265	1.4
12.9957	24.0043	90.0043	-0.00029	46.6043	0.000211	2.4
12.9908	24.0596	90.0092	-0.00111	46.6092	0.002387	2.6
12.995	24.005	90.005	-0.0003	46.605	0.000562	2.9

Table 5.6: Verification of estimated parameters A, B and α_i from multiple runs
(3rd set of experiments)

A	B	α_0	α_1	α_2	α_3	Run #
13.0101	24.146	89.9899	0.00178	46.5897	-0.00569	Run 1
12.9963	24.0037	90.0037	-0.00086	46.6037	0.000305	Run 2
13.0103	24.1458	89.9897	0.002199	46.5894	-0.00558	Run 3
13.0035	23.9965	89.9965	0.00077	46.5965	-0.00272	Run 6
12.9989	23.3761	90.0011	7.32E-05	46.6012	-0.00064	Run 8
13.0005	24.1557	89.9994	0.000331	46.5994	-0.00136	Run 9
12.9854	24.1707	90.0143	-0.00262	46.6143	0.004972	Run 10

Figure 5.3: Comparison of measured and predicted load using estimated parameters

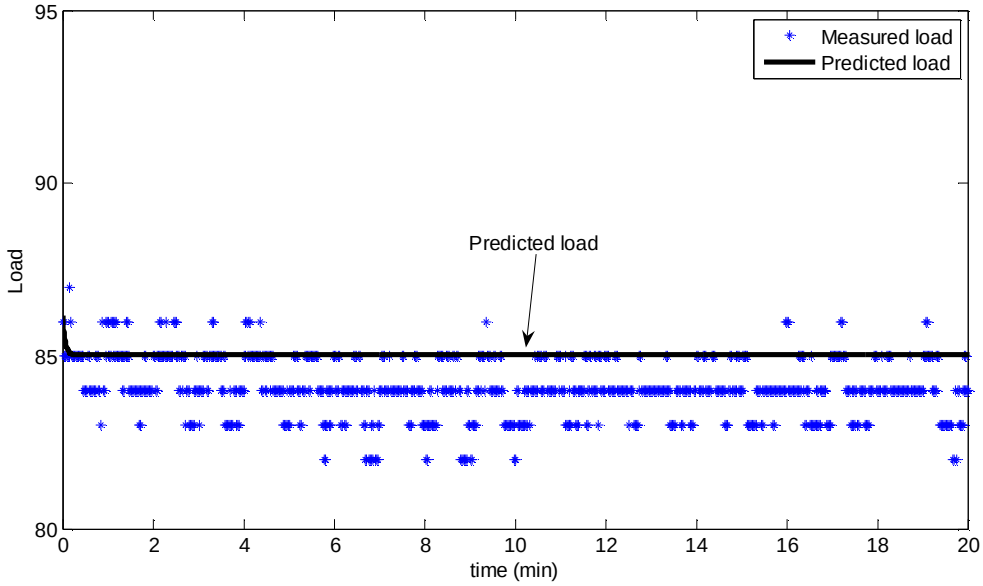

5.3 Die Pressure Parameters Identification

The die pressure relation in equation 3.14 involves unknown parameters β_i that need to be identified from measured input-output data. These parameters will in general vary, due to variations in process conditions, raw materials, composition, etc., and need to be identified on-line.

$$DP = \beta_1 Q_0 + \beta_2 Q_0 \Delta x_0 - \beta_3 Q_0 \Delta Q_0 - \beta_4 Q_0 \Delta T \quad \textbf{(3.14)}$$

One of the important features of this equation is that it relates changes in process inputs such as feed rate, and materials composition to changes in process output such as die pressure. In addition, the parameters β_i have a physical significance owing to their relationship to the melt viscosity of the compound or equivalently the melt volume flow rate. This relation of β_i with melt flow rate will be explained in chapter 6 of this thesis. Another important feature of this equation is that it is linear with respect to the parameters β_i. This linearity with respect to parameters allows use of on-line recursive adaptation techniques. In this study for identification of the parameters, we provided excitation to the system via variation in the inputs (feed-rates and screw speed) and recorded the corresponding die pressure measurement with sampling frequency of 2 Hz as explained in section 4.2 of this thesis. In this section, the method of recursive adaptation for identification of the die pressure parameters will be explained.

5.3.1 Recursive Parameter Estimation (RPE)

The method for computing online model parameters is called recursive parameter estimation. The general recursive identification algorithm is given by the following equation:

$$\hat{\beta}(t) = \hat{\beta}(t-1) + K(t)*[DP(t) - \widehat{DP}(t)] \quad \textbf{(5.6)}$$

$\hat{\beta}(t)$ is the parameter estimate at time *t*. DP*(t)* is the observed die pressure at time *t* and $\widehat{DP}(t)$ is the prediction of DP*(t)* based on observations up to time *t-1*. The gain, *K (t)*, determines how much the current prediction error [DP *(t)* - $\widehat{DP}(t)$] affects the update of the parameter

estimate. The estimation algorithms minimize the prediction-error term [DP *(t)* - $\widehat{DP}$(t)]. The gain has the following general form:

$$K(t) = q(t) * \psi(t) \quad \textbf{(5.7)}$$

The specific form of ψ(t) in the linearized die pressure model having ommitted the last two terms is :

$$\psi(t) = [Q(t) \;\; Q(t)\Delta x(t)]^T \quad \textbf{(5.8)}$$

In linear regression equations, the predicted output is given by the following equation:

$$\widehat{DP}(t) = \psi^T(t) * \hat{\beta}(t-1) \quad \textbf{(5.9)}$$

The following set of equations summarizes the *Kalman filter* adaptation algorithm [33]:

$\widehat{\beta}(t) = \hat{\beta}(t-1) + K(t) * [DP(t) - \widehat{DP}(t)]$

$\widehat{DP}(t) = \psi^T(t) * \hat{\beta}(t-1)$

$K(t) = q(t) * \psi(t)$

$q(t) = \frac{P(t-1)}{R_2 + \psi^T(t) * P(t-1) * \psi(t)}$

$P(t) = P(t-1) + R_1 - \frac{P(t-1) * \psi(t) * \psi^T(t) * P(t-1)}{R_2 + \psi^T(t) * P(t-1) * \psi(t)}$ **(5.10)**

The Kalman filter algorithm is entirely specified by the sequence of data DP*(t)*, the gradient $\psi^T(t)$, R_1, R_2, and the initial conditions β(t=0) (initial guess of the parameters) and P(t=0) (covariance matrix that indicates parameters errors). In our approach, we adopted the recursive least-squares formulation and to simplify, we scaled R_1, R_2, and P(t=0) of the original problem by the same value such that R_2 is equal to 1 and R_1 is equal to 0.

In this work, the parameters to be recursively identified are denoted by $\beta_i = [\beta_1 \quad \beta_2]^T$. In addition, ψ(t)=$[Q\ (t)\ \ Q\ (t)\Delta x(t)]^T$ denotes the coefficients of these parameters in the die pressure relation and *P(t)* is the parameter covariance matrix. The covariance matrix *P (t)* is initialized with a pre-selected positive definite covariance matrix. For identification of the die pressure model by the Kalman filter algorithm, a M-matlab file was written and is attached in appendix C of this thesis.

5.3.2 Die Pressure Parameters Identification Results

Since real time estimation facilities were not available in our experiments, we applied recursive parameter estimation to the data that were recorded using the data acquisition system. In particular, the measured process inputs (feed-rates and screw speed) are fed to the model and its prediction for the die pressure is compared with the measurements to generate the residual error. The recursive parameter capability for multiple runs with variations in raw material and composition from nominal conditions was tested off-line. The results of the model predictions compared with the measurements for some representative runs are shown in this section.

Figure 5.4 demonstrates the excitation in process conditions. In this experiment, the total feed rate and the polycarbonate feed rate have been decreased by 51 while screw speed has been kept constant.

Figure 5.4: Excitation in process conditions, Run 2-3, day 1 of the 2nd set of experiments

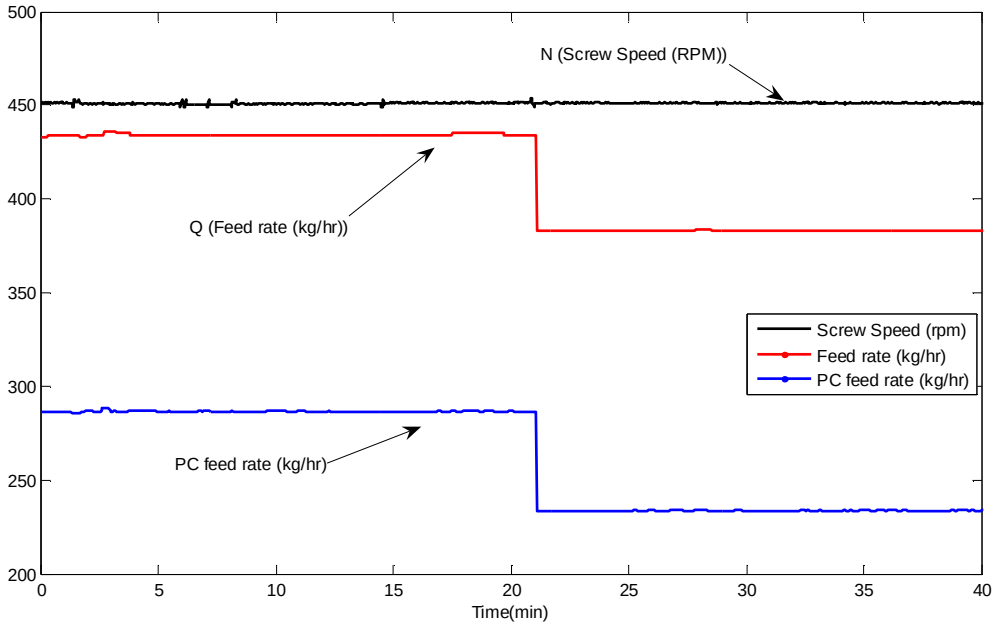

Figure 5.5 shows the die pressure changes in response to the changes in process conditions. In this Figure, as polycarbonate feed rate decreases the melt viscosity decreases thereby decreasing die pressure. Furthermore, as the total feed rate decreases, the outlet flow rate decreases thereby decreasing die pressure.

Figure 5.5 Die pressure measurements, Run 2-3, day 1 of the 2nd set of experiments

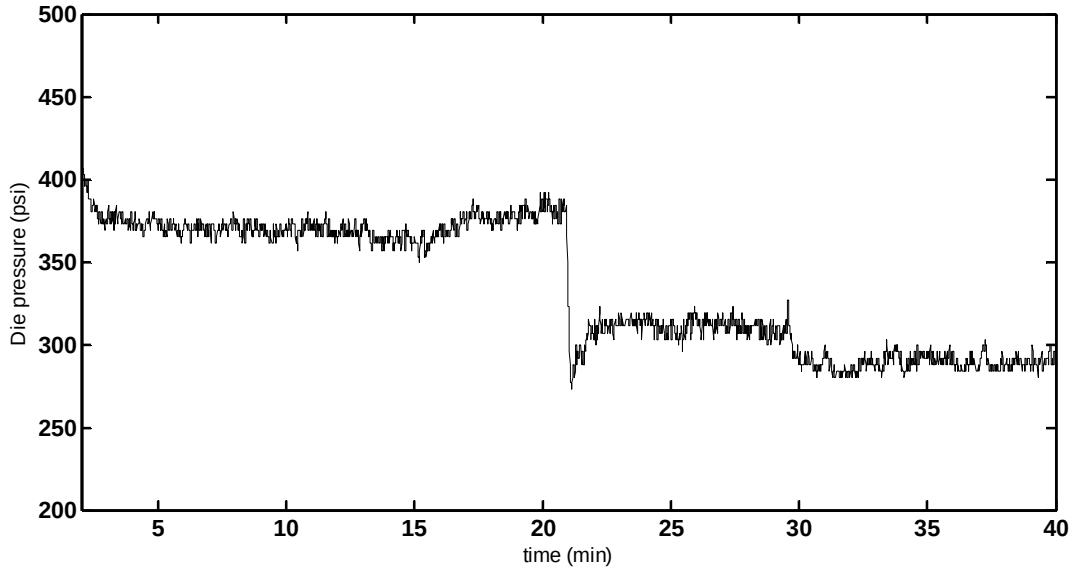

Figure 5.6 shows good agreement between the die pressure predictions of the extruder model and the measurements obtained in these consecutive runs. During this experiment, the parameters β_i were adapted following the above recursive least squares method. As shown in figure 5.5, the die pressure during this two runs is decreased with decreasing feed rate of PC. This is expected, since the lower PC composition causes a lower product viscosity and hence lower die pressure. As shown in figure 5.6, the parameters β_i adapted to match the model predictions to the measurements and capture the effect of the change in composition of feed. The residual plot in the lower section of figure 5.6 does not show any irregular patterns.

Figure 5.6: Comparison of measured and predicted die pressure, Run 2-3, day 1 of the 2nd set of experiments

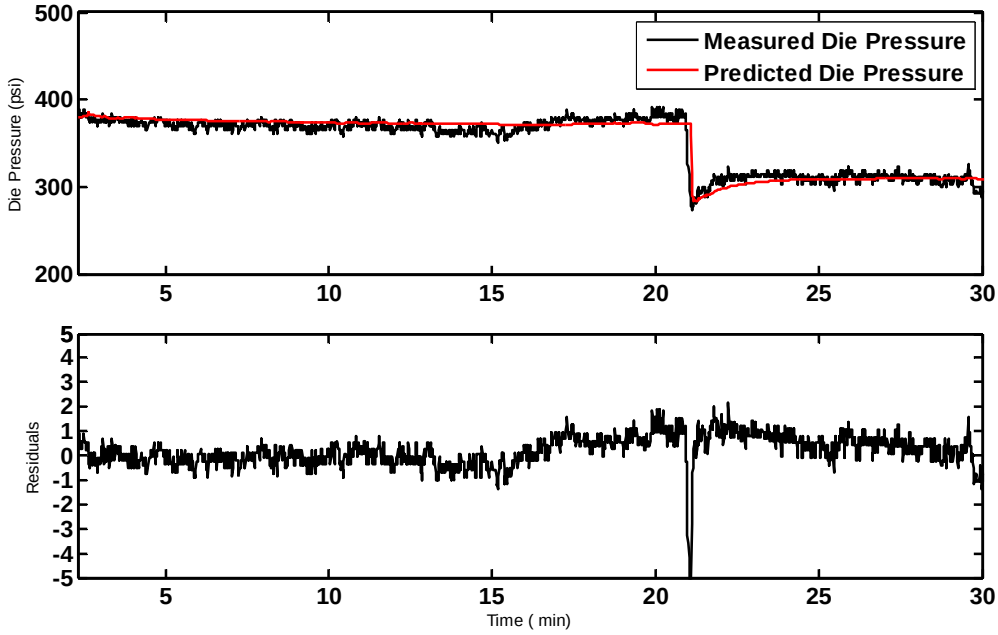

Figure 5.7 shows the agreement between the die pressure predictions of the extruder model and measurements obtained in experiment runs 6 and 7 on day 1 of the 2nd set of experiments. During this experiment, the inputs (PC, PBT feed-rates and screw speed) were varied and the parameters β_i were adapted following the recursive least squares method. The die pressure during these two runs (Figure 5.7) increases with increasing feed rate of PC and decreasing screw speed. This is expected, since the higher PC composition implies a higher product viscosity and hence higher die pressure.

Figure 5.7: Comparison of measured and predicted die pressure, Run 6-7, day 1 of the 2nd set of experiments

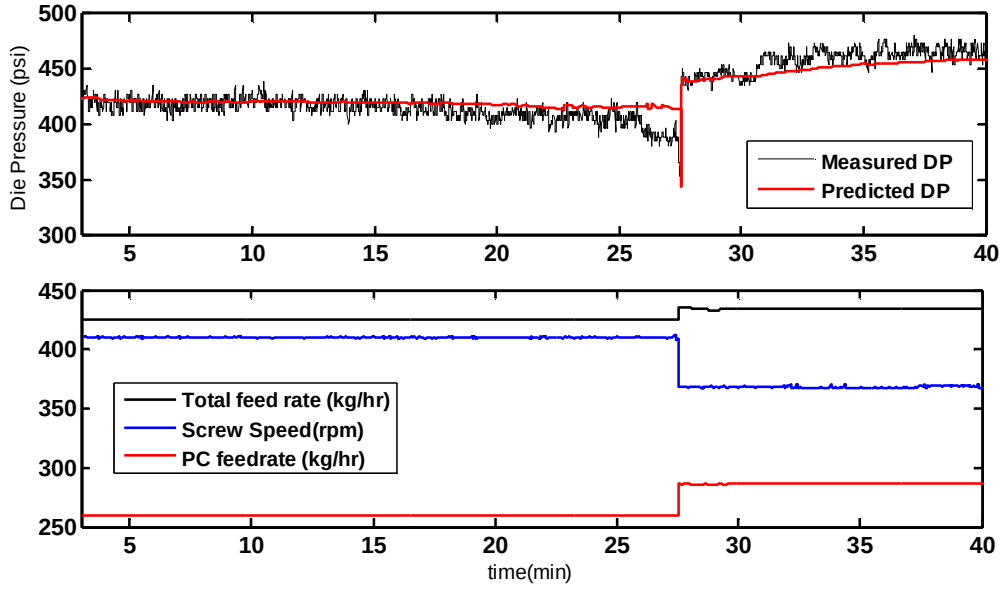

As shown in the representative runs from day 1 of the 2nd set of experimental runs, process dependent parameters in die pressure relations change depending on changes in raw materials and feed composition. In the presence of deviations from nominal conditions, these parameters will need to be adapted. The recursive identification of the parameters seems to capture very well the effects of changes in raw material and/or composition on die pressure.

Chapter 6

Melt Flow Rate Measurements and Fault Identification Results

In plastic compounding operations, product melt volume flow rate (MVR) is one of the quality characteristic that usually is measured off-line in a quality control lab on an extrusion plastometer. For such a measurement, typically a target value representing the desired value of the quality characteristics for an in-control process, along with upper and lower control limits, are specified. As long as the MVR measurement is within the control limits, the sample is approved and the product is assumed to meet the specification. However, a point outside of the control limits is interpreted as evidence that the product does not meet QA requirements and would be rejected. Because of infrequent discrete sampling, corrective action is usually applied with delay thus resulting in wasted material. The ability to monitor product MVR on-line from output process variables enables quick quality control to maintain products within specification limits and minimize waste production. In section 6.1 through 6.4 of this chapter, a simple model was developed for inferential estimation of MVR from die pressure model parameters and its validity was checked using experiments conducted on day 1 and day 2 of the 2nd set of experiments. In section 6.5, the usefulness of the die pressure model for fault identification is demonstrated.

6.1 MVR Model

The parameters β_i in the linear die pressure model [23] for twin screw extruder have physical meaning.

$$DP = \beta_1 Q_0 + \beta_2 Q_0 \Delta x_0 - \beta_3 Q_0 \Delta Q_0 - \beta_4 Q_0 \Delta T \quad \textbf{(3.14)}$$

Disregarding the shear rate and temperature effects since these are fixed for the lab measurements, leads to:

$$DP = \beta_1 Q_0 + \beta_2 Q_0 \Delta x_0 \quad \textbf{(6.1)}$$

In the above equation, β_1 and β_2 can be related to melt viscosity as:

$$\beta_1 = k\mu_0 \quad \& \quad \beta_2 = k\,\mu_1 \quad \textbf{(3.15)}$$

In the above linear approximation for viscosity, μ_0 denotes the nominal viscosity at the nominal operating point, while μ_1 denotes the gradient of viscosity with respect to composition. Viscosity has a reciprocal relationship with melt flow rate (MVR), i.e., the viscosity of the melt decreases with increasing melt flow rate and accordingly viscosity increases with decreasing melt flow rate. Substituting reciprocal of melt flow rate instead of viscosity leads to:

$$MVR = MVR_1 + MVR_2(x_0 - \overline{x_0}) \qquad \text{where} \quad MVR_1 = \frac{K}{\beta_1} \text{ and } MVR_2 = \frac{K}{\beta_2} \qquad \textbf{(6.2)}$$

In the above linear approximation for MVR, MVR_1 denotes the nominal melt flow rate at the nominal operating point, while MVR_2 denote the gradient of melt flow rate with respect to composition. In particular, as the raw materials or feed compositions change, melt flow rate will change.

6.2 MVR Measurement Results

During day 1 and day 2 of the 2nd set of experimental runs, polymer samples were collected as a function of time. MVR for each sample was measured on an extrusion plastometer at SABIC Innovative Plastics by the method described in chapter 4. Each MVR measurement took approximately 20 minutes. The MVR measurement results are shown in tables 6.1 and 6.2. Runs 2, 11, and 12 show missing samples indicated by" –".

Table 6.1: MVR measurement results on QA lab for day 1 of the 2nd set of experiments

Run	*N (rpm)*	*Q (Kg/hr)*	*X1 (Wt% PC)*	*X2 (Wt% PBT)*	*MVR measurements*										
					Sampling time (min) intervals										
					0.5	*1*	*1.5*	*2*	*2.5*	*3*	*3.5*	*4*	*9*	*14*	*19*
1	**410**	**425**	**0.61**	**0.39**	15.4	14.2	15.8	14.8	18.7	17.2	17.4	16.8	16.8	17.2	17.2
2	**451**	**434**	**0.66**	**0.34**	16.9	16.7	13.8	15.4	15.6	14.9	15.6	15.6	15	--	12.4
3	**451**	**383**	**0.61**	**0.39**	18.2	19.5	17.9	18.9	18.6	18.8	19.4	19.1	20	20.9	20.7
4	**410**	**425**	**0.61**	**0.39**	17.2	16.4	16.3	16.1	15.8	16.2	16.6	16.3	15.8	15.7	16.3
5	**369**	**383**	**0.61**	**0.39**	16.5	16.7	17	15.9	16.4	16.1	16.1	16.1	16.3	17.5	16.3
6	**410**	**425**	**0.61**	**0.39**	16.8	16.4	16.2	16.8	15.4	16	15.6	15.4	18.2	18.5	17.2
7	**369**	**434**	**0.66**	**0.34**	15.9	15.9	16.5	16	15	14.7	15	14.5	13.3	13.4	13.2
8	**451**	**468**	**0.61**	**0.39**	17.8	18.1	16.8	16.3	17.1	17	16.5	16.4	16.8	15.7	17.6
9	**410**	**425**	**0.61**	**0.39**	14.5	15.4	15.2	15.8	15.8	16.2	13.9	16.3	17.4	16.8	17.1
10	**451**	**416**	**0.56**	**0.44**	20.6	21.3	21.6	20.7	21	20.6	21.8	22.4	21	20.3	21.4
11	**410**	**468**	**0.61**	**0.39**	15.3	15.7	16.6	16.3	19.8	16.4	15.6	15.2	15.2	--	--
12	**369**	**416**	**0.56**	**0.44**	16.9	16	16.6	16.4	16.9	16.9	17.3	17.2	17.4	--	--
13	**410**	**425**	**0.61**	**0.39**	16.8	17.2	16.8	17.1	17.6	17.8	18.3	17.4	17.4	18	17.7

Table 6.2: MVR measurement results on QA lab for day 2 of the 2nd set of experiments

Run	*N (rpm)*	*Q (Kg/hr)*	*X1 (Wt% PC)*	*X2 Wt% PBT)*	*MVR measurements*											
					Sampling time (min) intervals											
					0.5	*1*	*1.5*	*2*	*2.5*	*3*	*3.5*	*4*	*6*	*8*	*10*	*15*
1	**410**	**425**	**0.61**	**0.39**	16.2	17.7	18.7	18.2	18.7	20.5	19.4	18.0	16.8	18.5	15.3	18.6
2	**451**	**456**	**0.63**	**0.34**	17.4	15.6	18.4	17.0	19.9	20.1	19.0	19.0	20.4	19.3	20.7	19.5
3	**451**	**383**	**0.61**	**0.39**	21.7	23.0	23.4	26.3	26.0	25.5	24.5	25.0	24.8	24.3	25.4	23.8
4	**410**	**425**	**0.61**	**0.39**	18.5	19.1	19.0	18.7	18.6	18.8	18.8	19.1	19.2	19.3	20.1	19.2
5	**369**	**383**	**0.61**	**0.39**	17.9	19.5	18.9	19.0	18.7	18.8	19.1	20.0	18.2	19.2	19.5	17.9
6	**410**	**425**	**0.61**	**0.39**	16.7	18.2	19.0	18.8	19.3	19.8	18.6	18.9	19.3	19.1	19.4	19.8
7	**390**	**434**	**0.66**	**0.34**	17.9	16.9	16.5	18.6	17.5	17.5	17.5	16.2	16.9	17.4	16.4	17.3
8	**451**	**468**	**0.61**	**0.39**	20.5	20.5	20.4	20.6	20.9	20.1	20.3	20.5	20.9	20.4	21.0	20.1
9	**410**	**425**	**0.61**	**0.39**	19.2	19.3	19.6	18.6	19.4	20.3	19.3	20.5	20.2	20.7	21.2	20.3
10	**451**	**416**	**0.56**	**0.44**	25.8	25.0	25.3	25.0	25.0	24.9	25.9	25.0	25.9	24.0	25.7	26.4
11	**451**	**468**	**0.61**	**0.39**	19.5	20.5	20.6	21.0	20.9	20.9	20.0	23.0	19.8	20.0	20.5	20.4
12	**369**	**416**	**0.56**	**0.44**	20.5	20.2	20.3	19.8	20.4	20.1	21.5	20.8	19.7	19.6	19.5	20.5
13	**410**	**425**	**0.61**	**0.39**	18.3	19.6	20.0	20.0	20.1	20.3	20.9	20.6	21.1	21.0	20.2	20.8

Some MVR measurements are randomly repeated to compute the variability of measurements. This variability will give an indication of the random error in the measurements (e.g., due to variability in the measurement instrument), because the replicated observations are measured under identical conditions. Results of measurements variability were shown in tables 6.3 and 6.4.

Table 6.3: MVR measurements variability for day 1 experiments

Run	1st MVR measurement	2nd MVR measurement
1.1.11*	17.05	17.35
1.5.11	15.96	16.69
1.10.11	20.27	22.56
1.13.11	17.7	17.76

1.1.11* means sample number 11 that was collected during run number 1of day 1

Table 6.4: MVR measurements variability for day 2 experiments

Run	1st MVR measurement	2nd MVR measurement
2.1.11*	15.38	14.26
2.2.11	20.7	19.78
2.3.11	25.4	24.52
2.4.11	20.12	20.25
2.5.11	19.58	20.03
2.6.11	19.44	19.38
2.7.11	16.48	16.64
2.8.11	21.04	20.89
2.9.11	21.22	20.56
2.0.11	25.76	25.91
2.11.11	20.5	20.78
2.12.11	19.55	19.32
2.13.11	20.21	19.96

2.1.11* means sample number 11 that was collected during run number one of day 2

It is typical in multisampling studies to pool the r sample variance to arrive at a single estimate of the standard deviation associated with responses derived from all r samples. If r numerical samples of respective size n_1 , n_2 ,…, n_r produce sample variances ${S_1}^2$, ${S_2}^2$,…, ${S_r}^2$,the pooled sample variance , ${S_p}^2$, is [34]:

$${S_p}^2 = \frac{(n_1-1)*{S_1}^2+(n_2-1)*{S_2}^2+\cdots+(n_r-1)*{S_r}^2}{(n_1-1)+(n_2-1)+\cdots+(n_r-1)}$$

The pooled sample standard deviation, S_p, is the square root of ${S_p}^2$. In MVR measurement data, each of n_1 , n_2 ,…, n_r is 2. Using the above equation:

$${S_p}^2 = \frac{(2-1)*{S_1}^2+(2-1)*{S_2}^2+\cdots+(2-1)*{S_r}^2}{(2-1)+(2-1)+\cdots+(2-1)} = \frac{0.045+0.26645+2.62205+0.0018}{4} = 0.733$$

And thus S_p=$\sqrt{0.733}$ =0.856

We repeated the same calculation for MVR measurements from day 2 experiments and a standard deviation of 0.38221 was obtained. It should be noted that S_p here represents the contribution to the overall measurement error variance coming from the MVR measuring device. These pooled standard deviations for both days of the experiments are small and can be ignored.

6.3 Estimation of Parameter K in MVR Model

As shown in chapter 3 of this thesis, equation 3.12 relates pressure drop [23] to the volumetric flow rate, viscosity of melt and geometry of die as:

$$DP = KQ_0\mu \quad \textbf{(3.12)}$$

In the above die pressure model, Q_0 is the flow rate of the product through the die plate. Substituting the reciprocal of melt flow volume rate instead of viscosity leads to:

$$DP = KQ_0/MVR \quad \textbf{(6.3)}$$

At steady state, K (machine/die/product grade dependent calibration parameter) can be calculated by equation 6.4:

$$K = DP * MVR\ /Q \quad \textbf{(6.4)}$$

The last column of Table 6.5 shows the value of K obtained from the runs conducted on day 2 of the 2nd set of experiments. The validity of the estimated value of K was checked by using the average value of K to predict MVR values for the experiments conducted in the 3rd set of experiments. Table 6.7 represents output of this calculation. The results showed that the MVR model validates very well against the measured MVR data. Figure 6.1 shows the comparison of the measured and predicted MVR using K=33.327.

Table 6.5: Estimation of K from steady state variables

Run #	Q (KG/hr)	N (rpm)	X1 %wt PC	Die Diameter (mm)	MVR	DP	$K = DP * MVR / Q$
2.1	425	410	0.61	**3**	19	703	31.44
2.2	434	451	0.63	**3**	20.24	676	31.54
2.3	383	451	0.61	**3**	24.96	519	33.87
2.4	425	410	0.61	**3**	20.19	683	32.48
2.5	383	369	0.61	**3**	19.81	677	35.06
2.6	425	410	0.61	**3**	19.41	689	31.48
2.7	434	390	0.66	**3**	16.56	741	28.28
2.8	468	451	0.61	**3**	20.97	674	30.23
2.9	425	410	0.61	**3**	20.89	666	32.75
2.1	416	451	0.56	**3**	25.84	559	34.72
2.11	468	451	0.61	**3**	20.64	680	30.00
2.12	416	369	0.56	**3**	19.44	732	34.21
2.13	425	410	0.61	**3**	20.09	665	31.45

Table 6.6: Basic Statistics for parameter K

Variable	N	Mean	StDev
K	13	32.121	1.996

Table 6.7: Estimation of MVR using K= 33.327 from 3rd set of experiments

Run	Q	N	X1	MVR (measured)	DP	MVR=K*Q/DP
1	425	410	0.61	19.88	761	18.61
2	425	410	0.61	20.36	776	18.25
3	425	410	0.61	19.22	807	17.55
4	425	410	0.61	19.69	776	18.25
5	425	410	0.61	20.87	772	18.34
6	425	410	0.61	19.21	772	18.34
7	425	410	0.61	18.71	780	18.15
8	425	410	0.61	19.25	776	18.25
9	425	410	0.61	18.01	799	17.72

Figure 6.1: Comparison of measured and predicted MVR using data from 3rd set of experiments

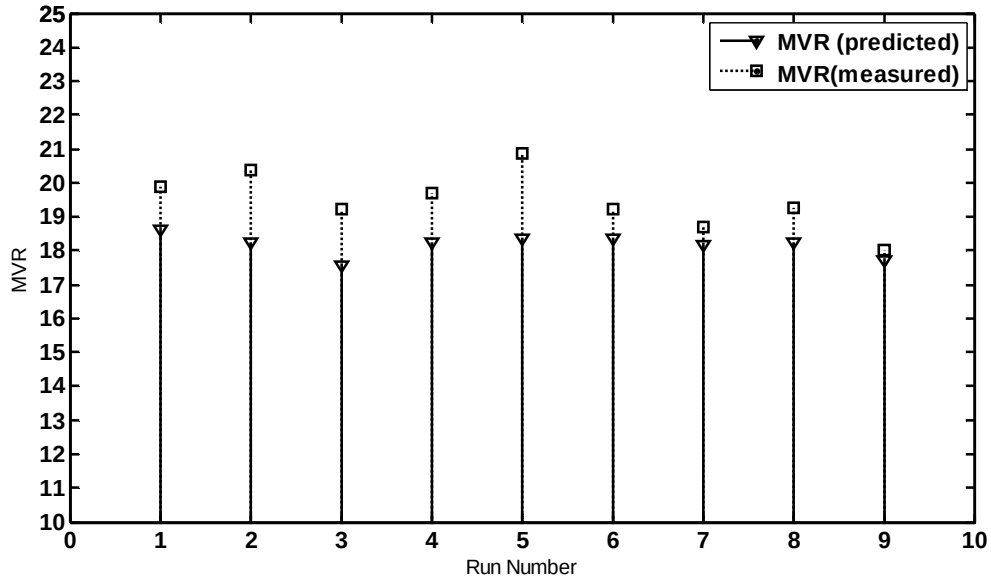

6.4 Inferential Estimation of MVR

As shown in equation 6.2, MVR can be inferentially estimated using the die pressure parameters β_1 and β_1 . In this section, we will show the comparison of the melt volume flow rate estimates with the lab MVR measurements of samples collected at multiple conditions with different compositions during each run.

Figure 6.2 shows the MVR estimation results using equation 6.2 for day 1 of the 2nd set of experiments. During these experiments one of the variables perturbed was the polycarbonate (PC) composition which was increased and decreased from the nominal compositions as explained in chapter 4. The overall estimation results seem promising. Two samples show poor fit. Run number 2 corresponds to very high PC content and thus low MVR. Run 10 corresponds to very low PC content and thus high MVR. These samples correspond to the maximum deviation from the nominal composition and the linear approximation for MVR as a function of composition used in the die pressure model becomes inaccurate under these extreme deviations, thus leading to larger error. Adding higher order nonlinear terms in the dependence of MVR on composition of PC may decrease this error under these extreme composition limits but it makes the model complicated for identification of parameters using the recursive method.

Figure 6.3 shows the MVR estimation results using equation 6.2 for runs two and three from day 1 of the 2nd set of experiments with nominal raw materials and higher composition of PC. The estimation results shown by star are compared with the corresponding lab measurements of samples collected during intervals in each run. The lower graph in Figure 6.3 also shows the predicted and measured die pressure for the same runs.

Figure 6.2: Comparison of predicted &measured MVR, day 1 of the 2nd set of experiments

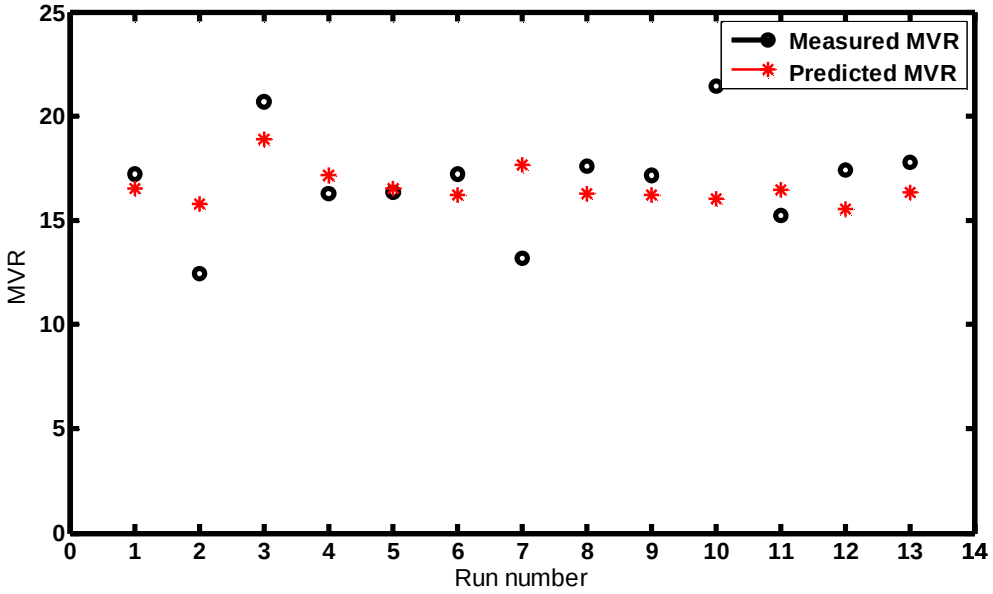

Figure 6.3 Comparison of predicted and measured MVR and Die Pressure, Run 2-3 (Day 1)

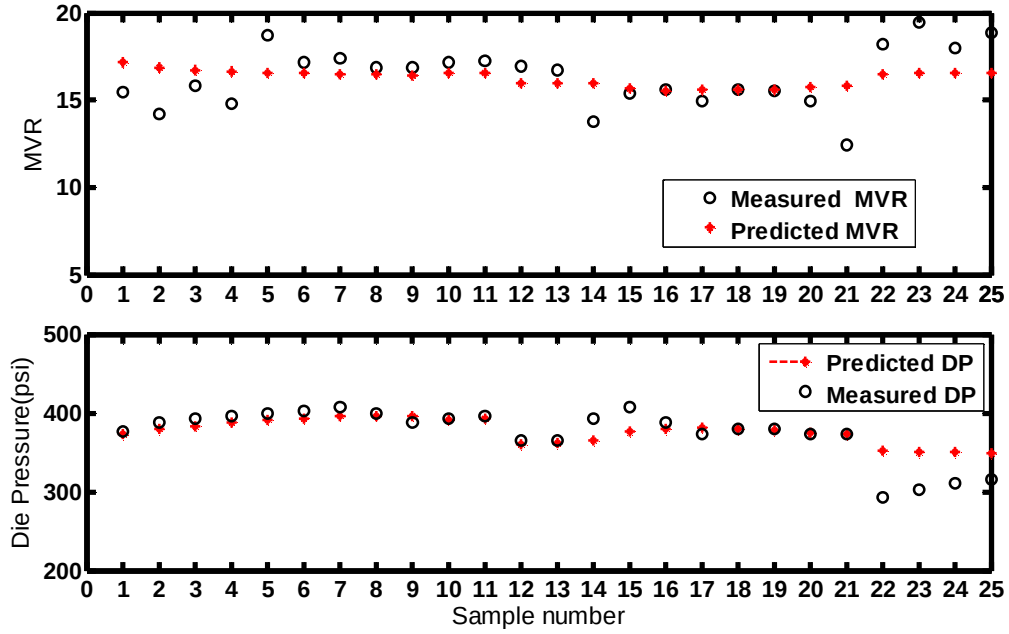

Figure 6.4 shows the MVR estimation results for runs 12 and 13 of day 2 of the 2nd set of experiments with nominal raw materials and higher PC composition. The lower graph in Figure 6.4 also shows the residuals predicted and measured MVR for same runs. Figure 6.5 also shows the MVR estimation results for runs 6-7 of day 2 of the 2nd set of experiments with nominal raw materials and higher PC composition. Again the lower graph in Figure 6.5 shows the residual predicted and measured MVR for the same runs.

As shown in these representative runs, the parameters β_i in die pressure model have a physical significance owing to their relationship to the melt flow rate. These parameters in die pressure can be estimated using recursive adaptation techniques and can be used for monitoring the quality (MVR) of PC/PBT blends.

Figure 6.4: Comparison of Predicted &Measured MVR, Run 12-13, day 2 of the 2nd set of experiments

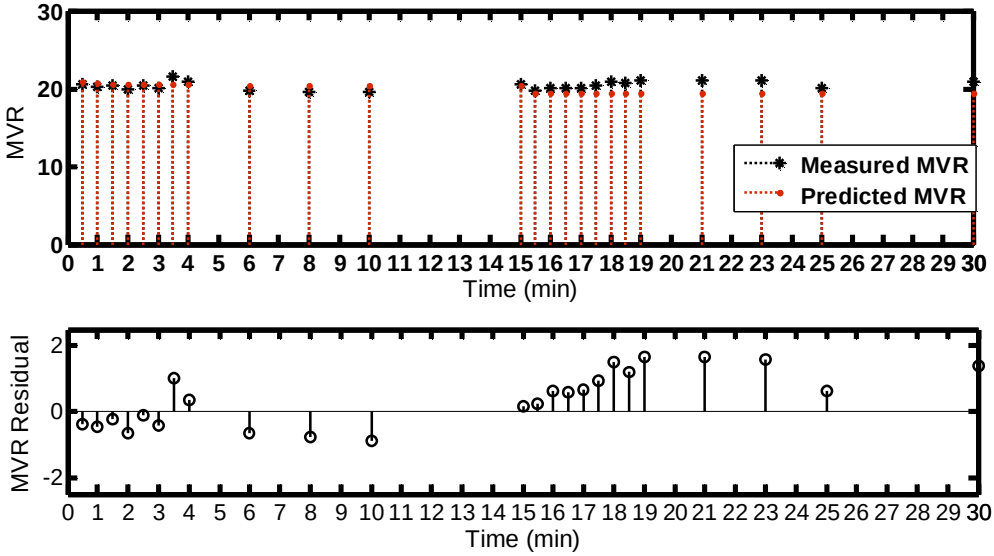

Figure 6.5: Comparison of MVR, Run 6-7, day 2 of 2nd set of experiments

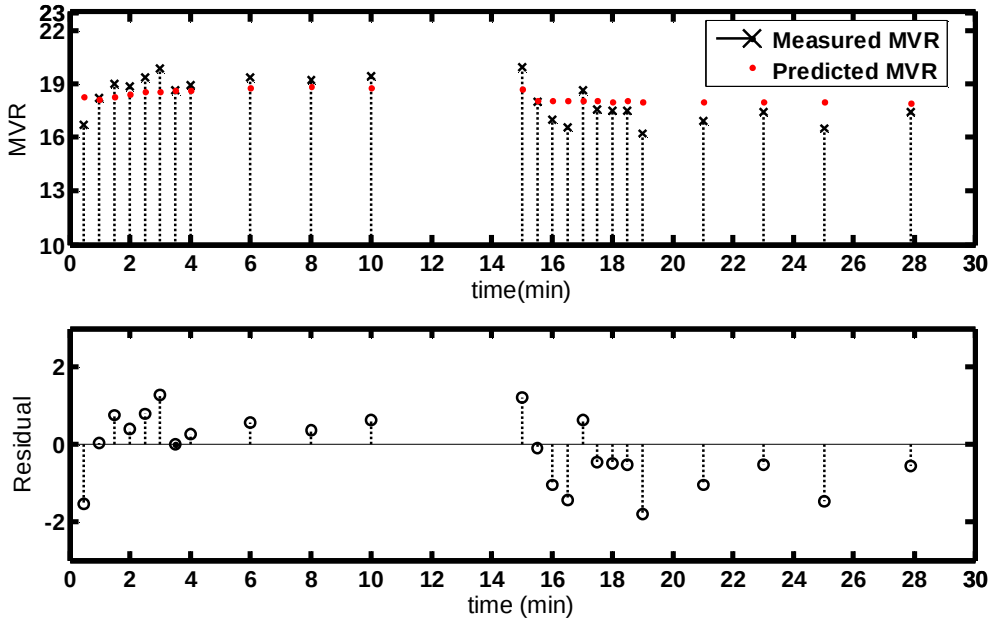

6.5 Fault Identification using the Die Pressure Parameters

The manufacturing process must be capable of operating with little variability around the target or nominal value. In any production process, a certain amount of inherent variability will always exist. Other kinds of variability and fault in MVR usually arise from three sources: machine malfunctions, operator errors, or material fluctuations. Among these possible sources of faults, the major ones that affect product quality are associated with variations in raw material and feeder variations. Motivated by this, we will focus on the detection of raw material and feeder variation, using available simulated off-line measurements from days 1 and 2 of the 2^{nd} set of experimental runs. In this section, the problem of fault identification because of variation in raw materials will be addressed for the compounding of PC/PBT on a twin screw extruder (TSE) using the developed modeling and adaptation methods which are described in the previous sections of this thesis.

6.5.1 Fault Identification Results

A major objective of process control for compounding of PC/PBT on a TSE is to quickly detect the occurrence of faults. After identification of this fault, corrective action can be undertaken to eliminate the fault. This quick identification of a fault and a corrective action in successive stages will reduce significantly nonconforming products. Fault identification methods for the extruder using the developed modeling and adaptation methods described in the previous sections will only detect faults. An additional step of subsequent corrective action will be necessary to eliminate the cause.

As explained in chapter 4 of this thesis, multiple experiments with different raw materials were conducted over two days to test the performance of the fault diagnostics. In particular, the PC or PBT feed-rates and screw speed were varied. Then, the off-line simulations of recursive parameter identification were performed on actual recorded input/output data from the experiments.

Here, some representative runs are shown. More runs from 2nd and 3rd set of experiments have been presented in appendix B of this thesis. In all these figures from representative runs, we consider the scenario of starting with nominal operation, and then a fault (PC changed from nominal to lower or higher polycarbonate composition) is introduced and the die pressure increase or decrease significantly as consequent of change in input variable such as feed-rates and screw speed. As shown in all of these excitations, the fault is detected and the model parameters are updated using the recursive adaptation method.

Fault detection can be achieved by monitoring the residual error between the measured die pressure and the model prediction (or accordingly by monitoring the die pressure parameters). Figure 6.6 shows the sequence of fault occurrence, detection and identification in the representative runs 7 and 8 of day 1 experiments. Details of these two runs are summarized in Table 6.8. As shown in figure 6.6, we consider the scenario of starting with nominal operation, and then a fault (as shown by arrow in Figure 6.6) occurs – a change in composition of PC from nominal (X=0.66) to lower (X=0.61) composition.

Under nominal conditions, the measured value for die pressure matches well with the model prediction using the nominal parameters. However, after the fault, i.e. the transition from nominal (X= 0.66) raw materials to a lower PC (X=0.61), the product viscosity drops. Accordingly the die pressure drops significantly. This leads to a mismatch between the measured die pressure and the model prediction. A fault, i.e., variation in the feed-rates and screw speed was detected by this residual error between the measured die pressure and the nominal model prediction. The detection of a fault initiates the fault identification. In this identification phase, the model parameters are updated using the simulated off-line recursive adaptation method. Finally, the new adapted parameters, i.e. beta1 (β_1) and beta2 (β_2) (or equivalently MVR_1 and MVR_2), are compared with the nominal values and identify the specific fault. The lower two plots in Figure 6.6 show the plots of the two parameters beta 1 and beta 2. The parameters beta1 and beta2, or equivalently MVR_1 and MVR_2 converge to a value lower than that for nominal conditions.

By monitoring these parameters, a fault can be identified. An appropriate corrective action such as returning raw material feeders speeds to nominal conditions can be taken to bring the process back on-spec, and prevent production of waste compounds of PC/PBT.

Figure 6.6: Fault Identification using die pressure parameters, Run 7-8, day 1

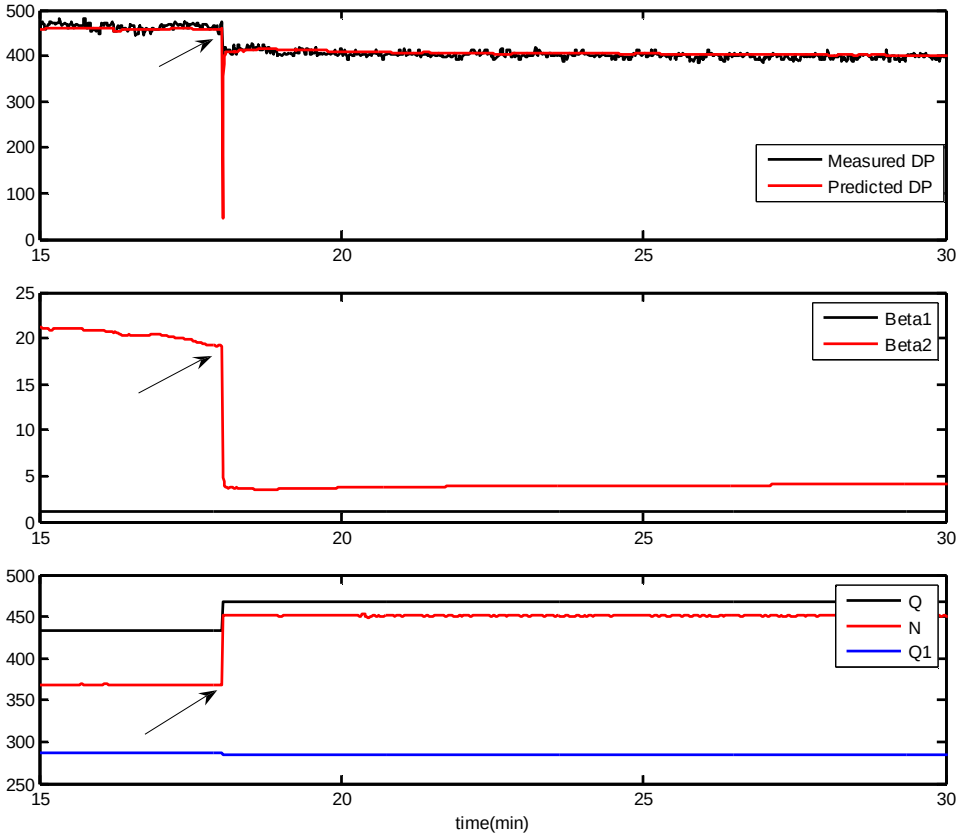

Table 6.8: Summary of excitation, Run 7-8 from day 1 of the 2nd set of experiments

Run number	N (rpm)	Q (kg/hr)	x_{pc} (wt %)	x_{PBT} (wt %)
7	369	434	0.66	0.34
8	451	468	0.61	0.39

We also used data from day 2 experiments to validate fault detection by monitoring the die pressure parameters. Again an excitation (as shown by arrow in Figure 6.7) to the system was made by variation in the inputs (feed rates and screw speed) and the corresponding die pressure measurements were recorded. Details of these excitations are summarized in table 6.9 and also in the lower parts of Figure 6.7. The fault detection is achieved by monitoring the die pressure parameters and the residual error between measured die pressure and the model prediction. The upper plot of Figure 6.7 shows recorded die pressure and predicted die pressure by the recursive parameter estimation method and the sequence of fault occurrence, detection and identification in a representative run 10 and 11 of day 2 experiments. Again, under nominal conditions, the measured value for die pressure matches well with the model prediction using nominal parameters. However, after the fault, i.e. the transition from nominal (X= 0.56) raw materials to a higher PC (X=0.61), the die pressure drops. This leads to a mismatch (as shown by arrow in Figure 6.7) between the measured die pressure and the model prediction. A fault, i.e., variation in the feed-rates and screw speed detected by this residual error between the measured die pressure and the nominal model prediction and the model parameters are updated using the simulated off-line recursive adaptation. The second plot in Figure 6.7 shows the beta1 and beta2 parameters. The parameters beta 1 and beta 2 converge to a value higher than that for nominal conditions. Finally, comparing the new adapted parameters, i.e. beta1 (β_1) and beta2 (β_2) with the nominal values identifies the specific fault.

Another representative run from day 2 experiments is shown in Figure 6.8 in which the inputs (feed rates and screw speed) were varied and corresponding die pressure measurements were recorded. Details of these excitations in inputs are summarized in table 6.10 and also in lower parts of Figure 6.8. As shown in this Figure, the fault is detected by monitoring the die pressure parameters and the model parameters are updated using the recursive adaptation.

Figure 6.7: Fault Identification using Die pressure parameters, Run 10-11, day 2

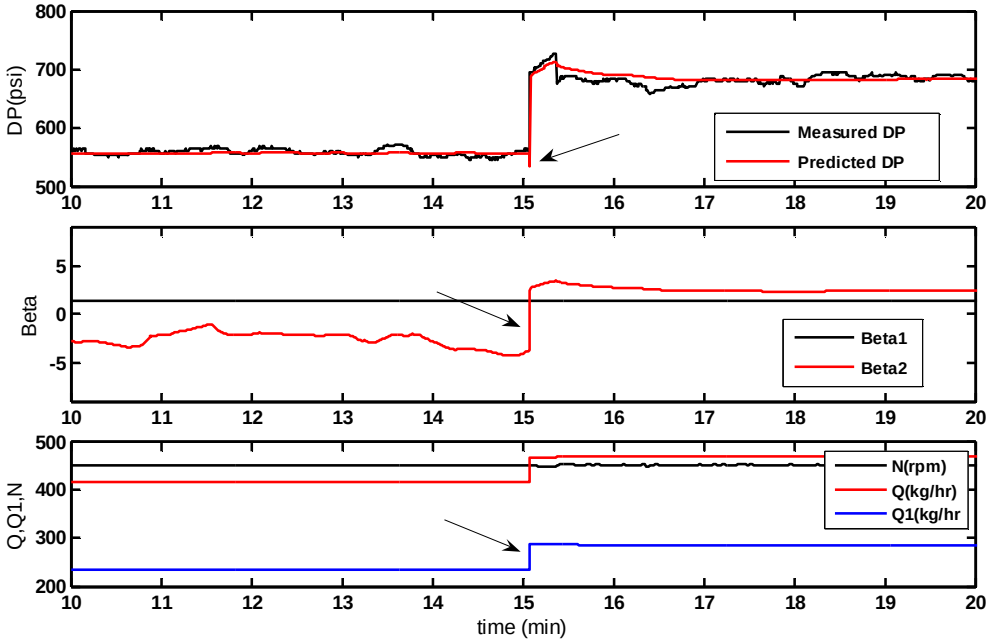

Table 6.9: Summary of excitation, Run 10-11 from day 2 of the 2nd set of experiments

Run # (Apr 12)	Q (kg/hr)	N (rpm)	X,PC	Average DP
10	416	451	0.56	560
11	468	451	0.61	680

Figure 6.8: Fault Identification using Die pressure parameters, Run 6-7, day 2

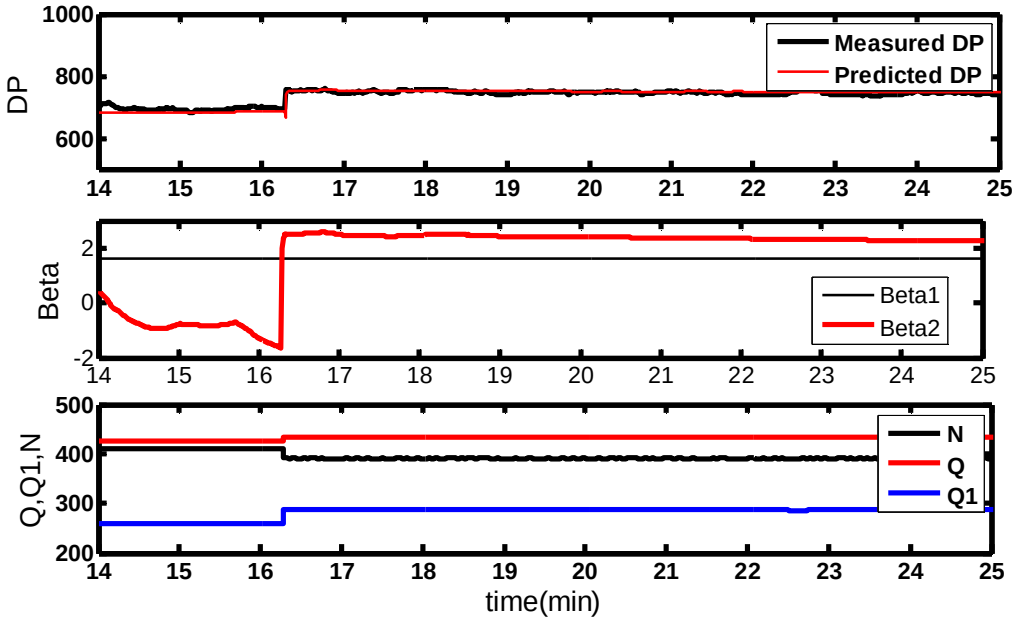

Table 6.10: Excitation to input variables (Q, N), Run 6, 7, day 2

Run # (Apr 12)	Q (kg/hr)	N (rpm)	X,PC	Average DP
6	425	410	0.61	680
7	434	390	0.66	740

Chapter 7
Conclusions and Recommendations

The purpose of this study was to examine the compounding operation of PC/PBT blend on twin screw extruder and to develop a methodology that can be applied on-line for monitoring properties of blend on the industrial compounding operation and decrease waste products and have consistent quality product. To achieve these objectives, the model developed by Kumar et al. [23, 24] was examined and adapted for our purpose and verified through designed experiments. The results showed that the model has capability of identifying fault in polymer compounding operation on the twin screw extruder. As explained and described in chapter 6, this model has ability to monitor product MVR on-line from output process variables such as die pressure which enables quick quality control to maintain products within specification limits and minimize waste production. This not only allows great reduction in waste materials and energy but also could maintain customer satisfied through consistent quality of polymer compounds.

Parameters for the torque and the die pressure in the twin screw extruders flow model have unknown parameters that depend on the specific extruder geometry and the product application. As demonstrated in Chapter 5, Matlab M-file programs were developed and adapted to identify theses unknown parameters from measured Input/output data using Levenberg Marquardt Algorithm (LMA) and Recursive Parameter Estimation (RSE) algorithm. All the algorithms developed in this work can be verified and implemented in compounding operations for process control purpose. Fault identification and MVR estimation capability of this model were demonstrated on experiments performed on a 58 mm co-rotating twin-screw extruder for an industrial compounding operation. Chapter 6 summarized the approach for inferential adaptive control of MVR using the flow model. The linearized model for MVR predicts MVR using output process data such as die pressure parameters with applying adaptive identification of parameters. This on-line estimation of MVR in comparison to discrete lab measurements has a significant advantage for continues

quality control and improvement of product. It was also shown only using die pressure parameters it is possible to identify fault and inferentially estimate MVR.

Although, the methodology developed was for compounding of PC/PBT, it can be extended for any compounds on twin screw extruder only by re-identification of product dependent parameters in the model.

7.1 Recommendations for Future Work

In this project, all the results are based on simulated offline data, which were analyzed using Matlab. It seems more work is needed to be done to implement this methodology for real time polymer compounding operation. Demonstrated approach during this study can be used only for fault identification (i.e., capturing the blend composition changes and variations in incoming raw material). A subsequent appropriate corrective action such as returning raw material feeders speeds to nominal condition should be taken to bring the process back on-spec, and prevent production of waste compounds. To do so, some work has to be done to develop and implement a closed-loop system that integrates all fault identification and corrective action i.e., to monitor viscosity or MVR with die pressure model parameters, to identify faults, and initiate corrective action such as re-fixing the raw material feeder speeds to bring the quality of polymer compounds back on-spec. It seems possible to develop a commercialization plan to apply the research results to typical polymer compounding operation lines which in turn can save lots of energy, materials and services.

REFERENCES

1- L. A. Utracki," Polymer Blends Handbook "Kluwer Publishers, Dordrecht /Boston (2002)

2- H. Bertilsson, B. Franzen, J. Kubat,"Ageing of PC/PBT Blends. I. Impact Properties", Plast. Rubber. Process. Appl., 10, 137-144 (1988)

3- R. S. Halder, M. Joshi, A. Misra," Morphological studies on the blends of poly (butylene terephthalate) and bisphenol-A polycarbonate", J. Appl. Polym. Sci., 39, 1251 – 1264 (1990)

4- J M. R. C. A. Santosa, J. T. Guthrie, "Polymer blends: the PC–PBT case", J. Mater. Chem., 16, 237-245 (2006)

5- T. W. Tseng, J. S. Lee," Functional MBS impact modifiers for PC/PBT alloy", J. Appl. Polym. Sci., 76, 1280–1284 (2000)

6- H. Bai, Y. Zhang, W. Zhou, "Toughening modification of PBT/PC blends ", Polym. Testing, 24, 235-240 (2005)

7-J.Wu, Y. W. Mai, B. Cotterell, "Fracture toughness and fracture mechanisms PBT/PC/IM blend", J. Mater. Sci., 28, 3373-3384 (1993)

8- S. S. Pesetskii, B. Jurkowski, V. N. Koval, "Polycarbonate/polyalkylene terephthalate blends: Interphase interactions and impact strength", J. Appl. Polym. Sci., 84, 1277 – 1285 (2002)

9- J. Devaux, P. Godard, J. P. Mercier, "The transesterification of bisphenol-a polycarbonate (PC) and polybutylene terephthalate (PBT): A new route to block copolycondensates", J. Polym. Eng. Sci., 22, 229-233 (1982)

10- S. B. Tattum, D. Cole, A. N. Wilkinson," Controlled Transesterification and Its Effects on Structure Development in Polycarbonate-Poly(Butylene Terephthalate) Melt Blends ", J. Macromol. Sci., Part B, 39, 459-479 (2000)

11-I. Hopfe, G. Pompe and K.J. Eichhorn, "Ordered structures and progressive transesterification in PC/PBT melt blends studied by FT i.r. spectroscopy combined with d.s.c. and n.m.r.", Polymer, 38, 2321-2327 (1997)

12- P. Marchese, A. Celli, M. Fiorini, "Influence of the Activity of Transesterification Catalysts on the Phase Behavior of PC-PET Blends ", Macromol. Chem. Phys., 203,

695-704 (2002)
13- D. C. Wahrmund, D. R. Paul, J. W. Barlow, " Polyester-polycarbonate blends. I. Poly (butylene terephthalate)", J. Appl. Polym. Sci., 22, 2155 - 2164 (197)
14- W. Birley, X.Y. Chen," Further studies of polycarbonate-poly(butylene terephthalate) blends" , Br. Polym. J., 17, 297 – 305 (1985)
15- S. Y. Hobbs, M. E. J. Dekkers and V. H. Watkins, "The morphology and deformation behavior of poly (butylene terephthalate)/BPA polycarbonate blends", Polym. Bul., 17, 341-345 (1987)
16- D. Delimoy, C. Bailly, J. Devaux, R. Legras , "Morphological studies of polycarbonate-poly(butylene terephthalate) blends by transmission electron microscopy" , Polym. Eng. Sci., 28, 104 (1988)
17- H. E. H. Meijer, P. H. M. Elemans, "The Modeling of Continuous Mixers. Part I: The Co-rotating Twin-Screw Extruder", Polym. Eng. Sci., 28 (1988)
18- K.E. Kinnear," Advances in Genetic Programming ", MIT Press (1994)
19-McKay, B. Lennox, B. Willis, M. Barton, G.W. Montague, "Extruder modeling: a comparison of two paradigms", IEEE, 2, 734- 739 (1996)
20- J. M. Dealy, T. O. Broadhead, "Process rheometers for molten plastics: A survey of existing technology", Polym. Eng. Sci., 33, 1513 – 1523 (1993)
21- J. M. Dealy' "Challenges in process rheometers", Rheolg. Acta, 29, 519-522 (1990)
22- J. Gao, G. C. Walsh , D. Bigio , R. M. Briber, Mark D. Wetzel , "Mean residence time analysis for twin screw extruders" , Polym. Eng. Sci., 40, 227-237 (2000)
23- A. Kumar, S. A. Eker, P.K. Houpt, "A model based approach for estimation and control for polymer compounding ", IEEE, 1, 729 – 735 (2003)
24- A. Kumar, A. Eker, M. Giammatia, P. Houpt, O. Montero, M. Shah, N. Silvi, T. Cribbs, "Intelligent Extruder for Polymer Compounding ", GE Global Research Report (2002)
25- Chris J. Rauwendaal," Analysis and experimental evaluation of twin screw extruders", Polym. Eng. Sci., 21, 1092 – 1100 (1981)
26- R. J. Crawford, "Plastics Engineering", Elsevier Science, Oxford (1999)

27- D. Bigio, R. M. Briber, M. D. Wetzel, “Mean residence time analysis for twin screw extruders”, Polym. Eng. Sci., 40, 227-237 (2000)
28-D.C. Montgomery, “Design and Analysis of Experiments”, 2nd edition, Wiley and Sons, US (2000)
29- A. V. Shenoy, D. R. Saini, “Melt Flow Index: More Than Just A Quality Control Rheological Parameter. Part I”, Adv. Polym. Tech., 6, 1-58 (1986)
30- ASTM D1238, Standard Test Method for Melt Flow Rates of Thermoplastics by Extrusion Plastometer
31- ASTM D256, Standard Test Methods for Determining the Izod Pendulum Impact Resistance of Plastics
32- P. E. Gill, W. Murray, “Algorithms for the Solution of the Nonlinear Least-Squares Problem”, J. Numerical. Analysis, 15, 977-992 (1978)
33- L. Ljung, “System Identification: Theory for the User”, Prentice Hall, N.J. (1987)
34- S. B. Vardeman, “Statistics for Engineering Problem Solving “, PWS, Boston (1994)
35- G.C. Derringer and R. Suich, “Simultaneous Optimization of Several Response Variables”, J. Quality. Tech., 12, 214-219 (1980)

Appendix A
Central Composite Design Results

In the first set of experiment conducted at the SABIC Innovative Plastics plant, the primary objective was to understand the compounding process of PC/PBT on a twin screw extruder. To address this, we used central composite design. An overview of this response surface methodology (RSM), experimental set up and material used were explained in chapter 4 of this thesis. The independent variables were the die temperature, the feed rate, and the screw Speed (rpm). The dependent variables examined include the load, specific energy consumption (SEC), melt temperature, melt flow rate and impact strength. In this Appendix, the correlations of the dependent variables with the independent variables are evaluated with the Minitab statistical analysis package**.** The correlations among several of the dependent variables are also evaluated and explained.

A.1 Experiments Results

Practically die temperature could not been maintained as per set points , so it was taken as response , Table A.1 presents summary of design and response where Q is feed rate (Kg/hr) , N is screw speed(rpm) , SEC is specific energy consumption , MVR is average of melt flow rate ($cm^3/10\text{min}$) from 5 replicates at each run and T is die temperature. All experiment runs could not be made under homogeneous conditions and time. Since each start up potentially may has effect on response, blocking method was applied for reducing the background noise in the experiment. The blocks for our experimental runs have shown in table A.2. In this table block 1, was run on morning, block 2 run afternoons and accordingly block 3 runs at evening of same day.

Table A.1: Variables and responses of the CCD design

Run	Q	N	T	%Load	SEC	MVR	Impact
1	400	410	292	82	0.213205	**30.49**	**14.98**
2	450	450	290	85	0.215284	**29.91**	14.63
3	400	343	285	93	0.202221	**26.57**	14.72
4	400	477	293	77	0.231244	**36.37**	13.24
5	400	410	290	84	0.218651	**31.04**	**14.81**
6	450	400	291	95	0.214979	**26.9**	14.61
7	350	450	291	71	0.232154	**39.87**	12.95
8	350	370	286	81	0.216795	**30.73**	13.64
9	400	410	289	84	0.217297	**31.38**	**13.46**
10	350	370	300	80	0.215531	**31.18**	13.78
11	484	420	295	97	0.211648	**27.62**	15.40
12	400	410	290	84	0.218001	**29.18**	**15.73**
13	400	410	289	83	0.216907	**31.19**	**15.42**
14	450	400	290	94	0.212746	**28.03**	15.53
15	450	450	294	87	0.22014	**30.11**	12.85
16	350	450	293	71	0.23034	**40.14**	12.38
17	400	410	291	84	0.216887	**32.01**	**14.66**
18	316	410	291	68	0.212876	**40.63**	12.92
19	400	410	305	82	0.214167	**32.76**	**14.11**
20	400	410	296	82	0.212977	**29.05**	**14.67**

Table A.2: The block design

Block 1	Block 2	Block 3
Runs: 4,5,6,7,8,9	Runs : 10,11,12,13,14,15,16,17,18	Runs: 1,2,3,19,20

A.2 Power Consumption

The first characteristic determined was the feed rate, screw speed and load relationship. Figure A.1 shows the relationship between load, screw speed and throughput for the all 20 runs. All lines are almost straight. Load on a co-rotating extruder is determined from torque. In figure A.1, moving sequentially along the path of steepest decent, that is, in the direction of increase in throughput and decrease in screw speed, load increases steadily.

The nature of this curve depends on machine geometry, operating conditions, and material properties. Table A.3 shows response surface regression of load versus throughput and screw speed. The Model for load gives good fit with reliability of 98.8%. Analysis of variance (lower portion of Table A.3) for load indicates that feed rate and screw speed significantly affect the load. Lack of fit test was used to check the adequacy of the straight line model. Since, P- value for lack of fit not small, there is no indication of a lack of fit.

Figure A.1: Control Plot of motor load versus feed rate (kg/hr) and screw speed (rpm)

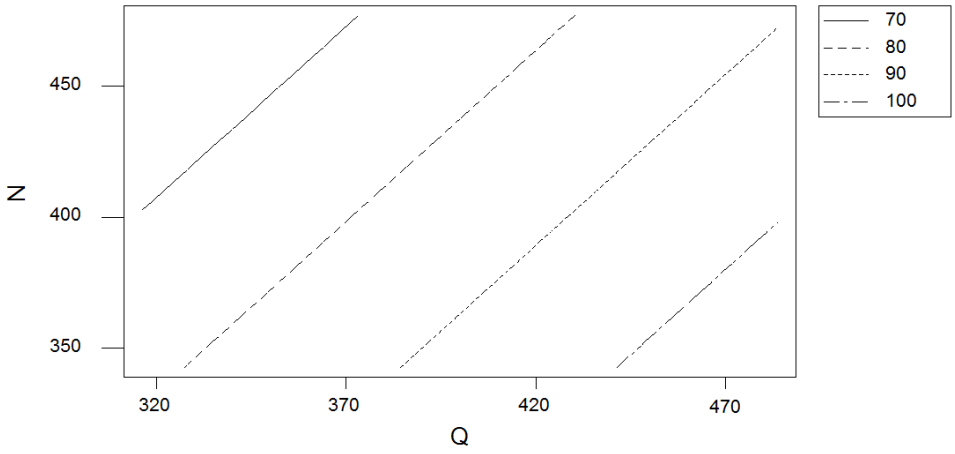

Table A.3 Response Surface Regression: Load versus Q, N

The analysis was done using uncoded units.

Estimated Regression Coefficients for Load

Term	Coef	SE Coef	T	P
Constant	68.7234	3.04794	22.547	0.000
Block 1	1.0462	0.29477	3.549	0.003
Block 2	0.0334	0.26157	0.128	0.900
Q	0.1751	0.00486	36.011	0.000
N	-0.1344	0.00661	-20.327	0.000

S = 0.8705 R-Sq = 99.0% R-Sq(adj) = 98.8

Analysis of Variance for Load

Source	DF	Seq SS	Adj SS	Adj MS	F	P
Blocks	2	26.68	11.47	5.734	7.57	0.005
Regression	2	1127.29	1127.29	563.647	743.85	0.000
Linear	2	1127.29	1127.29	563.647	743.85	0.000
Residual Error	15	11.37	11.37	0.758		
Lack-of-Fit	13	11.31	11.31	0.870	32.21	0.249
Pure Error	2	0.05	0.05	0.027		
Total	19	1165.34				

SEC is an important process parameter in any type of mixing. The specific energy consumption (SEC) which represents the amount of energy required per unit mass of material can be derived by dividing load by the throughput. Unit of SEC is Kw.h/kg. SEC is a measure of the total deformation that the material is exposed during the extrusion process and the stress that is required to bring about this deformation [25]. Contour plot and surface plot of SEC versus feed rate and screw speed are shown figure 4.2 and figure A.3. The Model for SEC gives good fit with reliability of 87.1. Analysis of variance (Table 4.5) indicates that feed rate and screw speed significantly affect the SEC.

In design region, all contour lines have straight lines with SEC increasing sharply at low throughputs. As shown in plots, the lowest value of SEC can be obtained at high throughputs and low screw speed. The mechanical energy is transformed in the extruder into heat by frictional and viscous heat generation. Thus, the higher the SEC the higher will be the temperature rise of the material.

Figure A.2: Control Plot of SEC versus feed rate (kg/hr) and screw speed (rpm)

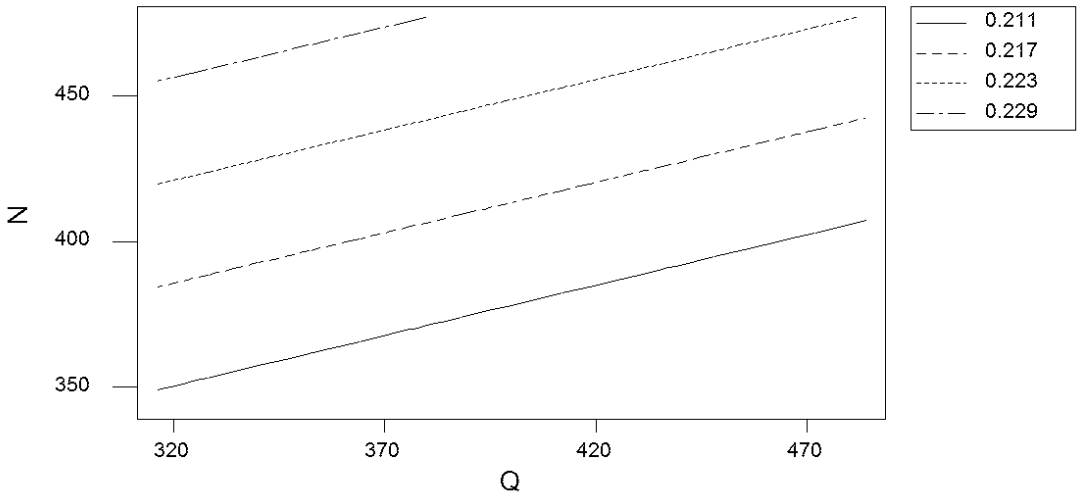

Figure A.3: Surface Plot of SEC versus feed rate (kg/hr) and screw speed (rpm)

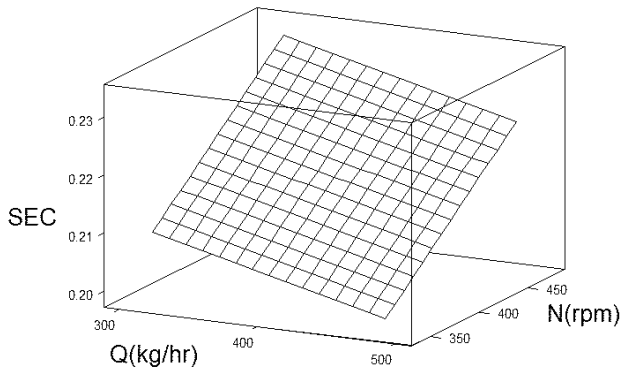

Table A.5 Response Surface Regression: SEC versus Q, N

The analysis was done using uncoded units.
Estimated Regression Coefficients for SEC

Term	Coef	SE Coef	T	P
Constant	0.170296	0.010041	16.960	0.000
Block 1	0.003305	0.000971	3.403	0.004
Block 2	0.000045	0.000862	0.052	0.959
Q	-0.000059	0.000016	-3.667	0.002
N	0.000170	0.000022	7.799	0.000

S = 0.002868 R-Sq = 87.1% R-Sq(adj) = 83.6%

Analysis of Variance for SEC

Source	DF	Seq SS	Adj SS	Adj MS	F	P
Blocks	2	0.000288	0.000113	0.000056	6.84	0.008
Regression	2	0.000542	0.000542	0.000271	32.93	0.000
Linear	2	0.000542	0.000542	0.000271	32.93	0.000
Residual Error	15	0.000123	0.000123	0.000008		
Lack-of-Fit	13	0.000123	0.000123	0.000009	29.20	0.034
Pure Error	2	0.000001	0.000001	0.000000		
Total	19	0.000953				

Figure A.4 shows the Xbar chart for MVR versus Run number .The upper and lower control limits for Xbar chart were set as per the SABIC Innovative Plastics quality control spec. This chart monitors both the mean value of the MVR and its variability. Examining Xbar chart indicates that run numbers 7, 16 and 18 are out of range. These run are in low level of feed rate and high level of screw speed. At low throughput, there must be a significant increase in resident time .Furthermore, SEC increasing sharply at low throughputs and high screw speed so material are stayed longer in extruder and expose to more energy which in turns results in decrease of viscosity and increase of MVR.

Figure A.5 shows comparisons of Load with reciprocal of Melt flow rate for 20 experimental runs. As shown, in this figure, MVR are closely correlated with reciprocal of Load. Least square method was used to find relation between MVR and Load as shown in Table A.6. From examining this model, one can see that with increasing Load, MVR decreases. As explained above the load are also affected by processing conditions such as feed rate and

screw speed. That is, with increase in throughput and decrease in screw speed thus increase in Q/N, load increases steadily. An increase in load which is resulted from more shear and stress causes a decrease in viscosity of blends and according an increase in MVR.

Table A.6 Regression Analysis: MVR versus Load

```
The regression equation is MVR = 73.1 - 0.497 Load
Predictor        Coef     SE Coef          T        P
Constant       73.103       4.300      17.00    0.000
Load         -0.49654     0.05143      -9.66    0.000
S = 1.756       R-Sq = 83.8%     R-Sq(adj) = 82.9%
```

Figure A.4: Control Chart for MVR

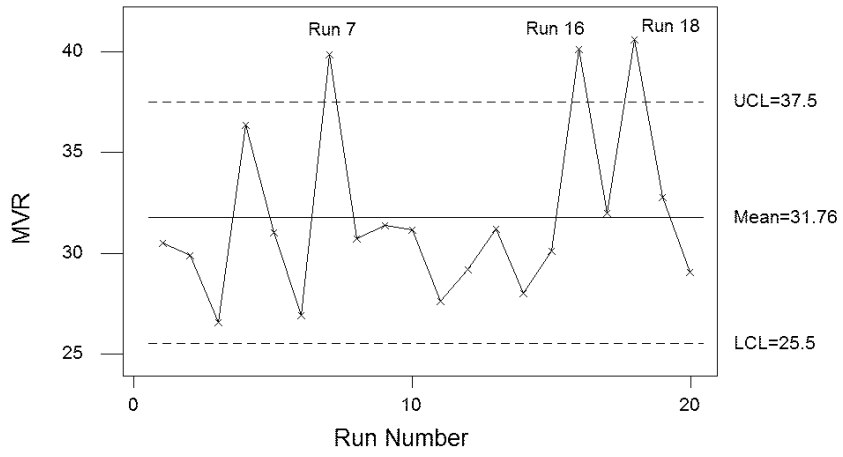

Figure A.5: Comparison of 1/MVR with motor load

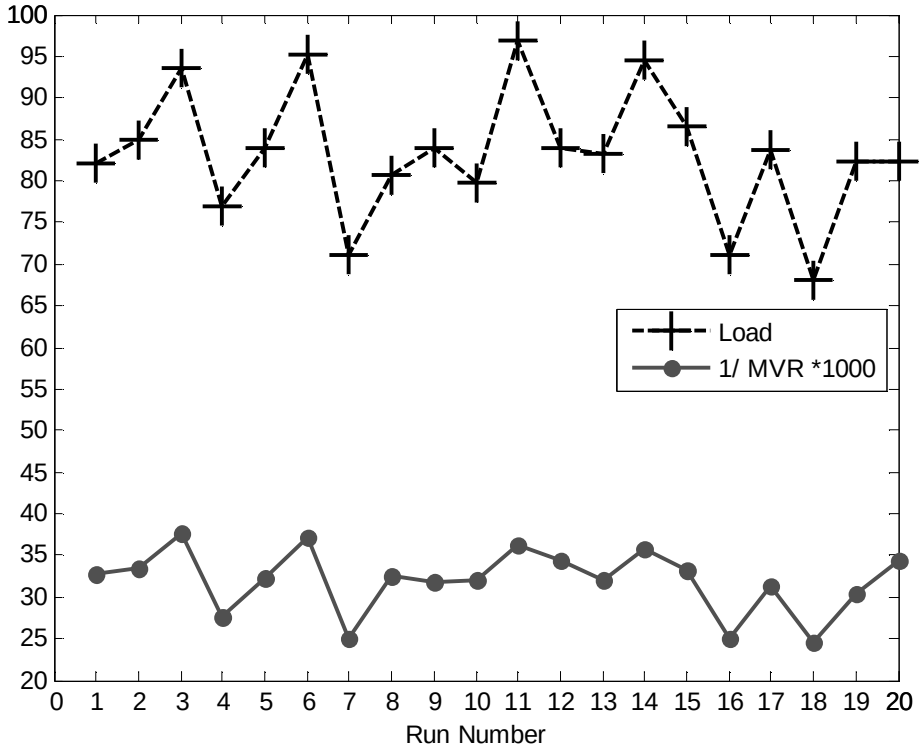

A.3 Optimization of Multiple Responses

In our experimental runs MVR and impact were measured as responses. First , an appropriate response surface for melt volume rate were build as function of process variables Q , and N. then it was repeated for impact strength . For the analysis of these responses simultaneously and finding the set of operating conditions that keeps these responses in desired ranges, these response surface were overlaid. Details of these results will be shown and discussed in this section.

As regression analysis shows (Table A. 7) the melt flow rate depends on the feed rate and screw speed and it can be concluded that Q and N will significantly affect MVR. A multiple regression model that might describes this relation is

MVR = 28.8 - 0.0812 *Q + 0.0856* N+ϵ

By assuming the expected value of error as zero, the regression model can be shown as

E (MVR) = 28.8 - 0.0812 Q + 0.0856 N

Parameters of $b_1 = -0.0812$ and $b_2 = 0.0856$ measures the expected change in melt flow rate per unit change in N when Q is held constant and vise versa. Figure A.6 shows a contour plot of the regression model –that is, lines of constant E(Y) as a function of Q and N .The contour lines in this plot seems straight lines.

Same procedures were repeated for impact strength. As regression analysis shows (Table A.8) the impact strength depends on the feed rate and screw speed. Accordingly the regression model for impact strength can be shown as

E (Impact) = 14.6 + 0.0150 Q - 0.0153 N

Parameters of $b_1 = -0.015$ and $b_2 = 0.0153$ measures the expected change in impact strength per unit change in N when Q is held constant and vise versa. Figure A.7 shows a contour plot of the regression model with the contour lines of straight.

Table A.7 Regression Analysis: MVR versus Q, N

Predictor	Coef	SE Coef	T	P
Constant	28.810	4.994	5.77	0.000
Q	-0.081185	0.007826	-10.37	0.000
N	0.08564	0.01060	8.08	0.000

S = 1.429 R-Sq = 89.9% R-Sq(adj) = 88.7%

Figure A.6: Control Plot of MVR versus feed rate (kg/hr) and screw speed (rpm)

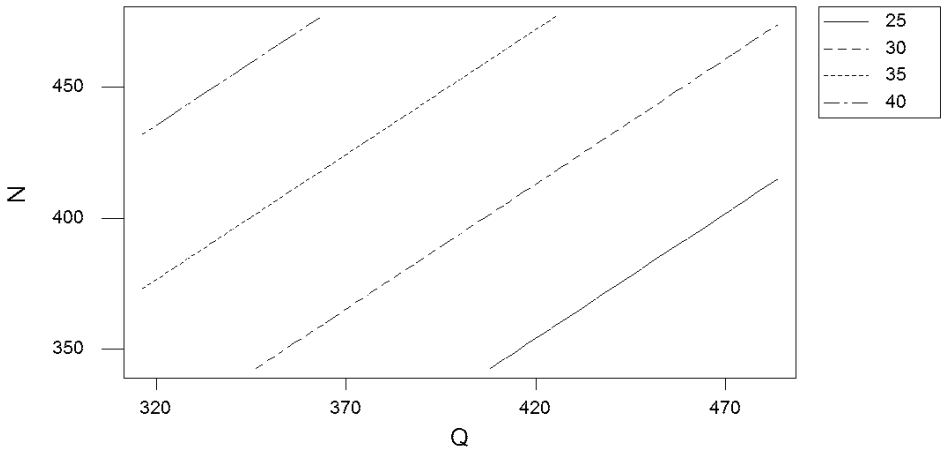

Table A.8 Regression Analysis: impact versus Q, N

The regression equation is

Predictor	Coef	SE Coef	T	P
Constant	14.551	2.563	5.68	0.000
Q	0.014963	0.004017	3.73	0.002
N	-0.015260	0.005440	-2.81	0.012

S = 0.7334 R-Sq = 52.8% R-Sq(adj) = 47.2%

Figure A.7: Control Plot of Impact versus feed rate (kg/hr) and screw speed (rpm)

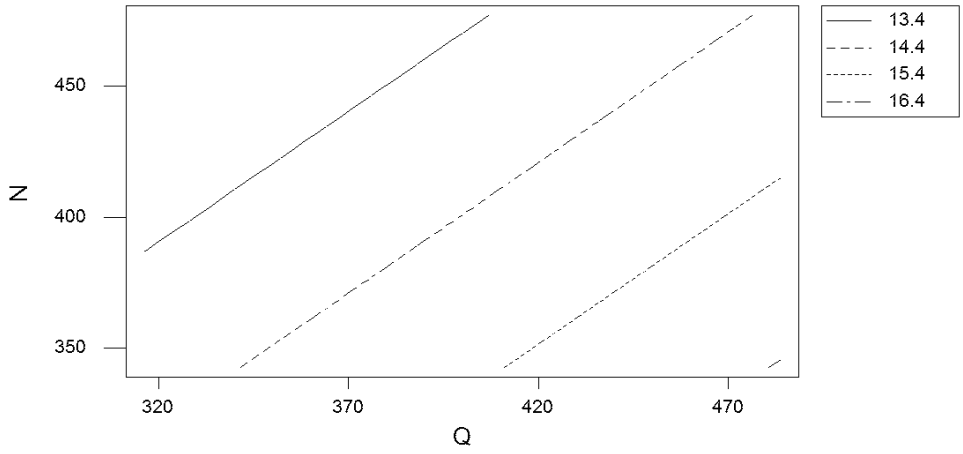

One of the general methods for optimization of multiple responses is using overlaid contour plots [28] for each response when there are only a few process variables. In this technique, by setting processing variables boundaries, it is possible to examine feasible area that will result in product with desired quality characteristics. Figure A.8 shows an overlay plot for the three responses with contours for melt flow rate, impact strength and load. These boundaries represent typical important conditions that must be met by the compounding process for production of typical product quality constrains of MVR (25.5, 37.5) and impact strength (12, 30) for special grades of compound. As shown in figure A.8, there are a number of combinations of process variables i.e. Q and N that will results in satisfactory process. We can visually examine the feasible area which has been shown by white area.

Another useful approach to optimization of multiple responses is to use the technique popularized by Derringer and Suich [35] using desirability functions. The general approach is to first convert each response y_i into an individual desirability function d_i that changes over the range d (0 1). If the response y_i is at its goal or target, then $d_i = 1$ and if the response is outside an acceptable region $d_i = 0$. Then the design variables are choosen to maximize the overall desirability. The overall desirability is the product of individual desirability function and can be calculated by

$D = (d_1 . d_2 \dots \dots d_m)^{1/m}$ Where there are m responses

We might formulate the problem as we get to target of MVR =28 and impact=15.5, Where process constrains are Q (316, 484) and N (343, 477). Minitab software solves this version of problem using a direct search procedure as shown in Table A.9. Desirability function for melt flow is 0.98 and for impact strength is 0.853 and the overall desirability is:

$D = \sqrt[2]{0.98 * 0.853} = 0.92$

This solution is in feasible region of the design space and near to the boundary of the constraints. These plots can be used to set processing condition (N, Q) for achieving characteristic quality properties (MVR, Impact strength). In typical compounding process, this technique can be used to reduce significantly time needed to reach optimal setting of process variables.

Figure A.8: Overlaid Plot

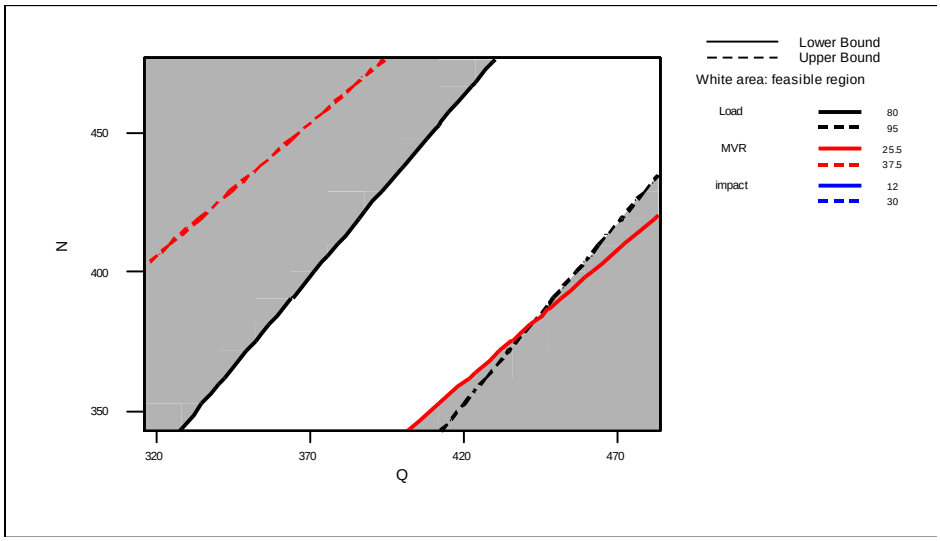

Table A.9 Response Optimization

Parameters

	Goal	Lower	Target	Upper	Weight
MVR	Target	25.5	28.0	37.5	1
impact	Target	12.0	15.5	40.0	1

Starting Point

Q	=	400
N	=	400

Global Solution

Q	=	420.709
N	=	391.572

Predicted Responses

MVR = 28.1262, desirability = 0.98672
impact = 14.9879, desirability = 0.85367

Composite Desirability = 0.91779

Appendix B

Experimental Figures

B.1 Day 1 of the 2nd set of Experimental Runs

Figure B1: Changes in input variables of day 1 Experiments

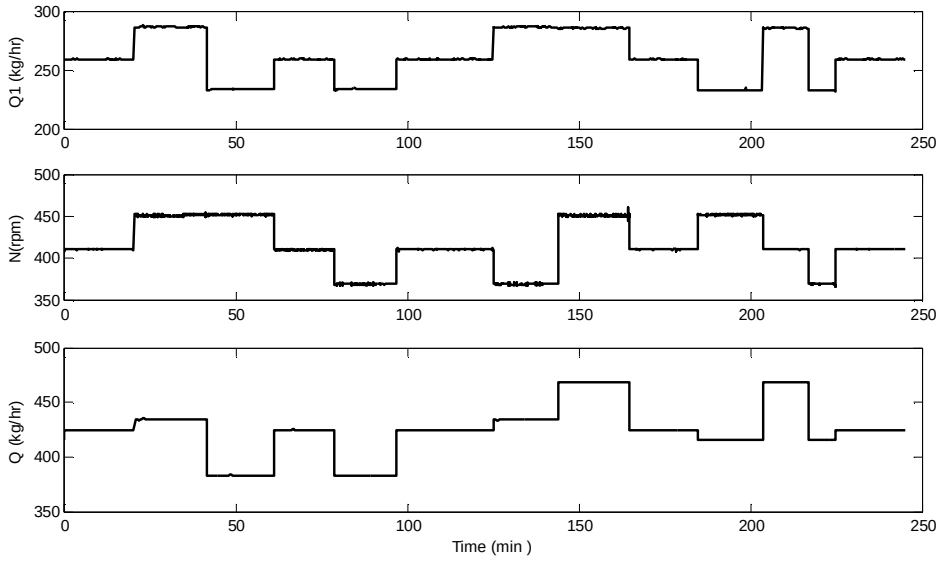

Figure B.2: Output Variables of day 1 Experiments

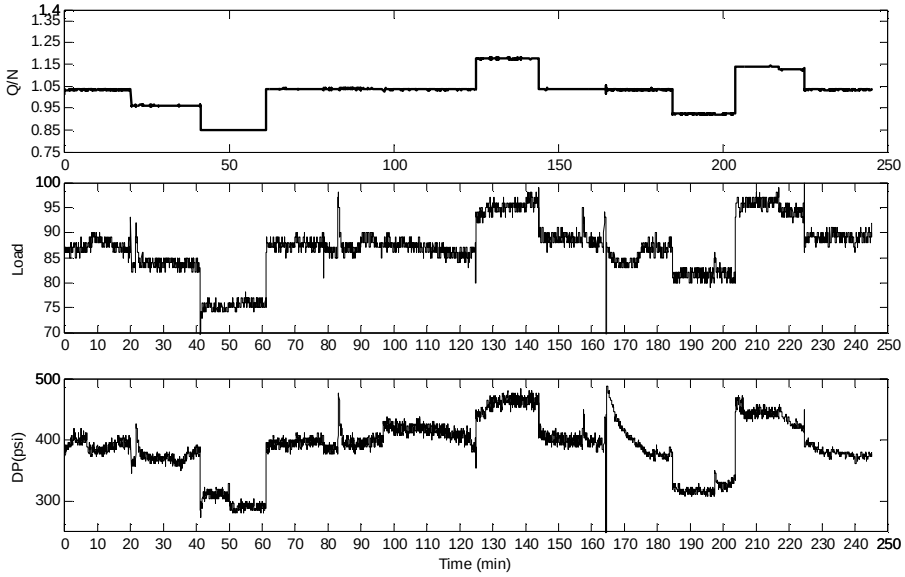

Figure B.3: Comparison of predicted and measured Die Pressure, Run 1-2, day 1

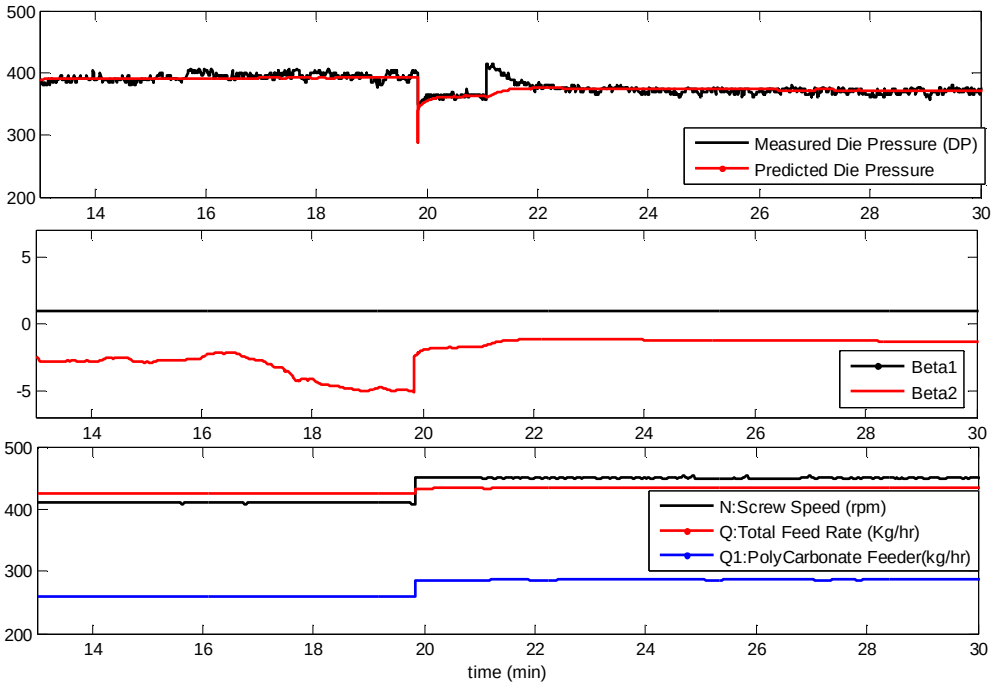

Figure B.4: Comparison of predicted and measured Die Pressure, Run 6-7, day 1

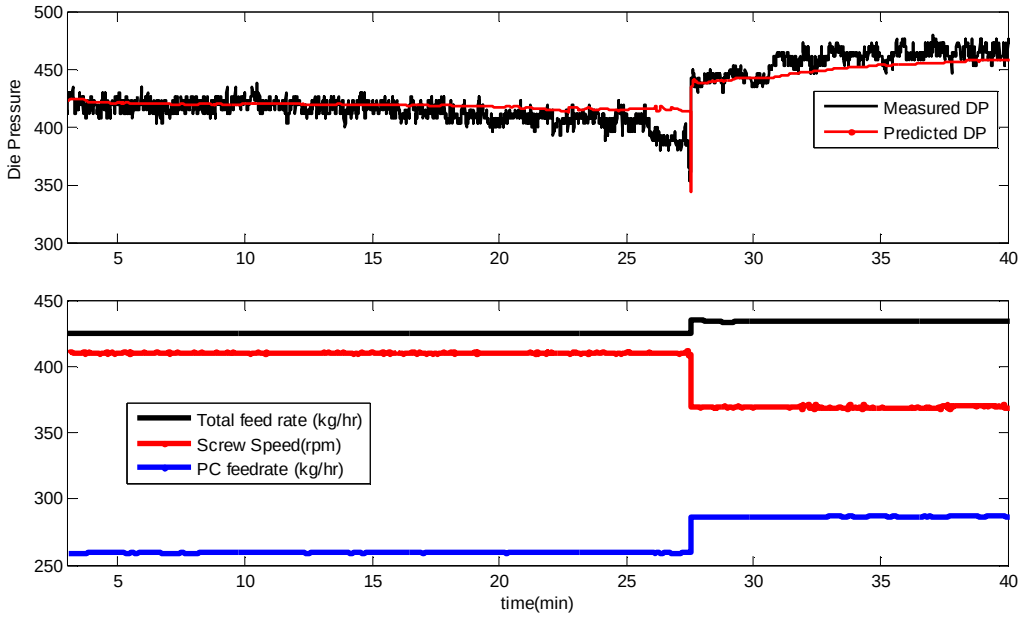

Figure B.5: Comparison of predicted and measured Die Pressure, Run 7-8, day 1

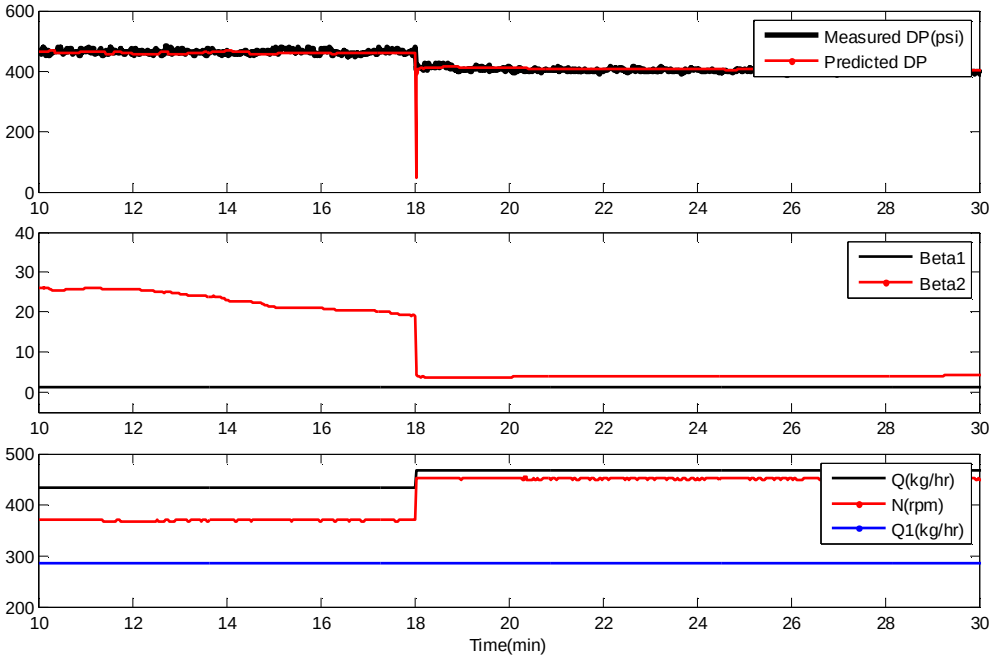

Figure B.6: Comparison of predicted and measured Die Pressure, Run 9-10, day 1

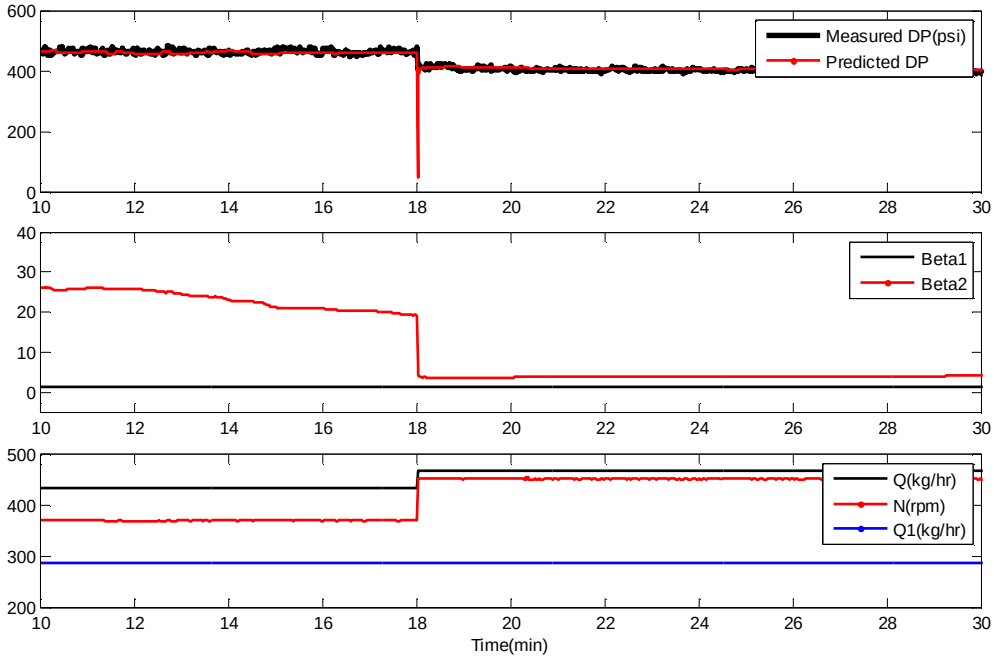

Figure B.7: Comparison of predicted and measured Die Pressure, Run 10-11, day1

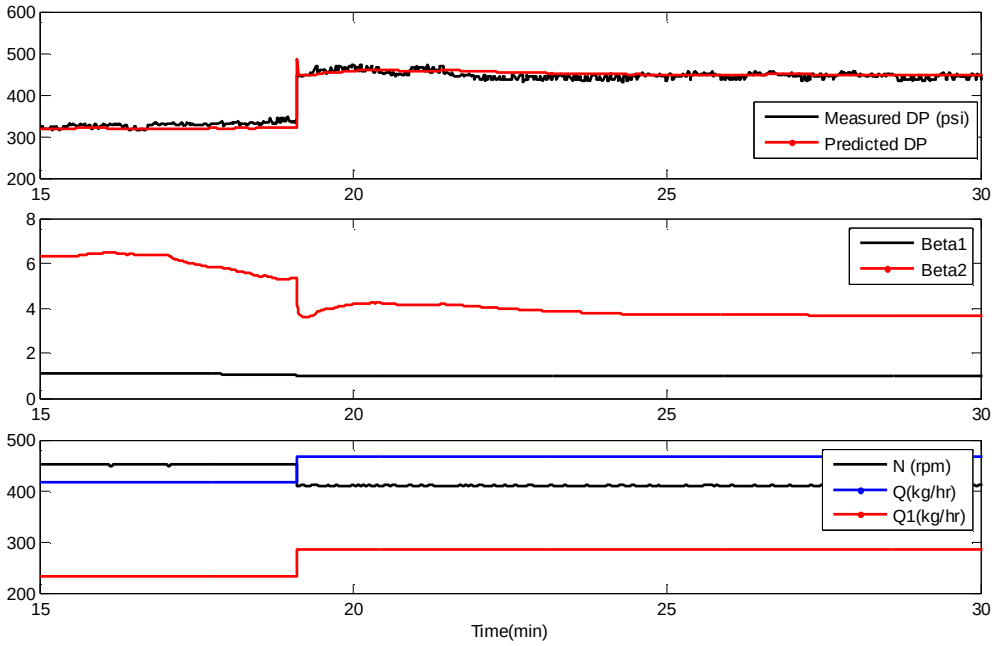

Figure B.8: Comparison of predicted and measured Die Pressure, Run 11-12, day 1

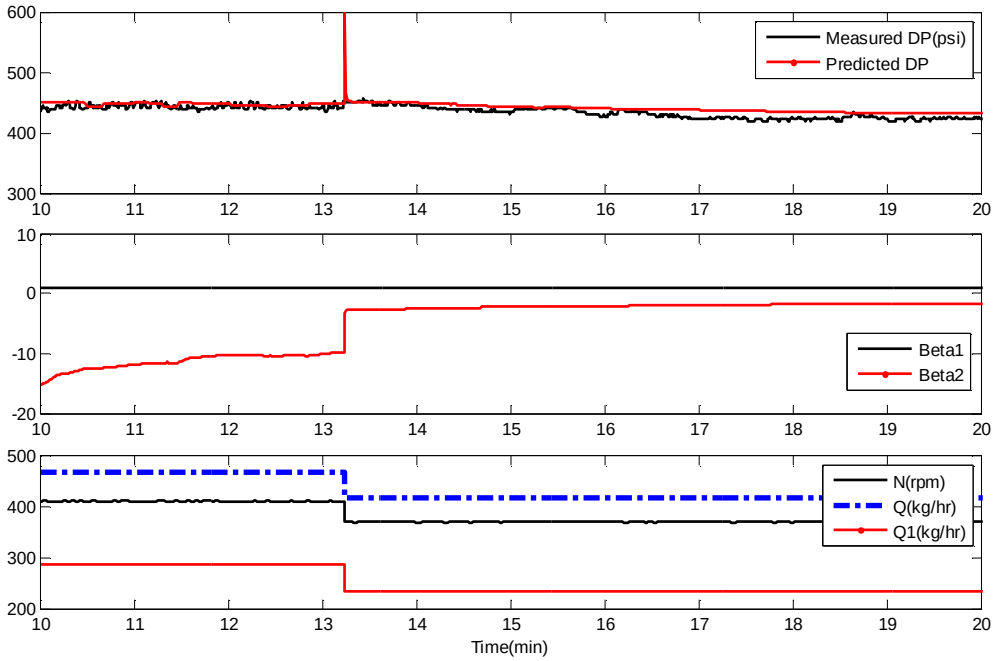

B.2 Day 2 of the 2nd Set of Experimental Runs

Figure B.9: Changes in input variables of day 2 experiments

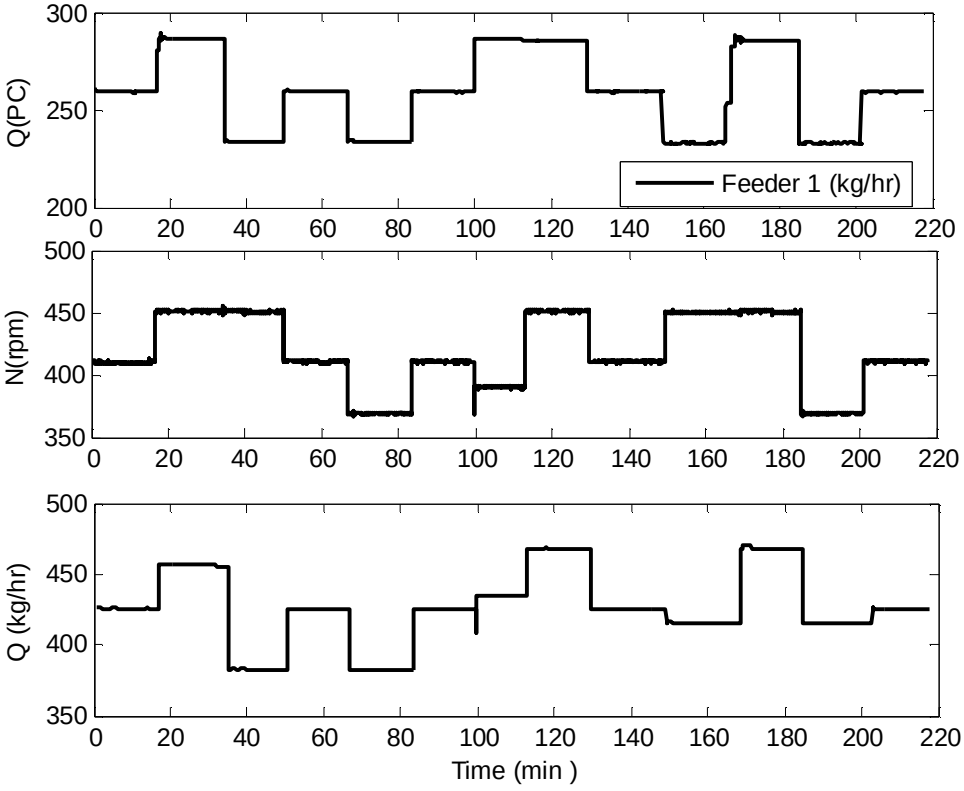

Figure B.10: Output variables of day 2 Experiments

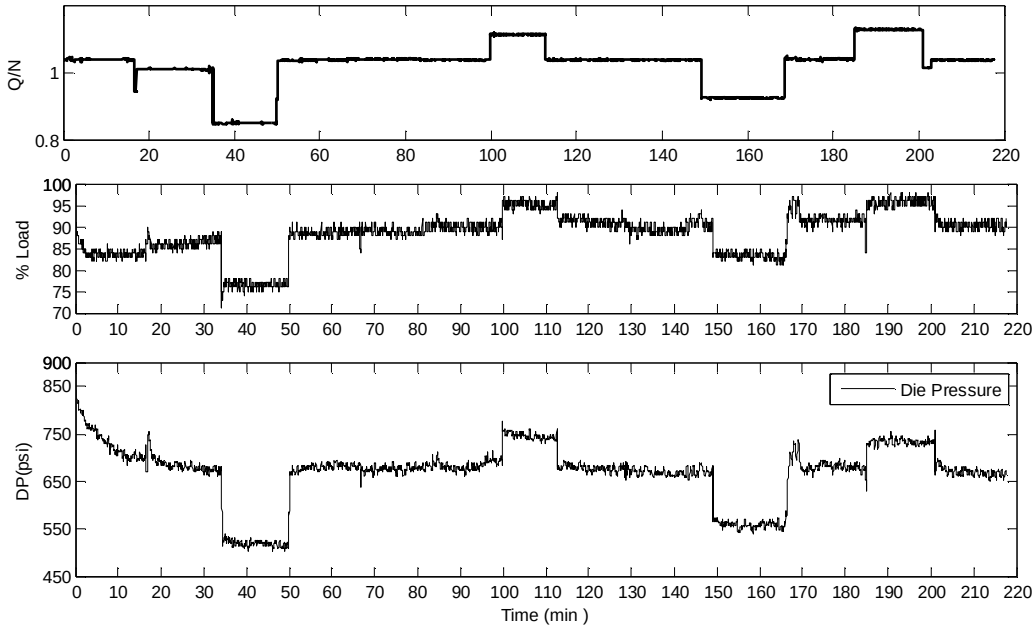

Figure B.11: Comparison of predicted and measured Die Pressure, Run 6-7, Day 2

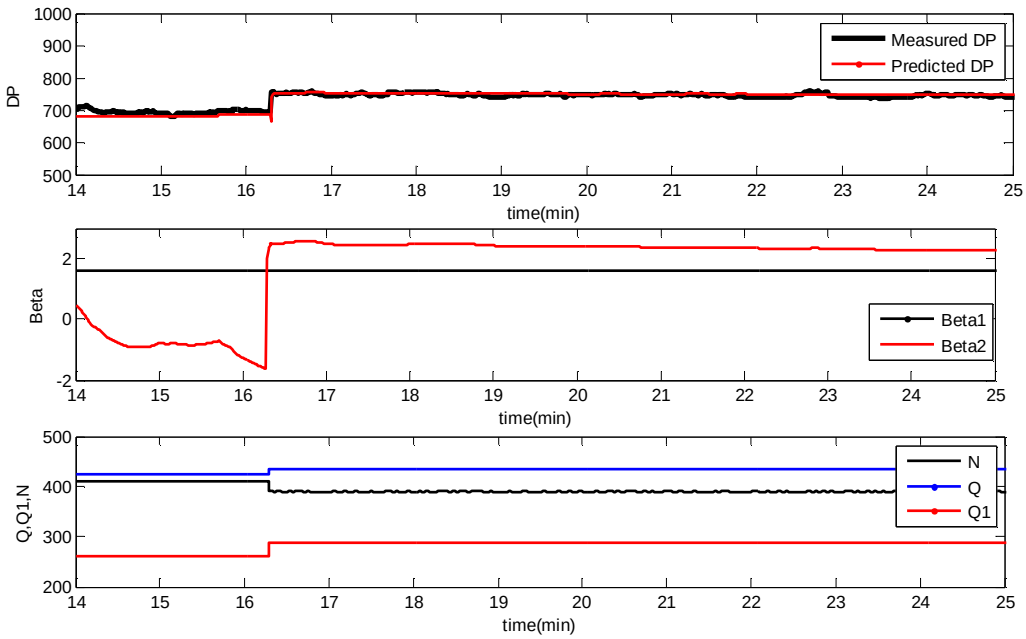

Figure B.12: Comparison of predicted and measured Die Pressure, Run 7-8, day 2

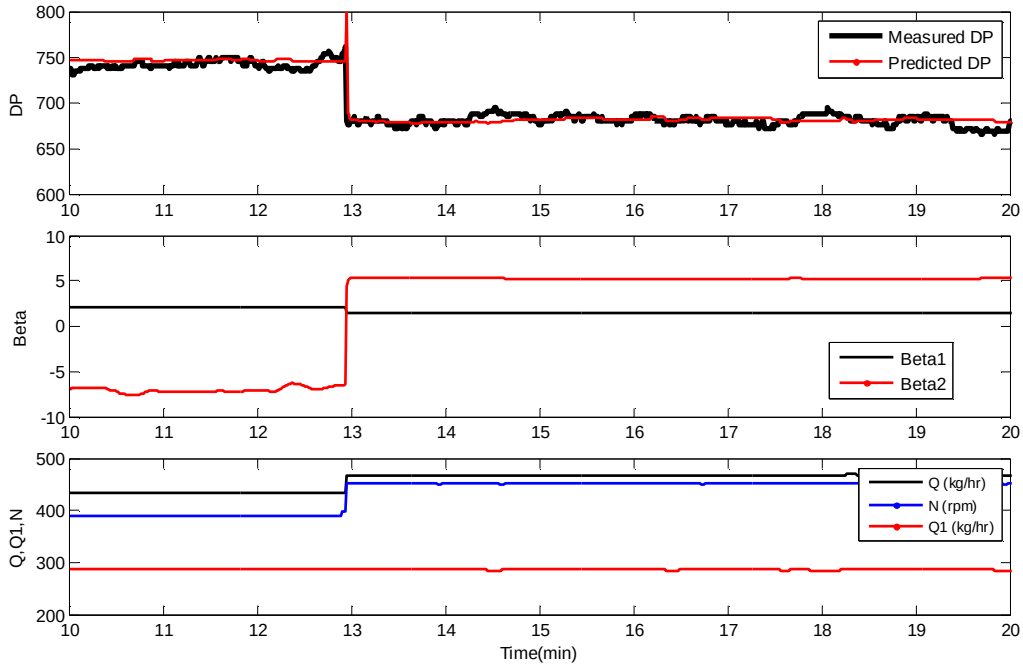

Figure B13: Comparison of predicted and measured Die Pressure, Run 9-10, day 2

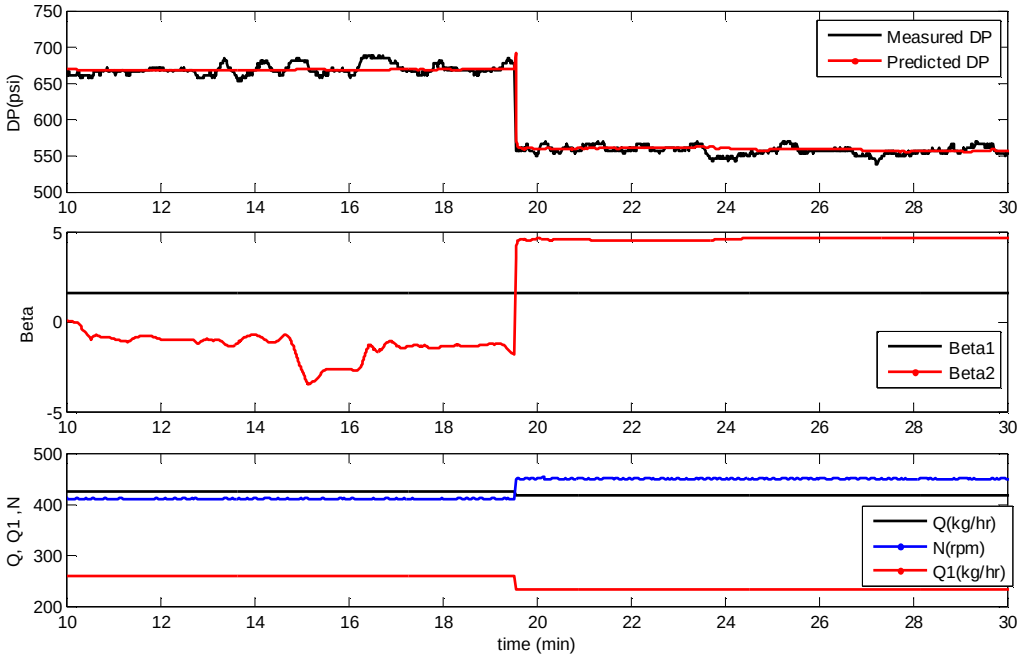

Figure B14: Comparison of predicted and measured Die Pressure, Run 10-11, day 2

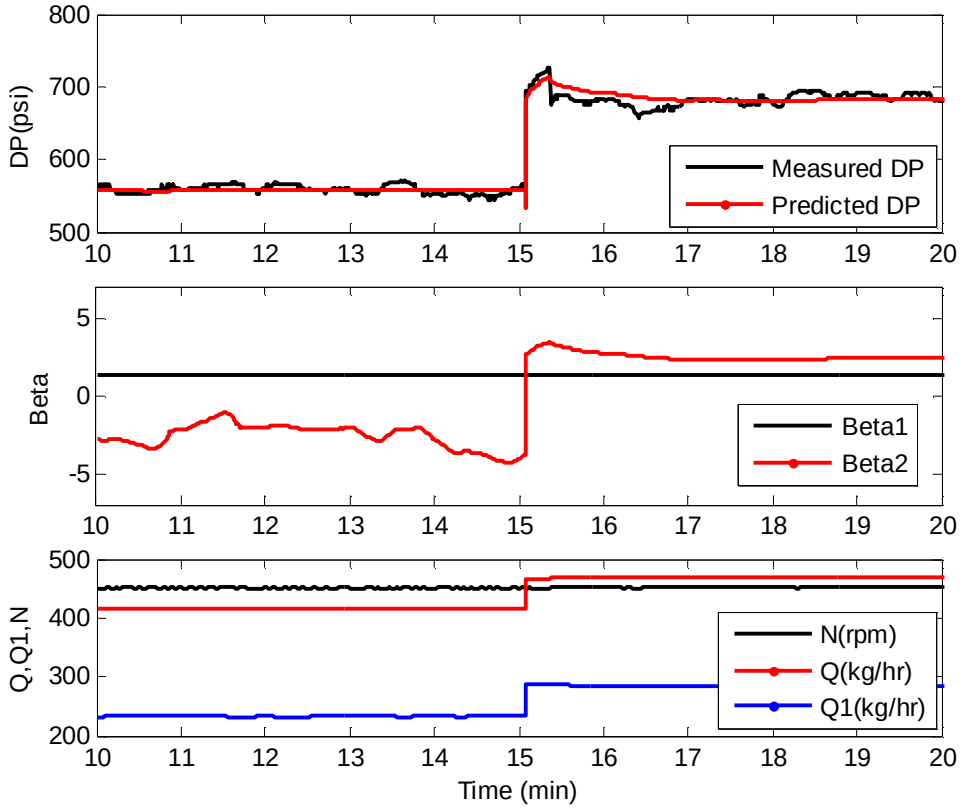

Figure B.15: Comparison of predicted and measured Die Pressure, Run 11-12, day 2

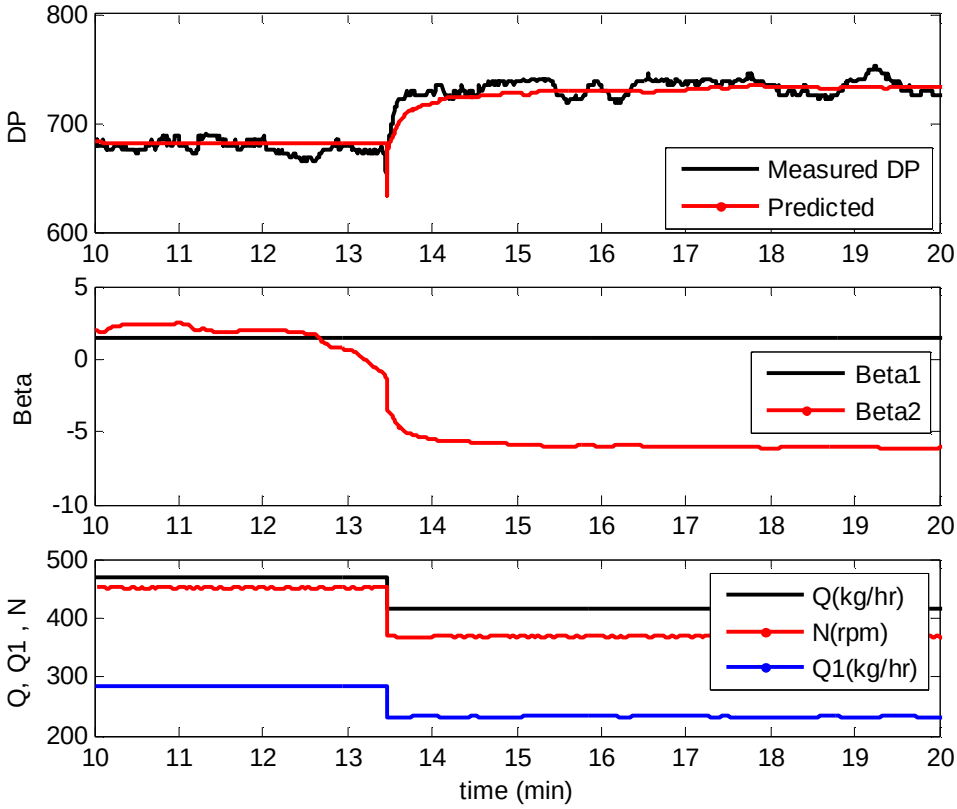

B.3 3rd Set of Experimental Runs

Figure B.16: Comparison of predicted and measured Die Pressure, Run 1-2
3rd Set of Experiments

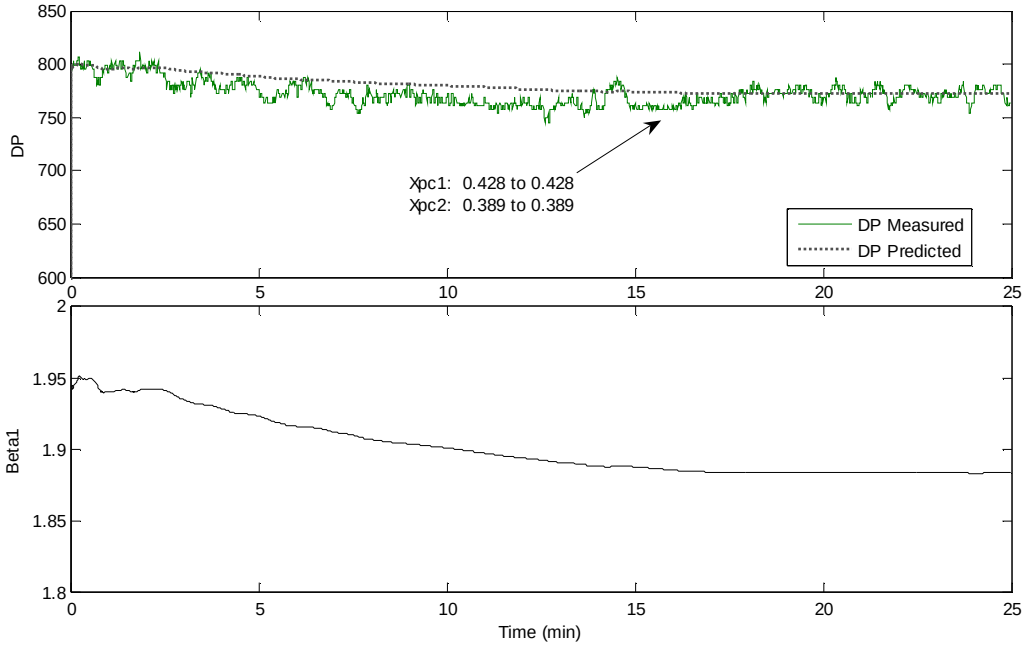

Figure B.17: Comparison of predicted and measured Die Pressure, Run 3-4, 3rd Set of Experiments

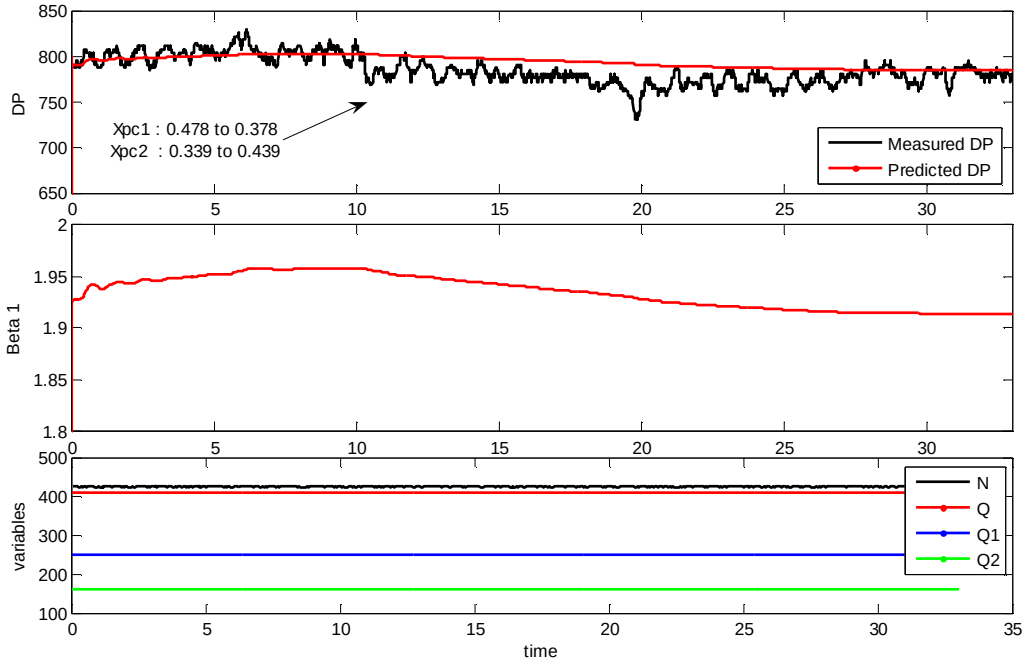

Figure B18: Comparison of predicted and measured Die Pressure, Run 6-7, 3rd Set of Experiments

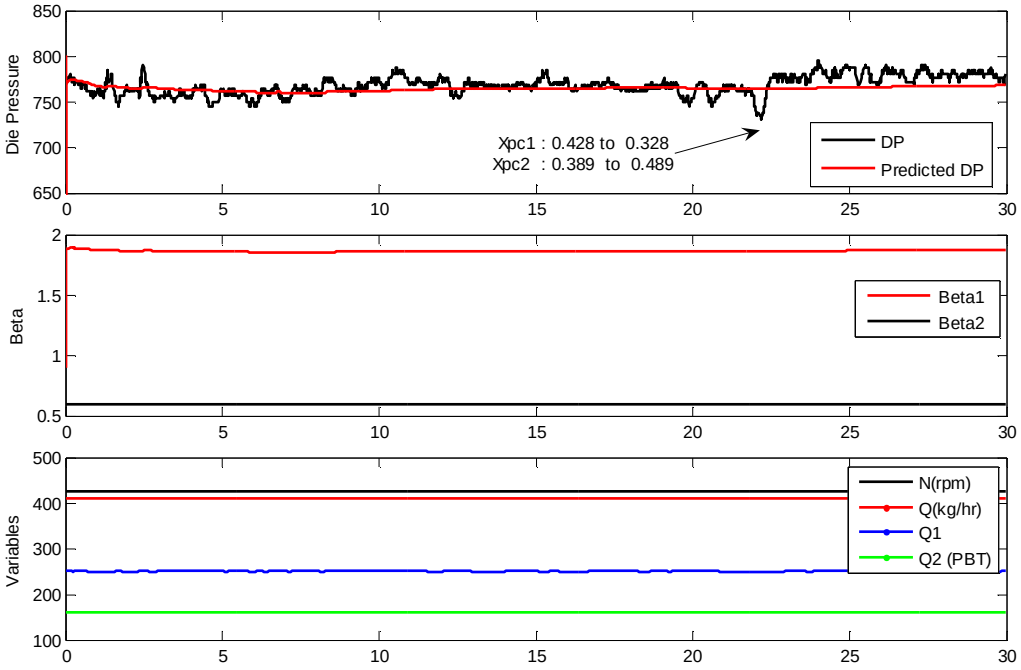

Figure B19: Comparison of predicted and measured Die Pressure, Run 7-8 , 3rd Set of Experiments

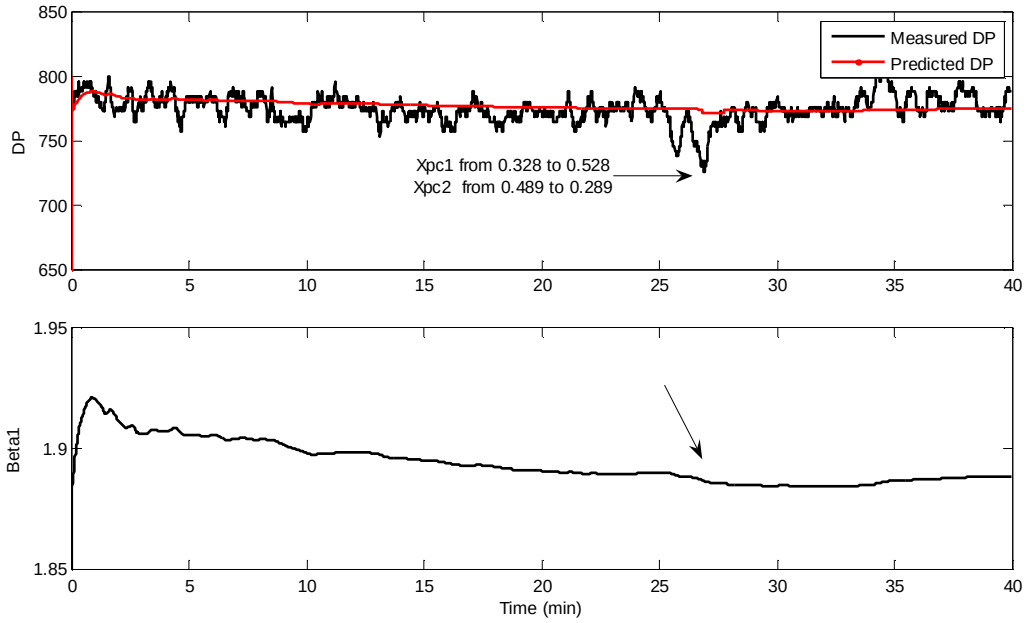

Figure B20: Comparison of predicted and measured Die Pressure, Run 8-9, 3rd Set of Experiments

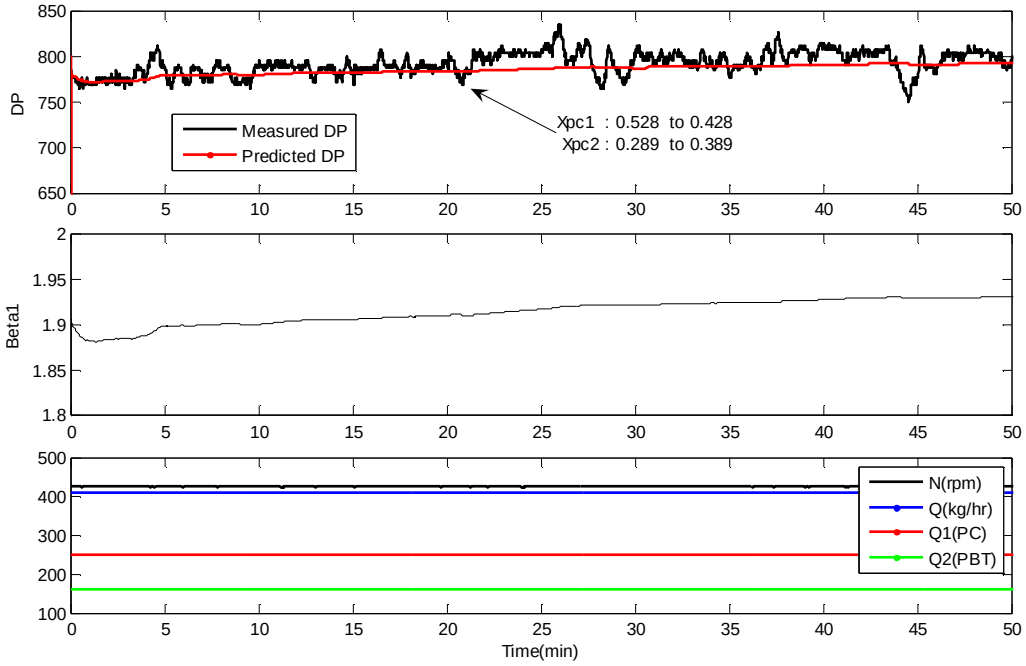

Appendix C

Matlab M-Files

C.1 Recursive Parameter Estimation (RPE)

%this program was written to estimate the die pressure parameters using

% Kalman filter algorithm

%first, Q, Qdx, and DP vectors should be imported to the Matlab workspace
%then this M-file should be run

Matlab M-file

```
---------------------------------------------------------------------------------------------------------------
P {1} = [5 0; 0 5];                % initial value of covariance matrix
teta{1}=[0.9 ; 1.6];               % initial value of Beta
yhat(1)= 560;                       % yhat(1)= G{1}'*teta{initial}

j = input('what is i');
for i=1:j
   G{i} = [Q(i,1) ; Qdx(i,1)];   % G is design vector
end

for i=2:j
   P{i} = P{i-1}-((P{i-1}*G{i}*G{i}'*P{i-1}) / (1 + (G{i}'*P{i-1}*G{i})));
end

for i=2:j
   q{i}=P{i-1}/(1+(G{i}'*P{i-1}*G{i}));
end

for i=2:j
   K{i}=q{i}*G{i};        %K is gain
end

for i=2:j

%    teta{i-1}
      yhat(i)=G{i}'*teta{i-1};
      teta{i}=teta{i-1}+K{i}*(DP(i)-yhat(i));

end
---------------------------------------------------------------------------------------------------------------
```

```
%running this M-file will produce yhat, K, Teta, G, P, and q matrices in the Matlab
%workspace
%after that type     Beta=cell2mat(teta(:,[1: i]))'  which will give die pressure parameters
%matrices
```

C.2 Torque Model Parameter Estimation using Levenberg Marquardt Algorithm

```
% first, t (time) and T (load) vectors should be imported to workspace of Matlab

p0= [13 24 90 0.000278    46.6    -0.00111]

% initial values of parameters P [A B a0 a1 a2 a3]

N=410; Q=425; Xi=0.61; M0=20;    % process variables values
```

Matlab M-file

```
function e = cost(p, t,T)
%p: Load parameters
%t:time
%T:Load
%N:screw speed
%Q:total feed rate
%Xi:wt fraction of polycarbonate
%M0: initial value of mass holdup

A=p(1);
B=p(2);
a0=p(3);
a1=p(4);
a2=p(5);
a3=p(6);
N=410;Q=425;Xi=0.61;M0=20;
yhat= a0+a1*((M0*N-B*Q)*exp(-N*t/B)+B*Q)/N*(a2+N)*Xi+a3*A*N*Xi;
e = yhat-T;
```

```
optim_options = optimset('Display','iter','LevenbergMarquardt','on','TolFun', 1e-
4,'MaxFunEvals',600);

% this command gives options for calculating load parameters using LMA
```

```
[p,resnorm,RESIDUAL,EXITFLAG,OUTPUT,LAMBDA,Jacobian] =lsqnonlin(@cost, p0,
[],[],optim_options, t,T);

% this command calculate parameters by iteration


------------------ Plotting results ----------------------------------------------------------------------
    plot(t, T,'*')
    hold on
    plot(t,p(3)+p(4)*((M0*N-p(2)*Q)*exp(-
N*t/p(2))+p(2)*Q)/N*(p(5)+N)*Xi+p(6)*p(1)*N*Xi,'r' )
```